

**Regulation of G protein-activated inwardly rectifying  
potassium channels by the neural cell adhesion molecule  
NCAM**

Dissertation

zur Erlangung des Doktorgrades des Fachbereiches Chemie  
der Universität Hamburg

vorgelegt von Markus Delling

Hamburg, 2001

**Gutachter: Herr Prof. Dr. G. Gercken**  
**Frau Prof. Dr. M. Schachner**

## Content

I	INTRODUCTION .....	1
1	The neural cell adhesion molecule NCAM .....	1
1.1	NCAM deficient mice .....	4
1.2	NCAM-mediated signal transduction.....	6
1.3	NCAM-mediated modulation of potassium channels .....	7
2	Inwardly rectifying K <sup>+</sup> channels.....	7
2.1	G protein-activated inwardly rectifying K <sup>+</sup> (Kir3) channels.....	8
2.2	Modulation of Kir channels by phosphorylation.....	10
2.3	Modulation of Kir channels by other proteins.....	11
2.4	Regulation of postsynaptic neural excitability by Kir3 channels.....	11
II	AIM OF THE STUDY .....	13
III	MATERIALS .....	14
1	Chemicals .....	14
2	Solutions and buffers .....	14
3	Bacterial media .....	18
4	Bacterial strains and cell lines .....	19
5	Cell culture media.....	19
6	Molecular weight standards.....	20
7	Plasmids.....	21
8	Antibodies.....	22
8.1	Primary antibodies.....	22
8.2	Secondary antibodies.....	23
IV	METHODS.....	24
1	Molecular biology.....	24
1.1	Bacterial strains .....	24
1.1.1	Maintenance of bacterial strains.....	24
1.1.2	Production of competent bacteria.....	24
1.1.3	Transformation of bacteria .....	24
1.2	Plasmid isolation of E. coli.....	25
1.2.1	Plasmid isolation from 3 ml cultures (Minipreps).....	25
1.2.2	Plasmid isolation from 15 ml-cultures.....	25

1.2.3	Plasmid isolation from 500 ml-cultures (Maxipreps).....	25
1.3	Enzymatic modification of DNA.....	26
1.3.1	Digestion of DNA.....	26
1.3.2	Dephosphorylation of Plasmid-DNA .....	26
1.3.3	Polishing of sticky ends.....	27
1.3.4	Ligation of DNA-fragments .....	27
1.4	Polymerase chain reaction (PCR).....	27
1.4.1	Standard PCR .....	27
1.4.2	Site-directed Mutagenesis.....	28
1.4.3	Single Colony PCR.....	30
1.4.4	Splicing by overlap extension (SOE) PCR.....	30
1.5	DNA Gel-electrophoresis .....	31
1.6	Extraction of DNA fragments from agarose gels .....	32
1.7	Purification of DNA fragments .....	32
1.8	Determination of DNA concentrations.....	32
1.9	DNA Sequencing.....	33
1.10	RNA techniques.....	33
1.10.1	In vitro-transcription.....	33
2	Protein-biochemical methods .....	33
2.1	SDS-poly-acrylamide gel electrophoresis .....	33
2.1.1	Coomassie-staining of poly-acrylamide gels.....	34
2.2	Western Blot-analysis.....	34
2.2.1	Electrophoretic transfer .....	34
2.2.2	Immunological detection of proteins on Nitrocellulose membranes.....	35
2.2.3	Immunological detection using enhanced chemiluminescence.....	35
2.2.4	Densitometric evaluation of band intensity .....	35
2.3	Recombinant expression of proteins in <i>Escherichia coli</i> .....	36
2.3.1	Expression in E. coli using the pET-system.....	36
2.3.2	Expression in E. coli using the pQE-system.....	36
2.4	Lysis of bacteria.....	37
2.4.1	Sonification.....	37
2.4.2	French press.....	37
2.5	Determination of protein concentration (BCA).....	37

2.6	Preparation of the Lovastatin open acid form .....	38
3	Cell culture .....	38
3.1	CHO and N <sub>2</sub> A cell culture .....	38
3.2	Transfection of CHO-cells.....	39
3.3	Lysis of CHO-cells .....	39
3.4	Co-immunoprecipitation and pull-down assays from transiently transfected CHO cells.....	39
3.5	Surface biotinylation and internalization measurements of transfected CHO cells.	40
3.6	Internalization assays with Tritc-transferrin and Tritc-dextran.....	41
3.7	NCAM-stimulation with polyclonal antibodies .....	41
3.8	Immunoprecipitation of tyrosine phosphorylated proteins.....	42
3.9	Isolation of detergent-resistant membrane fractions .....	42
3.10	Preparation of membrane and Triton X-100-insoluble fractions of CHO cells .....	43
3.11	Endoglycosidase H digestion of CHO cell lysates .....	43
3.12	Incubation of CHO cells with lovastatin and mevalonate .....	44
4	Immunocytochemistry .....	44
4.1	Immunocytochemistry of living cells.....	44
4.2	Fixation of CHO cells.....	44
4.3	Immunocytochemistry of fixed CHO cells and hippocampal neurons.....	45
4.4	Fluorescence measurements of <i>Xenopus</i> oocytes.....	45
4.5	Confocal laser-scanning microscopy.....	45
5	Electrophysiology.....	46
5.1	Heterologous expression in <i>Xenopus laevis</i> oocytes .....	46
5.2	Electrophysiological recordings from transfected CHO cells and hippocampal neurons.....	46
6	Computer based sequence analysis.....	46
V	RESULTS .....	47
1	Kir3 inward currents are increased in hippocampal neurons of NCAM <sup>-/-</sup> -mice.....	47
2	NCAM140 and NCAM180 reduce neuronal Kir3 currents in <i>Xenopus</i> oocytes and CHO cells.....	48
3	NCAM140 reduces surface localization of EGFP-tagged Kir3.2 channels in <i>Xenopus</i> oocytes .....	51
4	The NH <sub>2</sub> -terminus of Kir3.2 is the major structural determinant for NCAM-sensitivity	52

5	The intracellular domain of NCAM140 is not sufficient to inhibit Kir3-mediated currents .....	56
6	Stimulation of NCAM140 or NCAM180 associated signal transduction pathways did not alter surface localization of Kir3.1/3.2 .....	57
7	NCAM140 does not interact physically with the Kir3 channels .....	58
8	All NCAM isoforms are present in lipid raft microdomains.....	61
9	Mutation of palmitoylation sites abolishes the presence of NCAM140 in lipid rafts .....	63
10	Activation of the focal adhesion kinase FAK by NCAM140 is impaired when NCAM140 is excluded from lipid rafts.....	65
11	Impairment of NCAM140 raft association or disruption of intracellular rafts in CHO cells revert the inhibitory effect of NCAM140 on Kir3.1/3.2 surface localization.....	66
12	Kir3 channel reduction by NCAM140 - altered delivery to or internalization from the plasma membrane? .....	69
13	Kir3.1/3.2 or Kir3.1/3.4 do not shift to a certain intracellular compartment after cotransfection with NCAM140 or NCAM180 .....	75
VI	DISCUSSION.....	78
1	NCAM140 and NCAM180 reduce plasma membrane localization of Kir3 channels. ....	78
2	Two submembranous compartments contain NCAM-isoforms.....	79
3	Palmitoylation of NCAM140 is necessary for its localization in lipid rafts .....	80
4	NCAM140 regulates the transport of Kir3 channels to the cell membrane .....	81
5	Lipid rafts are involved in the transport of Kir3.1/3.2 channels to the membrane.....	82
6	Physiological relevance of adhesion molecules regulating the number of inhibitory potassium channels.....	85
VII	SUMMARY.....	86
VII	ZUSAMMENFASSUNG .....	88
VIII	REFERENCES .....	90
IX	APPENDIX .....	102
1	ABBREVIATIONS.....	102
2	Oligonucleotides.....	104
3	Accession numbers.....	105
4	Plasmids.....	106
4.1	Kir3 plasmids.....	106
4.1.1	Construction of Kir3.1/3.2 and Kir3.1/3.4-hybrids .....	107

4.1.1.1	COOH and NH <sub>2</sub> exchange .....	107
4.1.1.2	Single amino acid mutations in Kir3.2 and Kir3.4 .....	109
4.1.2	Construction of Kir3.1/3.2 and Kir3.1/3.4-EGFP and 6xHis-tag chimeras ...	109
4.1.3	Construction of Kir3.1flag/3.2 and Kir3.1flag/3.4 and Kir3.1flag/3.2- and Kir3.1flag/3.4-EGFP chimeras .....	111
4.2	NCAM plasmids .....	111
4.2.1	NCAM120 in pcDNA3 and psGEM .....	111
4.2.2	NCAM140 and NCAM180 in pcDNA3 and psGEM.....	112
4.2.3	NCAM 140Δ in pcDNA3 and psGEM.....	113
4.2.4	NCAM140-, NCAM180- and NCAM140Δ-EGFP in pcDNA3.....	113
4.2.5	NCAM140IC and NCAM180ICpcDNA3 and psGEM.....	115
4.2.6	NCAM140IC and NCAM180ICpQE30 .....	115
5	Publications and poster presentations.....	116
5.1	Poster presentations .....	116
5.2	Publications .....	116
6	Curriculum vitae .....	117
	Danksagung .....	118

# I Introduction

## 1 The neural cell adhesion molecule NCAM

NCAM belongs to the immunoglobulin (Ig) superfamily of cell recognition molecules, which are characterized by the presence of several Ig-modules (Fig. 1). The prototypical examples of this family are antibodies (Edelman et al., 1969) and MHC-antigens (Orr et al., 1979). Many of these Ig-molecules in the immune system like the T-cell receptor (Kronenberg et al., 1986) are involved in highly specific cell-cell recognition events (Springer, 1990). In contrast to the molecules specialized for antigen recognition, the polypeptide chains constructed by Ig-modules in cell-recognition molecules do not form intermolecular disulfide bridges. Many, if not most cell-recognition molecules in the nervous system such as NCAM and L1 are composed not only by Ig-modules, but combine them with other repeated structures. One of these structures is the fibronectin repeat of the subtype III (FNIII-domain). This motif was originally identified as a 90-residue repeated module in the extracellular matrix (ECM) molecule fibronectin (Kornblihtt et al., 1985), and found later in other ECM proteins (Engel, 1991). Functional analysis of fibronectin revealed that FN-domains are involved in cell-ECM interactions (Ruoslahti and Pierschbacher, 1987). Studies on the ECM-molecules tenascin-C and tenascin-R mapped several functions of these molecules, like promotion of neurite outgrowth, to the subsets of their FN-repeats (Dörries et al., 1996; Xiao et al., 1996).

NCAM was the first Ig-like cell adhesion molecule to be isolated and characterized in detail (Brackenbury et al., 1977; Thiery et al., 1977). It forms the prototype of neural adhesion molecules of the Ig-superfamily. Figure 1 lists some of the members of the Ig superfamily that have been found in the nervous system. The extracellular domain of NCAM mediates various  $\text{Ca}^{2+}$  independent cell-cell and cell-extracellular matrix interactions, involved in proliferation, cell migration, neurite outgrowth, axon fasciculation, and synaptic remodeling (Rutishauser and Jessell, 1988; Doherty et al., 1990; Schachner, 1991; Doherty et al., 1992; Doherty and Walsh, 1992; Sporns et al., 1995; Jorgensen, 1995; Fields and Itoh, 1996; Cremer et al., 1997). NCAM shows homophilic binding with a high rate of cooperativity, so that a twofold increase in NCAM level can increase adhesiveness more than 30 fold (Hoffman and Edelman, 1983). In an heterophilic interaction, NCAM can bind heparin, a major component of the extracellular matrix (Cole et al., 1986a; Cole et al., 1986b; Cole and Glaser, 1986), and

soluble NCAM, derived from proteolytic cleavage near the membrane, can bind to collagen I-VI and IX (Probstmeier et al., 1989). Furthermore, NCAM assists homophilic binding of another cell recognition molecule (L1) in “cis” configuration, that is, on the same cell membrane (Kadmon et al., 1990a; Kadmon et al., 1990b). It has been shown that the unglycosylated core protein, and even single domains can perform many of the cell recognition functions of NCAM. When coated as substrates, the domains IgI and IgII mediate adhesion of neuronal cell bodies in vitro, and IgI, IgII and IgIV are involved in migration of cells from cerebellar explants. Substrate-coated FnII, and to a lesser extent also IgI-V domains promote neurite outgrowth.

Several NCAM proteins are encoded by a single gene. Diversity of NCAM proteins is generated at different levels, including transcriptional and posttranslational modifications. Three major isoforms are generated by alternative splicing of a primary transcript leading to translation of three proteins having apparent molecular masses of 120, 140 and 180 kD, designated NCAM120, NCAM140 and NCAM180, respectively (Cunningham et al., 1987). All three isoforms consist of an extracellular domain containing five Ig-domains and two FN-domains, which is anchored in the cell membrane via a phosphatidyl inositol (NCAM120) or connected via a transmembrane domain to the cytoplasmic domain (NCAM140 and NCAM180). The intracellular domain differs between NCAM140 and NCAM180 only by the presence of an additional 261 amino acid insert in the intracellular region of NCAM140 (see Fig. 1). Homologues with the same domain composition, biochemical and functional properties have been identified in rodents, chicken and human. Potential species homologues are fasciclin II in grasshopper and *Drosophila* and apCAM in *Aplysia* (reviewed by Brümmendorf and Rathjen, 1994).

The expression of alternatively spliced forms of NCAM, in terms of time and cell-type specificity, is differentially regulated (for review, see Jorgensen, 1995). NCAM120 was considered to be the predominant isoform in glial cells while the larger isoforms are expressed in neurons (Keilhauer et al., 1985). Later, others showed that NCAM120 is also the major isoform in sensory neurons of dorsal root ganglia (Rosen et al., 1992). However, the sub-cellular distribution of different isoforms seems to be regulated. NCAM140 is detectable on pre- and post-synaptic membranes, whereas NCAM180 accumulates in the postsynaptic densities of synapses of mature neurons (Persohn et al., 1989; Pollerberg et al., 1985). Both transmembrane isoforms are downregulated in aging rodents. Additional to the major splicing events leading to largely different protein isoforms, several splicing events of exons as small as one single amino acid lead to at least 18 different proteins (Santoni et al., 1989).

Several posttranslational modifications of NCAM proteins are known, such as phosphorylation of serine and threonine residues (Mackie et al., 1989) or palmitoylation of cysteine residues in the cytoplasmic domain and glycosidation of asparagines in the extracellular domain. The physiological relevance of these intracellular modifications has so far not been elucidated. As many neural recognition molecules and adhesion molecules of the immune system, NCAM can carry the HNK-1 carbohydrate epitope which contains sulfated glucuronic acid (Schachner and Martini, 1995). Outstanding of these modifications, however, are developmentally regulated and functionally significant alterations in the amount and distribution of  $\alpha$ -2, 8-linked polysialic acid (PSA), a carbohydrate not found to be associated with other proteins of vertebrate origin. All isoforms of NCAM can carry PSA as long linear polymer chains composed up to 200 sialic acid residues (Schachner and Martini, 1995), but PSA is restricted to NCAM180 in the hippocampus (Doyle et al., 1992).

The PSA-carbohydrate epitope seems to decrease the adhesive cues of NCAM and to increase its neurite outgrowth promoting features (Rutishauser, 1990). Since it is reduced generally in adulthood, but retained in areas with lifelong structural remodeling, the PSA carbohydrate epitope has been suspected to be involved in regenerative processes and synaptic plasticity (Becker et al., 1996; Doherty et al., 1995; Eckhardt et al., 2000; Muller et al., 1996; Regan and Fox, 1995).

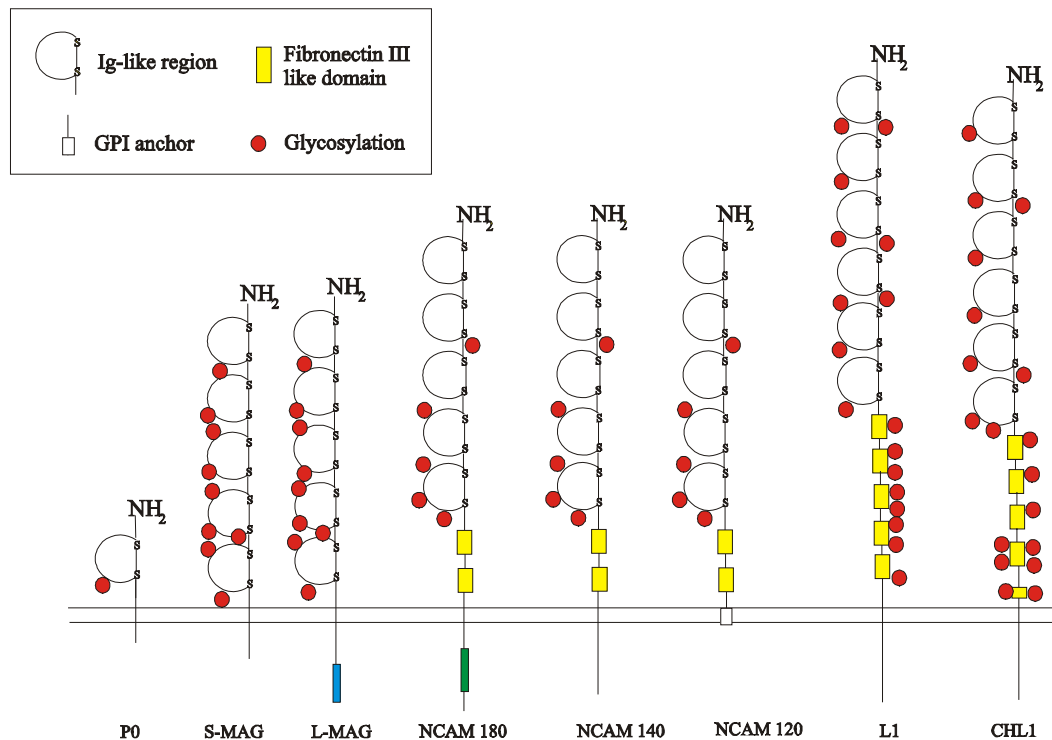


**Figure 1: Examples of members of the immunoglobulin superfamily.** Cell adhesion molecules belong to the Ig-superfamily. They consist of an extracellular domain with Ig-like domains and fibronectin type III repeats, a single transmembrane region or a GPI anchor and in most cases an intracellular domain.

## 1.1 NCAM deficient mice

In spite of its presumed role in CNS development, disruption of the NCAM gene in mice evokes only subtle morphological changes in the adult nervous system (Cremer et al., 1994; Cremer et al., 1997). The olfactory bulb of NCAM deficient mice (NCAM<sup>-/-</sup>) is reduced in size, probably as a result of disturbed cell migration. Similar observations have been reported for adult mice deficient for NCAM180 (Tomasiewicz et al., 1993) and for wild type mice treated with endoneuraminidase N to remove NCAM-associated polysialic acid (Ono et al., 1994), indicating that absence of PSA on migrating granule cells is a major factor for such abnormal development. Furthermore, disorganization of pyramidal cell layer in the hippocampal area CA3 and disorganized growth of mossy fiber bundles, with reduced fasciculation and quantitative reduction of mossy fibers and their terminals have been observed in NCAM<sup>-/-</sup> (Cremer et al., 1994; Cremer et al., 1997).

In addition to such altered morphology, behavioral changes are apparent in NCAM<sup>-/-</sup> mice. For instance, modest alteration of exploratory activity, deficits in special learning and strong increased intermale aggression have previously been observed (Cremer et al., 1994; Stork et al., 1997). Furthermore, NCAM<sup>-/-</sup> mice show increased anxiety-like behavior

compared to wild type mice that could be reduced by systemic administration of 5-HT<sub>1A</sub>-receptor agonists buspirone and 8-OH-DPAT. However, NCAM<sup>-/-</sup> mice showed anxiolytic-like effects at lower doses of buspirone and 8-OH-DPAT than wild type mice (Stork et al., 1999). Such increased response to 5-HT<sub>1A</sub>-receptor stimulation suggested a functional change in the serotonergic system of NCAM<sup>-/-</sup> mice, likely involved in the control of anxiety and aggression (for review, see Graeff et al., 1996). Nevertheless, 5-HT<sub>1A</sub>-receptor binding and tissue content of serotonin and its metabolite 5-hydroxy-indolacetic acid were found unaltered in every tested brain region of NCAM<sup>-/-</sup> mice indicating that affinity and expression of 5-HT<sub>1A</sub>-receptors as well as serotonin turnover are largely unchanged in NCAM<sup>-/-</sup> mice. Therefore, an involvement of NCAM in the serotonergic transmission via 5-HT<sub>1A</sub>-receptor and inwardly rectifying K<sup>+</sup> channels as the respective effector system was suggested (see Fig. 2 for schematic drawing).

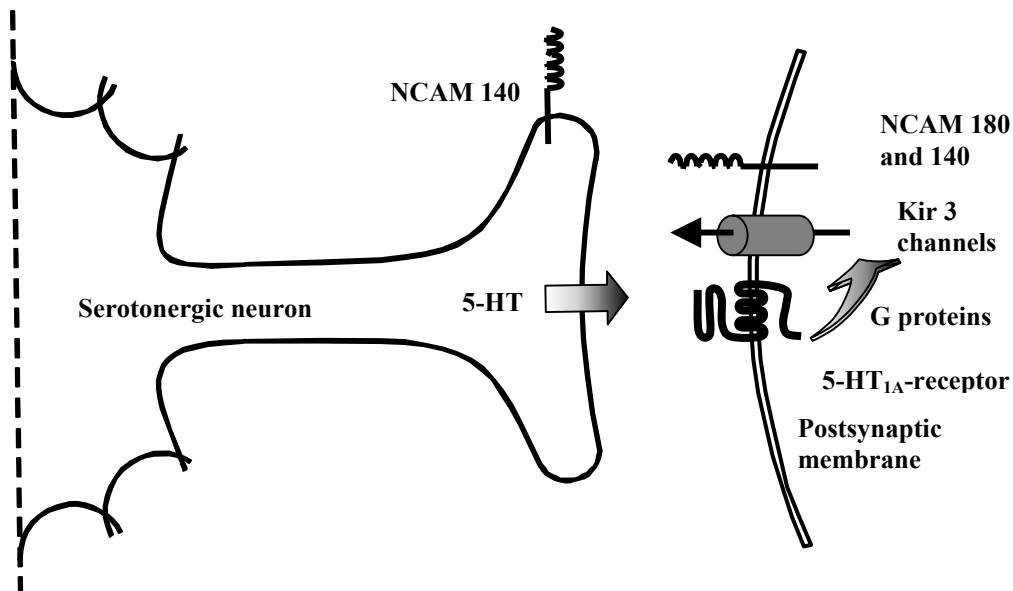


**Figure 2:** Schematic drawing of a serotonergic neuron demonstrating the localization of the 5-HT<sub>1A</sub> receptors, Kir3 channels and NCAM isoforms on the pre- and postsynapse. Serotonin is released into the synaptic cleft and stimulates 5-HT<sub>1A</sub> receptors, which in turn activate G proteins. The  $\beta\gamma$  subunits of the G proteins associate with the Kir3 potassium channels resulting in an opening of the K<sup>+</sup> channels. NCAM might influence this signaling system.

## 1.2 NCAM-mediated signal transduction

Neurite outgrowth is a major event in neural development being mediated by several members of the immunoglobulin superfamily of cell adhesion molecules, among them NCAM. Although NCAM plays a pivotal role in early brain development, synaptic plasticity, and memory consolidation (Ronn et al., 1998; Schachner, 1997; Murase and Schuman, 1999), NCAM-mediated signal-transduction has so far only been investigated extensively with respect to its ability to promote neurite outgrowth. NCAM-mediated neurite outgrowth is initiated upon homophilic or heterophilic engagement with other molecules on adjacent cell surfaces and in the extracellular matrix (for review see Crossin and Krushel, 2000). This implicates NCAM both as a ligand and a signal transducing receptor. Of the three major NCAM isoforms, all have been found to serve as neuritogenic ligands (Doherty et al., 1989; Doherty et al., 1990) due to their identical amino acid sequence of extracellular domains.

First attempts to elucidate the molecular events underlying NCAM mediated neuritogenesis have attributed a fundamental role to the fibroblast growth factor (FGF) receptor (Williams et al., 1995). Over-expression of a truncated FGF receptor-1 with a deleted kinase domain inhibited neurite outgrowth of PC12 cells when cultured on NCAM presenting fibroblasts (Saffell et al., 1997). The ability of NCAM to promote neurite outgrowth was therefore suggested to depend solely on the interaction between the extracellular domains of NCAM and the FGF receptor. Although there is no evidence for a direct interaction between NCAM and the FGF receptor, other mechanisms might function indirectly to dimerize and phosphorylate the FGF receptor, perhaps through NCAM clustering (Crossin and Krushel, 2000). According to this concept, the interaction of NCAM with the FGF receptor activates the receptor tyrosine kinase with subsequent activation of the receptors downstream signaling cascade, such as phospholipase C $\gamma$  (PLC $\gamma$ ). As a final consequence, increased Ca<sup>2+</sup> influx into the neurons results in neurite growth.

The view that the FGF receptor may not be the only mediator of NCAM-dependent signal transduction was indicated by data showing that NCAM-dependent neurite outgrowth is impaired in cultured neurons from mice deficient in the non-receptor tyrosine kinase *fyn*. Moreover, immunoprecipitation studies revealed an association of a minor portion of NCAM140 but not NCAM180 with *fyn* (Beggs et al., 1997). According to this model, NCAM clustering at the cell surface induces *fyn* phosphorylation with further recruitment of the focal adhesion kinase (FAK) to the NCAM/*fyn* complex. Activation of downstream kinases by this complex is then thought to be the initial step in NCAM-mediated neurite outgrowth. Although

the two signaling mechanisms would appear distinct at first sight, there are evidences that both pathways could be operant in cells expressing NCAM isoforms as receptors for neurite outgrowth (Kolkova et al., 2000a). Furthermore, NCAM stimulation has been shown to activate second-messenger cascades (Schuch et al., 1989) and to activate the transcription factor NF $\kappa$ B in cultured astrocytes and cerebellar neurons (Krushel et al., 1999). Both NCAM-mediated neurite outgrowth and NF $\kappa$ B activation could be partially blocked by the overexpression of an NCAM cytoplasmic domain construct (Kolkova et al., 2000b; Little et al., 2001). This finding indicated that the overexpressed domain exerted a dominant negative effect on NCAM-induced signal transduction and suggested that an intracellular interaction of this domain is involved in the signaling process. However, approaches to identify signaling proteins that interact with the intracellular domain of NCAM, such as the yeast two-hybrid system, failed so far.

### 1.3 NCAM-mediated modulation of potassium channels

So far, there are only a few reports which point towards a modulation of K<sup>+</sup> channels by NCAM and its homologues: Acute triggering of cultured glial precursor cells with NCAM antibodies induced a down-regulation of A-type and delayed rectifier amplitudes, an effect thought to be mediated by protein kinases such as protein kinase C (PKC) (Sontheimer et al., 1990). Another study identified FasII, the *Drosophila* homologue of NCAM, to cluster shaker potassium channels in the cell membrane via the intracellular linker protein discs-large (dlg). The shaker K<sup>+</sup> channel, which belong to the group of voltage-gated potassium channels, and FasII bind via their intracellular domains to Dlg, which mediates a co-localization of the two molecules. While the co-clustering with FasII does obviously not change single channel properties of the K<sup>+</sup> channel, the interaction is thought to be relevant for the structural organization of the synapse. However, this co-localization has not been observed for the mammalian homologues of fasII and dlg, namely NCAM and SAP-97 (Thomas et al., 1997).

## 2 Inwardly rectifying K<sup>+</sup> channels

The molecular nature of inwardly rectifying K<sup>+</sup> (Kir) channels was discovered in 1993, when the first two subunits (ROMK1/Kir1.1 and IRK1/Kir2.1) were cloned (Ho et al., 1993;

Kubo et al., 1993). Since then a large number of Kir proteins have been identified, and grouped in a  $K^+$  channel gene family, sharing a common feature of only two transmembrane segments in each of the four  $K^+$  channel subunits (Isomoto et al., 1997) (see Table 1 and Fig. 3).  $K^+$  channels formed out of Kir subunits elicit currents, which flow more readily in the inward direction than outward (Fakler et al., 1995) and are strongly modulated by intracellular factors and second messengers (Nichols and Lopatin, 1997; Ruppersberg, 2000; Ruppersberg and Fakler, 1996). These  $K^+$  channels play pivotal roles in maintenance of the resting membrane potential, in regulation of the action potential, in receptor-dependent inhibition of cellular excitability and in secretion and absorption of  $K^+$  ions across cell membrane. The best known examples of the physiological importance of Kir regulation are as follows: the ATP dependence of Kir6 channels in the control of insulin secretion (Ashcroft et al., 1984; Ashcroft and Rorsman, 1989) and the determination of myocardial resistance to hypoxia (Friedrich et al., 1990), the regulation of Kir3 channels by G-proteins to account for the vagal control of heart rate (Krapivinsky et al., 1995; Wickman and Clapham, 1995) and the regulation of Kir1 channels by intracellular  $K^+$  and pH, which controls  $K^+$  secretion in kidney (Wang et al., 1997).

Subfamilies	Subtypes	Chandy and Gutman's nomenclature
Classical inwardly rectifying $K^+$ channels	IRK 1, IRK2, IRK 3	Kir 2.1, Kir 2.2 Kir 2.3
G protein-activated $K^+$ channels	GIRK 1, GIRK 2 GIRK 3, GIRK4	Kir 3.1, Kir 3.2 Kir 3.3, Kir 3.4
ATP-sensitive $K^+$ channels	$uK_{ATP-1}$ , BIR	Kir 6.1 Kir 6.2
ATP-dependent $K^+$ channels	ROMK1 $K_{AB-2}$	Kir 1.1a Kir 4.1
Others	BIR9	Kir 5.1 Kir 7.1

**Table 1: Summary of the different Kir subunits, which have been identified so far.** The subunits can be subdivided into 4 different families, while two Kir5.1 and Kir7.1 cannot be accounted to a special family.

## 2.1 G protein-activated inwardly rectifying $K^+$ (Kir3) channels

In contrast to the constitutively active Kir1 and Kir2 groups, more than one subunit seems to be required to form a normal functional channel, thus Kir3 channels are normally

heterotetramers (Fig. 3). Kir3.1 alone does not produce functional channels when expressed in most cell lines tested (Chan et al., 1996b) and is not delivered to the cell membrane when transfected alone into oocytes (Stevens et al., 1997). Kir3.2 and Kir3.4 alone form G gated channels in various heterologous expression systems, but with rather aberrant single channel properties. The presence of Kir3.1 corrects the single channel properties to yield open times and amplitudes similar to those observed in cardiac and nerve cells (Lesage et al., 1995). The Kir3.1 subunit co-purifies with Kir3.2 and Kir3.4 (Chan et al., 1996a; Lesage et al., 1995) and has been shown by electrophysiological assays in heterologous expression systems to form functional channels with all other Kir3 subunits (for reviews see Mark and Herlitze, 2000; Isomoto et al., 1997). However, there are also studies reporting of functional Kir3.2 homomers and Kir3.2/3.3 combinations (Inanobe et al., 1999; Jelacic et al., 2000; Wischmeyer et al., 1997). Kir3.1, Kir3.2 and Kir3.3 subunits are abundantly expressed in several brain areas (Karschin and Karschin, 1997) and Kir3.1/3.2 and Kir3.1/3.3 channels are believed to be the main functional Kir3 combinations in the brain (Lüscher et al., 1997; Kofuji et al., 1995). In contrast, Kir3.4 subunits are mainly expressed in the heart (Karschin and Karschin, 1997) and form together with the Kir3.1 subunit the atrial K(ACh) channels. These channels are activated by acetylcholine via the muscarinic m2 receptor and are involved in slowing the heart rate (Mark and Herlitze, 2000). Thus, the Kir3.1/3.2 and Kir3.1/3.3 channels are commonly referred to as the neuronal Kir3 channels, whereas the Kir3.1/3.4 channel is depicted as the cardiac Kir3 channel.

The main stimulatory effect on Kir3 channels is caused by the  $G_{\beta\gamma}$  subunit of the heterotrimeric G-protein that binds to Kir3 channels and activates them (Huang et al., 1995; Slesinger et al., 1995; Wickman and Clapham, 1995). Inhibition of Kir3 channels by  $G_{\alpha}$  has also been described (Slesinger et al., 1995) but seems to be less potent than activation by  $G_{\beta\gamma}$  molecules. Microclusters in which Kir channels,  $G_{\alpha}$  subunits and receptors are bound to each other to form complexes may explain why, in several types of cells, Kir3 channels are opened only by particular receptors (e.g. M2-receptors but not  $\beta$ 1-receptors regulate Kir in atrial myocytes), even though Kir channels show no specificity for particular  $G_{\beta\gamma}$  subunits of certain G-protein subtypes.

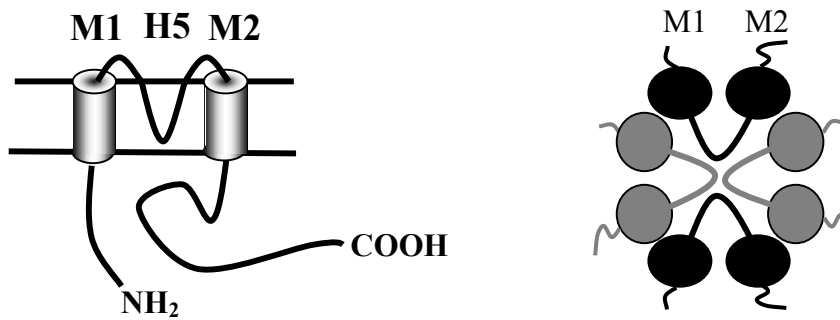


**Figure 3: Schematic drawing of a Kir subunit.** A: All Kir subunits consist of two transmembrane regions (M1 and M2) and a pore forming region (H5). Both the NH<sub>2</sub>- and the COOH-terminus are located intracellularly. B: hypothetical model of a functional Kir3 channel. The vast majority of Kir3 channels forms heterotetramers consisting of two Kir3.1 subunits and two variable subunits.

## 2.2 Modulation of Kir channels by phosphorylation

Protein kinase A and protein kinase C as well as tyrosine kinases, such as src kinase, regulate almost all kinds of ion channels. For the Kir channels, the effects of such kinases on K<sup>+</sup> current amplitude have been observed by many authors (Cohen et al., 1996; DiMagno et al., 1996; Fakler et al., 1994; Henry et al., 1996; McNicholas et al., 1994; Wischmeyer and Karschin, 1996). Some of these effects, such as current stimulation by activation of PKA, are common to all members of the Kir family and are not correlated to a particular phosphorylation site in the primary sequences. This may be because of the influence of kinases on other regulatory pathways, such as the phosphatidylinositol phosphate pathway. Other effects are highly subunit specific, such as the effect of PKC on Kir2.3 (Henry et al., 1996) and the nerve growth factor receptor-mediated tyrosine phosphorylation of the Kir2.1 subunit (Wischmeyer et al., 1998). Defined sites for phosphorylation in the C-terminal end of Kir2.1 and Kir2.3 (Cohen et al., 1996) have been confirmed biochemically. The interaction of these channels with PDZ domain-carrying proteins, such as PSD95, is thought to be regulated by this C-terminal phosphorylation site (Cohen et al., 1996). Implications of tyrosine phosphorylation for Kir3 channel function have so far only been reported for the Kir3.1/3.4 channel: TrkB stimulation resulted in tyrosine phosphorylation of the Kir3.4 subunit and thus in a strong inhibition of the basal activity of the channel (Rogalski et al., 2000).

### 2.3 Modulation of Kir channels by other proteins

$\beta$ -subunits that co-assemble with the pore forming  $\alpha$ -subunits and thus function as a regulatory subunits have been identified in almost all classes of ion channels. Among Kir channels, so far only Kir6 seems to have such an additional subunit, the sulphonylurea receptor: SUR1a, b and SUR2 (Babenko et al., 1998). It is presently assumed that the stimulatory effects of dinucleotides such as ADP are mediated by the SUR subunit (Gribble et al., 1997). The SUR subunit of ATP-sensitive  $K^+$  channels is thought to associate in a stoichiometry of one to one with the Kir6.2 subunit, forming a channel complex that consists of eight subunits in total (Aguilar-Bryan et al., 1998; Babenko et al., 1998). Both subunits have strong functional interactions: the SUR subunit mediates the sensitivity of Kir6 channels to stimulation by intracellular MgADP (Gribble et al., 1997; Hibino et al., 1997). The assembly of SUR and Kir6 channels is regulated by a sequence motif (arginine-lysine-arginine; RKR) in the C-termini of both SUR and Kir6.2 which inhibits the transport of these  $K^+$  ATP channel subunits to the surface membrane as long as they are not associated with each other (Zerangue et al., 1999).

A further protein-based regulation of Kir channels is the interaction of Kir3 channels with heterotrimeric GTP-binding proteins. So far, little is known about how interacting proteins, such as  $\beta$ -subunits or G-protein subunits, regulate Kir3 channels. Therefore, the published mechanistic models are rather speculative. It is presently assumed that  $G_{\beta\gamma}$  causes the opening of Kir3 channels primarily by binding to a C-terminal domain in the Kir3.1 subunit (Huang et al., 1995; Krapivinsky et al., 1998). An interaction with the N-terminus has also been discussed (Huang et al., 1997; Krapivinsky et al., 1998).  $G_{\alpha}$  probably associates with the N-terminus of the Kir3 channel subunit, perhaps while it is bound to the seven-membrane spanning receptor (Slesinger et al., 1995).

### 2.4 Regulation of postsynaptic neural excitability by Kir3 channels

Kir3 channels are coupled to several pertussis-sensitive G protein coupled receptors (GPCRs) in brain including opioid, adrenergic, muscarinic, dopaminergic and  $GABA_B$  receptors and are important for maintaining the resting potential and excitability of neurons (Hille, 1992). Disruption of this  $K^+$  channel could affect the signal transduction of several pathways in the CNS. The weaver (wv) mouse is the first neurological abnormality directly

linked to a genetic point mutation in the Kir3.2 protein. Homozygous *wv* mice were first characterized by their abnormal “weaving” when they walk, hence the name weaver which is due to a substantial loss of cerebellar granule neurons (Hess, 1996). This weaver mutation is the result of a Gly to Ser exchange in the highly conserved K<sup>+</sup> selectivity sequence, GYG. The mutant channel was also no longer inhibited by specific K<sup>+</sup> channel antagonists but could be blocked with the cation channel inhibitors verapamil, MK-801 and QX-314 (Kofuji et al., 1996). Similar properties were also exhibited with cultured *wv* granule cells. Mutant *wv* cerebellar neurons appeared to be leaky to Na<sup>+</sup>, chronically depolarized, unresponsive to neurotransmitters (Kofuji et al., 1996) and to have elevated intracellular Ca<sup>2+</sup> levels (Harkins et al., 2000). In 1997, Signorini et al. (1997) generated mutant mice lacking Kir3.2. Homozygous mice (-/-) were morphologically indistinguishable from their wild-type littermates (+/+) but displayed a dramatic decrease in Kir3.1 and Kir3.2 expression, an indication that Kir3.2, like Kir3.4, controls Kir3.1 expression, assembly and/or surface localization to a Kir3 heteromer and is involved in control of neural excitability (Kennedy et al., 1999; Liao et al., 1996; Signorini et al., 1997). To further investigate the importance of Kir3 channels in neural excitability, presynaptic and postsynaptic K<sup>+</sup> conductances were recorded from the hippocampal slices of Kir3.2 deficient mice. As Kir3.2 was previously shown to be predominantly in the dendrites of pyramidal cells (Drake et al., 1997), it was not surprising that stimulation of GPCRs by application of GABA<sub>B</sub>, adenosine A1 or 5HT<sub>1A</sub> failed to elicit postsynaptic K<sup>+</sup> currents from Kir3.2-deficient hippocampal neurons (Lüscher et al., 1997). Normal presynaptic inhibition of excitatory and inhibitory postsynaptic currents was detected in Kir3.2-deficient mice indicating that Kir3.2 is important for the modulation of postsynaptic but not presynaptic transmitter actions in hippocampal neurons.

## II Aim of the study

Mice deficient in the neural cell adhesion molecule NCAM show an increased anxiety-like behavior and an increased sensitivity of the 5-HT<sub>1A</sub> receptor to its agonists 8-hydroxydipropylaminotetralin (8-OH-DPAT) and buspirone (Stork et al., 1999). From these results, an interdependence of the 5-HT<sub>1A</sub> receptor system and NCAM and/or a convergence of their downstream signaling mechanisms was suggested. However, previous studies revealed that the 5-HT<sub>1A</sub> receptor itself is obviously not affected by NCAM at least in terms of its affinity and distribution in brain slices.

By this study, the question was addressed whether NCAM has a possible influence on the 5-HT<sub>1A</sub> receptor effector systems. G protein-coupled inwardly rectifying K<sup>+</sup> (Kir3) channels are the main targets of 5-HT<sub>1A</sub> receptors in the hippocampus. This study therefore focused on the question whether NCAM affects either directly or indirectly the Kir3 potassium channels by using biochemical, molecular biological and electrophysiological methods. Beyond that question, the putative signaling mechanisms were investigated by which NCAM might regulate these K<sup>+</sup> channels. For this purpose, combinations of the major NCAM isoforms, Kir3 channel subunits and the 5-HT<sub>1A</sub> receptor were co-expressed in the heterologous expression systems of oocytes and CHO cells and tested by various assay systems for a modulatory interplay between the main NCAM isoforms and Kir3 channels.

## III Material

### 1 Chemicals

All chemicals were obtained from the following companies in p.a. quality: GibcoBRL (Life technologies, Karlsruhe, Germany), Macherey-Nagel (Düren, Germany), Merck (Darmstadt, Germany), Serva (Heidelberg, Germany) and Sigma-Aldrich (Deisenhofen, Germany).

Restriction enzymes were obtained from New England Biolabs (Frankfurt am Main, Germany) and MBI Fermentas (St. Leon-Rot, Germany), molecular weight standards were obtained from Gibco. DNA Purification kits were purchased from Life Technologies (Karlsruhe, Germany), Pharmacia Biotech (Freiburg, Germany), Macherey & Nagel and Qiagen (Hilden, Germany). Plasmids and molecular cloning reagents were obtained from Clontech (Heidelberg, Germany), Invitrogen (Groningen, The Netherlands), Pharmacia Biotech, Promega (Mannheim, Germany), Qiagen and Stratagene (La Jolla, California, USA). Oligonucleotides were ordered from metabion (Munich, Germany). All oligonucleotides used are listed in the appendix. Cell culture material was ordered from Nunc (Roskilde, Denmark) or Life Technologies.

### 2 Solutions and buffers

(in alphabetical order)

Antibody buffer	0.3	% (w/v)	BSA in PBS pH 7,4
<i>(Immunocytochemistry)</i>	0.02	% (w/v)	Triton X-100
Blocking buffer	3	% (w/v)	BSA in PBS pH 7,4
<i>(Immunocytochemistry)</i>	0.2	% (w/v)	Triton X-100
Blocking buffer	1-4	% (w/v)	instant milk powder in TBS
<i>(Western Blot)</i>	or	1	% (v/v)
			block solution (boehringer) in TBS
Blotting buffer	25	mM	Tris

<i>(Western Blot)</i>	192	mM	Glycin
Boston buffer	50	mM	Tris, pH 8
<i>(lysis of Bacteria)</i>	1	% (w/v)	Triton X-100
	50	mM	KCl
	2.5	mM	EDTA
Citrate buffer (2x)	150	mM	Sodiumcitrate, pH5.5
<i>(EndoH digestion)</i>			
DNA-sample buffer (5x)	20	% (w/v)	glycerol in TAE buffer
<i>(DNA-gels)</i>	0,025	% (w/v)	orange G
dNTP-stock solutions	20	mM	each dATP, dCTP, dGTP, dTTP
<i>(PCR)</i>			
Ethidiumbromide-staining solution	10	µg/ml	ethidiumbromide in 1xTAE
<i>(DNA-gels)</i>			
Hypotonic lysis buffer	10	mM	HEPES, pH 7.4
<i>(cell lysis)</i>	0.5	mM	EDTA
Ligation buffer (10x)	200	mM	Tris-HCl, pH 7,9
	100	mM	MgCl <sub>2</sub>
	100	mM	Dithiothreitol (DTT)
	6	mM	ATP
Native lysis buffer	50	mM	NaH <sub>2</sub> PO <sub>4</sub> , pH 8.0
<i>(bacterial lysis)</i>	300	mM	NaCl

	10	mM	imidazole
NT-buffer	150	mM	NaCl
<i>(surface biotinylation)</i>	0,5	mM	CaCl <sub>2</sub> ,
	2	mM	MgCl <sub>2</sub> ,
	0.2	%	BSA
	20	mM	TABS, pH 8.6
Phosphate buffered saline (PBS)	150	mM	NaCl
	20	mM	Na <sub>3</sub> PO <sub>4</sub> pH 7.4
Phosphate buffered saline with Ca <sup>2+</sup> , Mg <sup>2+</sup> (PBSCM)	150	mM	NaCl
	20	mM	Na <sub>3</sub> PO <sub>4</sub> pH 7.4
	0.2	mM	CaCl <sub>2</sub>
	2	mM	MgCl <sub>2</sub>
Protease-inhibitors	COMPLETE™ pills. resuspending 1 tablet in 2 ml solution results in a 25xstock solution		
RIPA-buffer	50	mM	Tris-HCl, pH 7.4
<i>(cell lysis)</i>	1	% (w/v)	Triton X-100
	150	mM	NaCl
	1	mM	EGTA
	1	mM	Na <sub>3</sub> VO <sub>4</sub>
Running Gel 10% (8%)	3.92	ml (4.89 ml)	deionized water
<i>(protein gels)</i>	5.26	ml (5.26 ml)	1 M Tris pH 8.8
	0.14	ml (0.14 ml)	10% SDS
	4.70	ml (3.73 ml)	30% Acrylamide – Bis 29:1
	70.0	µl (70 µl)	10% APS
	7.00	µl (7 µl)	TEMED
Sample buffer (5x)	0.312	M	Tris-HCl pH 6.8

<i>(protein-gels)</i>	10	% (w/v)	SDS
	5	% (w/v)	β-Mercaptoethanol
	50	% (v/v)	Glycerol
	0.13	% (w/v)	Bromphenol blue
SDS running buffer (10x)	0.25	M	Tris-HCl, pH 8.3
<i>(protein-gels)</i>	1.92	M	glycine
	1	M	SDS
Stacking Gel 5%	3.77	ml	deionized water
<i>(protein gels)</i>	0.32	ml	1 M Tris pH 6.8
	0.05	ml	10% SDS
	0.83	ml	30% Acrylamide – Bis 29:1
	25.0	μl	10% APS
	7.00	μl	TEMED
Staining solution	40	% (v/v)	ethanol
<i>(Protein-gels)</i>	10	% (v/v)	acetic acid
	0,1	% (w/v)	Serva Blue R250
Stripping buffer	0.5	M	NaCl
<i>(Western blots)</i>	0.5	M	acetic acid
TAE (50x)	2	M	Tris-Acetat, pH 8,0
<i>(DNA-gels)</i>	100	mM	EDTA
TE (10x)	0,1	M	Tris-HCl, pH 7,5
	10	mM	EDTA
TNE-buffer, pH 7.4	25	mM	Tris-HCl, pH 7.5
<i>(lipid raft isolation)</i>	150	mM	NaCl
	5	mM	EDTA
	COMPLETE		

	0-80	% (w/v)	sucrose
TNE-buffer, pH 11	25	mM	Tris-HCl, pH 11
<i>(lipid raft isolation)</i>	150	mM	NaCl
	5	mM	EDTA
	COMPLETE		
	0-80	% (w/v)	sucrose
	0.1	M	Na <sub>2</sub> CO <sub>3</sub> until pH was adjusted to 1
Tris Buffered Saline (TBS)	10	mM	Tris-HCl, pH 8.0
	150	mM	NaCl

### 3 Bacterial media

(Media were autoclaved and antibiotics were supplemented prior to use)

LB-medium	10	g/l	Bacto-tryptone, pH 7,4
	10	g/l	NaCl
	5	g/l	yeast extract
LB/Amp-medium	100	mg/l	ampicillin in LB-Medium
LB/Amp-plates	20	g/l	agar in LB-Medium
	100	mg/l	ampicillin
LB/Amp/Kana-medium	20	g/l	agar in LB-Medium
	100	mg/l	ampicillin
	25	mg/l	kanamycin
LB/Tet-plates	20	g/l	agar in LB-Medium
	25	mg/l	tetracycline

#### 4 Bacterial strains and cell lines

CHO-K1 *Chinese Hamster Ovary*

N<sub>2</sub>A Mouse neuroblastoma cell line  
Origin: Established from the spontaneous tumor of a strain A albino

*Escherichia coli* DH5 $\alpha$  NEB

*Escherichia coli* M15pREP4 QIAGEN

*Escherichia coli* BL21(DE3) Novagene

*Escherichia coli* XL1-Blue Stratagene

#### 5 Cell culture media

Media were prepared from a 10X stock solution purchased from Gibco GBL

CHO-cell Medium Glasgow MEM (GMEM) (with nucleotides, L-Glutamine)  
supplemented with  
10 % (v/v) fetal calf serum (FCS)  
50 U/ml Penicilline/Streptomycine  
4 mM L-Glutamine

N<sub>2</sub>A-cell Medium Dulbecco MEM (DMEM)  
supplemented with  
10 % (v/v) fetal calf serum (FCS)  
50 U/ml Penicilline/Streptomycine

1 mM Pyruvate

Versene Gibco GBL

## 6 Molecular weight standards

1kb DNA ladder 14 bands within the range from 200-10000 bp  
(Gibco)

BenchMark™ 6 µl of the *BenchMark Prestained Protein Ladder* (Life Technologies) were loaded on the SDS-PAGE gel.

Band No.	apparent molecular weight (kDa)
1	195.9
2	125.6
3	89.4
4	64.9*
5	52.8
6	39.8
7	27.7
8	21.8
9	16.2
10	9.0

\*Orientation band (pink in color)

## 7 Plasmids

<i>pBluescript KS<sup>+</sup></i>	plasmid used for cloning and blue/white selection on X-gal containing plates. Amp-resistance (Stratagene)
psGEM	RNA-transcription plasmid. Contains 5' and 3' untranslated regions of the $\beta$ -Globine gene. Amp-resistance
pQE30	prokaryotic expression plasmid for recombinant expression of proteins. carrying a polyhistidine-domain (6xHis) at the 5' end of the multiple cloning site for purification. Amp-resistance (Qiagen)
pcDNA3	mammalian expression vector for transfection. Amp-resistance (Invitrogen)
pcDNA3.1Myc-HisA,B,C	mammalian expression vector containing a His- and a myc tag at the 3' end of the multiple cloning site. Amp-resistance (Invitrogen)
EGFP	Mammalian expression plasmid encoding for the enhanced green fluorescent protein. Kanamycin-resistance (Clontech)
pDsRed	Mammalian expression plasmid encoding for the red fluorescent protein. Kanamycine-resistance (Clontech)

## 8 Antibodies

### 8.1 Primary antibodies

anti-c-myc	mouse monoclonal antibody clone 9E10. Raised against the epitope EQKLISEEDLN (Santa Cruz) IB: 1:1000 (2% milk in TBS)
anti Kir3.1	polyclonal Kir3.1 antibody derived from a peptide encoding for the C-terminus of Kir3.1. (obtained from R. Veh, Berlin) IB: 1:1000 (1% milk in TBS) IH: 1:50
anti-NCAM	polyclonal antibody derived from the extracellular domain of mouse NCAM-Fact (produced in the lab of M. Schachner) IB: 1:5000 (4% milk in TBS) ICH: 1:800
P61	monoclonal antibody produced against the C-terminus of the intracellular domain of NCAM140 and NCAM180 IB: 1:10 (supernatant in 2% milk/TBS)
anti-flag	mouse monoclonal antibody M2 (Sigma) Recognizes the DYKDDDDK motif both terminally and intracellularly of the protein IH: 1:100
anti-MAP kinase, activated	mouse monoclonal antibody recognizes the diphosphorylated ERK-1&2 (Sigma) IB: 1:10000 (1% Boehringer block solution)

anti-phosphotyrosine	mouse monoclonal antibody, clone 4G10 (Upstate) IB: 1:5000 (1% milk in TBS)
anti-fyn	rabbit polyclonal antibody (Santa Cruz) IB: 1:1000 (2% milk in TBS)
anti-FAK	rabbit polyclonal antibody (Santa Cruz) IB: 1:1000 (2% milk in TBS)
Anti-Penta His	mouse monoclonal antibody, recognizes the 5xHis epitope (Qiagen) IB: 1:2000 (2% milk in TBS)

## 8.2 Secondary antibodies

All horseradish-coupled secondary antibodies were purchased from dianova (Hamburg, Germany) and used in a dilution of 1:10,000.

For immunocytochemistry, Cy3, Cy5, Fitc and Tritc-labeled secondary antibodies were obtained from dianova and used in a dilution of 1:200.

## IV Methods

### 1 Molecular biology

#### 1.1 Bacterial strains

##### 1.1.1 Maintenance of bacterial strains

(Sambrook et al., 1989)

Strains were stored as glycerol stocks (LB-medium, 25% (v/v) glycerol) at  $-70^{\circ}\text{C}$ .

An aliquot of the stock was streaked on an LB-plate containing the appropriate antibiotics and incubated overnight at  $37^{\circ}\text{C}$ . Plates were stored up to 6 weeks at  $4^{\circ}\text{C}$ .

##### 1.1.2 Production of competent bacteria

(Inoue et al., 1990)

DH5 $\alpha$  or XL1-Blue bacteria were streaked on LB-plates and grown overnight at  $37^{\circ}\text{C}$ . 50 ml of LB-medium was inoculated with 5 colonies and grown at  $37^{\circ}\text{C}$  until the culture had reached an optical density ( $\text{OD}_{600}$ ) of 0,3-0,5.

##### 1.1.3 Transformation of bacteria

(Sambrook et al., 1989)

To 100  $\mu\text{l}$  of competent XL1-Blue or DH5 $\alpha$  either 50-100 ng of plasmid DNA or 20  $\mu\text{l}$  of ligation mixture were added and incubated for 30 min on ice. After a heat shock (2 min,  $42^{\circ}\text{C}$ ) and successive incubation on ice (3 min), 800  $\mu\text{l}$  of LB-medium were added to the bacteria and incubated at  $37^{\circ}\text{C}$  for 30 min. Cells were then centrifuged (10000 x g, 1 min, RT) and the supernatant removed. Cells were resuspended 100  $\mu\text{l}$  LB medium and plated on LB plates containing the appropriate antibiotics. Plates were incubated at  $37^{\circ}\text{C}$  overnight.

## **1.2 Plasmid isolation of E. coli**

### **1.2.1 Plasmid isolation from 3 ml cultures (Minipreps)**

(see Sambrook et al., 1989 and Amersham Pharmacia Mini preparation kit)

3 ml LB/Amp-Medium (100 µg/ml ampicillin) were inoculated with a single colony and incubated over night at 37°C with constant agitation. Cultures were transferred into 2 ml Eppendorf tubes and cells were pelleted by centrifugation (12,000 rpm, 1min, RT). Plasmids were isolated from the bacteria according to the manufactures protocol. The DNA was eluted from the columns by addition of 50 µl Tris-HCl (10 mM, pH 8.0) with subsequent centrifugation (12,000 rpm, 2 min, RT).

### **1.2.2 Plasmid isolation from 15 ml-cultures**

(see Macherey-Nagel Nucleospin kit)

To obtain rapidly higher amounts of DNA, the Macherey-Nagel Nucleospin kit was used. 15 ml LB/Amp-Medium (100 µg/ml ampicillin) were inoculated with a single colony and incubated over night at 37°C with constant agitation. Cultures were transferred into 15 ml Falcon tubes and cells were pelleted by centrifugation (12,000 rpm, 1min, RT) in an eppendorf centrifuge. Plasmids were isolated from the bacteria according to the manufactures protocol with the exception that twice the suggested amount of buffers were used. DNA was eluted from the columns by adding twice 50 µl of prewarmed (70°C) TrisHCl (10 mM, pH 8.0) with subsequent centrifugation (12,000 rpm, 2 min, RT). Finally, the concentration was determined.

### **1.2.3 Plasmid isolation from 500 ml-cultures (Maxipreps)**

(see Qiagen Maxiprep kit)

For preparation of large quantities of DNA, the Qiagen Maxiprep kit was used. A single colony was inoculated in 2 ml LB/amp (100 µg/ml ampicillin) medium and grown at 37°C for 8 h with constant agitation. Afterwards, this culture was added to 500ml LB/amp medium (100 µg/ml ampicillin) and the culture was incubated at 37°C with constant agitation

overnight. Cells were pelleted in a Beckmann centrifuge (6,000g, 15 min, 4°C) and DNA was isolated as described in the manufactures protocol. Finally, the DNA pellet was resuspended in 600 µl of prewarmed (70°C) Tris-HCl (10 mM, pH 8.0) and the DNA concentration was determined.

### **1.3 Enzymatic modification of DNA**

#### **1.3.1 Digestion of DNA**

(Sambrook et al., 1989)

For restriction, the DNA was incubated with twice the recommended amount of appropriate enzymes in the recommended buffer for 2 h. Restriction was terminated by addition of sample buffer and applied on a agarose gel. If two enzymes were incompatible with each other, the DNA was digested successively with the enzymes. The DNA was purified between the two digestions using the rapid purification kit (Life technologies).

#### **1.3.2 Dephosphorylation of Plasmid-DNA**

(Sambrook et al., 1989)

After restriction the plasmid DNA was purified and SAP buffer (Boehringer Ingelheim) and 1 U SAP (s<sub>crim</sub>p<sub>s</sub> a<sub>l</sub>kine p<sub>h</sub>osphatase) per 100 ng plasmid DNA were added. The reaction was incubated at 37°C for 2 h and terminated by incubation at 70°C for 10 min. The plasmid DNA was used for ligation without further purification.

### 1.3.3 Polishing of sticky ends

(Sambrook et al., 1989)

Non-compatible sticky ends were blunted for ligation using Klenow enzyme. After purification of the DNA fragments, 125  $\mu$ M dNTPs and Klenow buffer (Boehringer) were added to the reaction volume. The Klenow-enzyme was added (1 U, 30 min, RT) and the reaction was terminated by incubation at 70°C for 10 min. The fragments were used for ligation without further purification.

### 1.3.4 Ligation of DNA-fragments

(Sambrook et al., 1989)

Ligation of DNA fragments was performed by mixing 50 ng vector DNA with the fivefold molar excess of insert DNA. 1  $\mu$ l of T4-Ligase and 2  $\mu$ l of ligation buffer were added and the reaction mix was brought to a final volume of 20  $\mu$ l. The reaction was incubated either for 2 h at room temperature or overnight at 16°C. The reaction mixture was used directly for transformation without any further purification.

## 1.4 Polymerase chain reaction (PCR)

### 1.4.1 Standard PCR

(Saiki et al., 1988)

Amplification of DNA fragments was performed in a 50  $\mu$ l reaction mix with thin-walled PCR tubes in MWG-PCR cyclers. *Turbo-Pfu*-Polymerase and the appropriate reaction buffer were obtained from Stratagene. The following reaction mixture was used:

Template	2-10 ng
Primer 1 (10pM)	1 $\mu$ l
Primer 2 (10pM)	1 $\mu$ l
Nucleotides (dNTPs) (20 mM)	1 $\mu$ l

PCR-buffer (10 x)	5 µl
<i>Turbo-pfu</i> - Polymerase	2,5 U
ddH <sub>2</sub> O	ad 50 µl

The PCR was performed with the following step gradient:

1) Initial denaturing	94°C	1 min
2) Denaturing	94°C	1 min
3) Annealing	T <sub>m</sub> -4°C	1 min
4) Synthesis	72°C	1 min/ 1kb DNA
5) Termination	72°C	10 min
6) Cooling	4°C	

The amplification procedure (steps 2-4) was repeated 30 times.

The melting temperature of the primers depends on the GC content and was calculated by the following formula:

$$T_m = 4 \times (G+C) + 2 \times (A+T)$$

If the two primers had different melting temperatures, the lower of both was used. Afterwards, the quality of the PCR product was monitored by gel electrophoresis and the PCR product was purified with the rapid PCR purification kit (III 1.7).

#### 1.4.2 Site-directed mutagenesis

(Quikchange Site-directed mutagenesis kit, Stratagene)

For mutation of single amino acids within a DNA fragment, the Quikchange Site-directed mutagenesis kit (Stratagene) was used. For detailed information, see the manufactures instruction.

In brief, primers were designed such that:

- 1) they contain the desired mutation and anneal to the same sequence on opposite strands of the plasmid.
- 2) the primers have a length between 25 and 45 bases and the melting temperature was greater than 78°C.
- 3) the desired mutation (deletion or insertion) was in the middle of the primer with 10~15 bases of correct sequence on both sites.

During PCR reaction, it is important to keep primer concentrations in excess. Therefore, the amount of template was varied while primer concentrations were kept constant.

The reaction mixture was prepared as followed with 4 different template concentrations:

Template	5, 10, 20, 50 ng
Mutation-Primer 1 (10 pM)	1 µl
Mutation-Primer 2 (10 pM)	1 µl
Nucleotides (dNTPs) (20 mM)	1 µl
PCR-buffer (10 x)	5 µl
<i>Turbo-pfu</i> - Polymerase	1 µl (2,5 U)
ddH <sub>2</sub> O	ad 50 µl

The following step gradient was applied for mutagenesis:

1) Initial denaturing	94°C	30 sec
2) Denaturing	94°C	30 sec
3) Annealing	55°C	1 min
4) Synthesis	72°C	2 min/ 1kb DNA
5) Cooling	4°C	

The number of cycles (steps 2-4) was set to 18 to minimize undesired mutations. For determining the length of step 4, the sizes of the insert and the plasmid have to be taken into account. After PCR reaction, 10 µl of the mixtures were applied on an agarose gel to check for sufficient amplification. The template DNA (e.g. non mutated DNA) in the amplification reaction was digested by adding 1 µl of Dpn I restriction enzyme directly into the amplification reaction with subsequent incubation for 1h at 37°C. Afterwards, the

amplification reaction was transformed into competent XL1-Blue bacteria as described. Single colonies were picked from the plate and inoculated into 3 ml cultures. Plasmid DNA was prepared and mutation was verified by sequencing.

### 1.4.3 Single Colony PCR

To screen a large amount of bacterial colonies for the desired insert, single colonies were picked from a transformation plate with a sterile tooth picker and dotted on a new LB plate. The rest of the colony on the tooth picker was lysed in 70  $\mu$ l boston buffer. 10  $\mu$ l of this lysate were used as a template for a PCR with the appropriate primers to test for the presence of the desired insert. In case of a positive result, a 3 ml culture was inoculated with the colony dotted on the LB-plate.

### 1.4.4 Splicing by overlap extension (SOE) PCR

(Retzer et al., 1996)

Partial substitution of the Kir3.2 NH<sub>2</sub>-terminus by the corresponding Kir3.4 sequence was performed by splicing by overlap extension (SOEing). In principle, a short stretch of the Kir3.4 N-terminus was amplified by PCR using a primer that partially overlapped both with a sequence within the Kir3.2 and Kir3.4 sequence at the exchange position. The initial PCR product was obtained with the standard PCR protocol (see III 1.4.1). The PCR product was purified by agarose gel electrophoresis (III 1.6) and the final concentration was determined (III 1.8). The purified PCR product was used as a primer in the subsequent SOE with 4 different concentrations to yield the hybrid product. The reaction mixture was designed as follows:

Template Kir3.2 cDNA	10 ng
Primer 1 (PCR product 15ng/ $\mu$ l)	1, 3, 6, 10 $\mu$ l
Primer 2 (10pM)	1 $\mu$ l
Nucleotides (dNTPs) (20 mM)	1 $\mu$ l
PCR-buffer (10 x)	5 $\mu$ l
<i>Turbo-pfu</i> - Polymerase	2,5 U



## **1.6 Extraction of DNA fragments from agarose gels**

(Rapid gel extraction kit, Life technologies)

For isolation and purification of DNA fragments from agarose gels, ethidiumbromide-stained gels were illuminated with UV-light and the appropriate DNA band was excised from the gel with a clean scalpel and transferred into an Eppendorf tube. The fragment was isolated following the manufactures protocol. The fragment was eluted from the column by addition of 50  $\mu$ l prewarmed (70°C) Tris-HCl (10 mM, pH 8.0). The DNA-concentration was determined using the undiluted eluate.

## **1.7 Purification of DNA fragments**

(Rapid PCR Purification kit, Life technologies)

For purification of DNA fragments, the Rapid PCR Purification kit was used according to the manufactures protocol. The DNA was eluted from the column by addition of 50  $\mu$ l prewarmed (70°C) Tris-HCl (10 mM, pH 8.0). The DNA-concentration was determined using the undiluted eluate.

## **1.8 Determination of DNA concentrations**

DNA concentrations were determined spectroscopically using an Amersham-Pharmacia spectrometer. The absolute volume necessary for measurement was 50  $\mu$ l. For determining the concentration of DNA preparations (III 1.2), the eluate was diluted 1:50 with water and the solution was pipetted into a 50  $\mu$ l cuvette. Concentration was determined by measuring the absorbance at 260 nm, 280 nm and 320 nm. Absorbance at 260 nm had to be higher than 0.1 but less than 0.6 for reliable determinations. A ratio of  $A_{260}/A_{280}$  between 1,8 and 2 monitored a sufficient purity of the DNA preparation.

## 1.9 DNA Sequencing

(Step-by-Step protocols for DNA-sequencing with Sequenase-Version 2.0, 5<sup>th</sup> ed., USB, 1990)

DNA sequencing was performed by the sequencing facility of the ZMNH. For preparation, 1 µg of DNA was diluted in 7 µl ddH<sub>2</sub>O and 1 µl of the appropriate sequencing primer (10 pM) was added.

## 1.10 RNA techniques

All materials used for handling mRNA were autoclaved. ddH<sub>2</sub>O was stirred overnight with 0.01% diethyl-pyrocabonate (DPEC) and was autoclaved afterwards.

### 1.10.1 *In vitro* transcription

(Ambion mMESSAGE mMACHINE™ *in vitro* Transcription Kit)

Inserts in the psGEM plasmid were used for transcription. 2 µg of the plasmid were linearized using Sfi, NheI or PacI (see appendix). Linearized DNA was purified using the rapid DNA purification kit. RNA was prepared as described by the manufacture.

## 2 Protein-biochemical methods

### 2.1 SDS-polyacrylamide gel electrophoresis

(Laemmli, 1970)

Separation of proteins was performed by means of the discontinuous SDS-polyacrylamide gel electrophoresis (SDS-PAGE) using the Mini-Protean III system (BioRad). The size of the running and stacking gel were as follows:

Running gel: height 4.5 cm, thickness 1 mm  
8 % or 10 % acrylamide solution

Stacking gel: height 0.8 cm, thickness 1 mm  
5% (v/v) acrylamide solution  
15-well combs

After complete polymerization of the gel, the chamber was assembled as described by the manufactures protocol. Up to 25 µl sample were loaded in the pockets and the gel was run at constant 80 V for 10 min and then at 140V for the remainder. The gel run was stopped when the bromphenolblue line had reached the end of the gel. Gels were then either stained or subjected to Western blotting.

### **2.1.1 Coomassie-staining of polyacrylamide gels**

(Ausrubel, 1996)

After SDS-PAGE, the gels were stained in staining solution (1h, RT) with constant agitation. The gels were then incubated in destaining solution until the background of the gel appeared nearly transparent.

## **2.2 Western Blot-analysis**

### **2.2.1 Electrophoretic transfer**

(Towbin et al., 1979)

Proteins were transferred from the SDS-gel on a Nitrocellulose membrane (Protran Nitrocellulose BA 85, 0,45 µm, Schleicher & Schüll) using a MINI TRANSBLOT-apparatus (BioRad). After equilibration of the SDS-PAGE in blot buffer for 5 min, the blotting sandwich was assembled as described in the manufactures protocol. Proteins were transferred electrophoretically at 4°C in blot buffer at constant voltage (70 V for 120 min or 35 V

overnight). The prestained marker BenchMark™ (Gibco BRL) was used as a molecular weight marker and to monitor electrophoretic transfer.

### **2.2.2 Immunological detection of proteins on nitrocellulose membranes**

(Ausubel, 1996)

After electrophoretic transfer, the membranes were removed from the sandwiches and placed protein-binding side up in glass vessels. Membranes were washed once in TBS and incubated in 8 ml blocking buffer for 1 h at room temperature. Afterwards, the primary antibody was added in the appropriate dilution either for 2 h at RT or overnight at 4°C. The primary antibody was removed by washing the membrane 5 x 5 min with TBS. The appropriate secondary antibody was applied for 2 h at RT. The membrane was washed again 5 x 5 min with TBS and immunoreactive bands were visualized using the enhanced chemiluminescence detection system (III 2.2.3).

### **2.2.3 Immunological detection using enhanced chemiluminescence**

The antibody bound to the membrane was detected using the enhanced chemiluminescence detection system (Pierce). The membrane was soaked for 1 min in detection solution (1:1 mixture of solutions I and II). The solution was removed and the blot was placed between to saran warp foils. The membrane was exposed to X-ray film (Biomax-MR, Kodak) for several time periods, starting with a 2 min exposure.

### **2.2.4 Densitometric evaluation of band intensity**

Band densities were quantified using the image processing software *Scion Image* (Scion Corporation, Frederick, MD, USA). The developed film was scanned and the digitized picture was exported to *Scion Image*. Band densities were evaluated using the “Gelplot2”-macro according to the manual.

## 2.3 Recombinant expression of proteins in *Escherichia coli*

(Ausubel, 1996)

For recombinant expression of proteins in *E. coli*, the corresponding cDNA of the protein was cloned in frame with the purification tag of the corresponding expression plasmid. The appropriate *E. coli* strain was transformed with the expression plasmid and streaked on LB plates supplemented with the appropriate antibiotic. A single colony was inoculated in a 50 ml LB culture with the appropriate antibiotic and incubated overnight at 37°C with constant agitation. Afterwards, the 50 ml were transferred into a 450 ml culture and incubated at 37°C under constant agitation until the culture had reached an optic density of 0.7. Protein expression was induced by adding IPTG (0,1-0,5 mM *f.c.*) to the culture with further incubation for 2-6 h at 37°C. Bacteria were collected by centrifugation and stored at -20°C. Protein expression was monitored by removing small aliquots of the culture every hour after IPTG induction. Bacteria were pelleted, lysed in sample buffer and applied on a SDS gel.

### 2.3.1 Expression in *E. coli* using the pET-system

(*pET System Manual*, 7<sup>th</sup> edition, Novagen 1997)

The protein was expressed with an N-terminal poly-His Tag in *E. coli*- BL21 (DE3). The cDNA was cloned into the PET20 plasmid.

### 2.3.2 Expression in *E. coli* using the pQE-system

(*The QIAexpressionist handbook*, Qiagen, 1997)

The cDNA was cloned into the pQE30 expression plasmid and transformed into *E. coli* M15pREP4-bacteria. The protein was expressed with an N-terminal poly-His Tag for purification. Induction of protein expression and purification of the protein were carried out as described in the *QIAexpressionist handbook*.

## **2.4 Lysis of bacteria**

### **2.4.1 Sonification**

(Frangioni and Neel, 1993)

The bacterial culture was centrifuged (8000 x g, 4°C, 10 min) and the pellet was resuspended in SDS sample buffer. The suspension was lysed using a sonicator (Branson Sonifier B15, level 6, 50% pulse, 5 x 20 s, in ice) and the debris was removed by centrifugation (10000 x g, 4°C, 10 min). The supernatant was subjected to SDS-PAGE.

### **2.4.2 French press**

Bacteria were pelleted (8000 x g, 4°C, 10 min) and resuspended in native lysis buffer (20 ml lysis buffer per 500 ml culture). The suspension was transferred into a precooled French-*Pressure-20K*-chamber (capacity: 40 ml). Bacteria were compressed (Spectronic Instruments/SLM Aminco, 10000 psi, 5 min) and lysed by opening the valve carefully. The procedure was repeated 3 times and then the suspension was centrifuged (15.000xg, 10 min, 4°C) in a Beckman centrifuge.

## **2.5 Determination of protein concentration (BCA)**

(Ausrubel, 1996)

The protein concentration of cell lysates was determined using the BCA kit (Pierce). Solution A and B were mixed in a ratio of 1:50 to give the BCA solution. 20 µl of the cell lysate were mixed with 200 µl BCA solution in microtiter plates and incubated for 30 min at 37°C. A BSA standard curve was co-incubated ranging from 100 µg/ml to 2 mg/ml. The extinction of the samples was determined at 568 nm in a microtiter plate reader.

## 2.6 Preparation of the Lovastatin open acid form

(Fenton et al., 1992)

Preparation of the open acid form of Lovastatin was essentially carried out as described. In brief, after dissolving 10 mg Lovastatin in 1 ml 100% ethanol, 700  $\mu$ l 10% NaOH were added and the solution was incubated at 50°C for 2 h. The reaction was terminated by addition of 2 ml H<sub>2</sub>O and neutralized by the addition of 3,7% HCl, until pH was 7. The solution was aliquoted and stored at -20°C.

## 3 Cell culture

### 3.1 CHO and N<sub>2</sub>A cell culture

CHO cells and neuro2A cells were either cultured in GMEM or DMEM, respectively, with 10 % FCS (fetal calf serum) and 2% Penicillin/Streptomycin (P/S) 37°C, 5 % CO<sub>2</sub> and 90 % relative humidity in 75 cm<sup>2</sup> flasks (Nunc) with 15 ml medium or in six-well plates (d = 35 mm; area = 9,69 cm<sup>2</sup>) with 2 ml medium. Cells were passaged when they were confluent (usually after 3-4 days). Medium was removed and cells were detached by incubation with 4 ml Versene for 5 min at 37°C. Cells were centrifuged (200xg, 5 min, RT) and the pellet was resuspended in 10 ml fresh medium. Cells were split 1:10 for maintenance or seeded in six-well plates for transfection (300  $\mu$ l per well)

For immunocytochemistry or electrophysiology, cells were seeded on poly-L-lysine coated coverslips (d=14 mm). Coverslips were first cleaned by extensive washing with acetone and then air-dried. Coverslips were coated with poly-L-lysine by constant agitation at 4°C overnight in a poly-L-lysine solution (50  $\mu$ g/ml in PBS). Finally, they were washed twice with ddH<sub>2</sub>O and dried under a sterile hood. Two coverslips were placed per 35 mm dish and cells were seeded with a density of 30 % confluency 24 h before use.

### 3.2 Transfection of CHO-cells

*(Lipofectamine Plus manual, Life technologies)*

For transfection of CHO cells, the Lipofectamine Plus kit (Life Technologies) was used. One day before transfection,  $2 \times 10^5$  cells were seeded per 35 mm dish. When cell density had reached 80-90% (usually after 18-24 h) the cells were washed with GMEM Ø FCS and antibiotics and transfected with 2 µg total DNA per 35 mm well. In case of double transfection or triple transfection, equal amounts of DNA were used. In case of co-transfection with EGFP, the NCAM and Kir3 plasmids were used in excess. 6 µl Plus reagent and 4 µl Lipofectamine were used per well. Transfection was performed as described in the manufacturers protocol. Transfection was terminated after 3 h by addition of an equal volume of GMEM, 10 % FCS, 2% PS. 24 h after transfection, cells were detached with 500 µl Versene per well and split either 1:2 for biochemical analysis or split 1:6 on coverslips for immunohistochemistry and electrophysiological recordings.

### 3.3 Lysis of CHO-cells

After maintenance of CHO cells in 35 mm-culture dishes, the medium was removed and cells were lysed in 400 µl RIPA buffer per 35 mm well with constant agitation (1 h, 4°C). Cells were scraped of the wells and transferred into a 1.5 ml Eppendorf tube. Debris was removed by centrifugation (15000 x g, 4°C, 10 min) and the supernatant was stored at -20°C.

### 3.4 Co-immunoprecipitation and pull-down assays from transiently transfected CHO cells

CHO cells were transfected with the plasmids encoding for the potassium channels or co-transfected with the different NCAM isoforms and the His-tagged potassium channels. Cells from two confluent 35 mm dishes were used per immunoprecipitation. 48 h after transfection, cells were lysed in 400 µl RIPA buffer containing 0.5 % Triton X-100 per 35 mm well. Debris was removed by centrifugation (15000 x g, 4°C, 10 min) and the supernatant was transferred in a 1.5 ml Eppendorf tube. The supernatant was diluted with RIPA buffer Ø Triton X-100 to give final concentrations of Triton X-100 between 0.1 and 0.3 % of the cell

lysate. For co-precipitation experiments, His-tagged potassium channels were precipitated by the addition of 30  $\mu$ l Ni-beads (Qiagen) with constant agitation (4°C, overnight). Ni-beads were collected by centrifugation (1000xg, 5 min, 4°C) and washed twice with RIPA buffer  $\emptyset$  Triton X-100. Proteins were eluted from the beads with SDS sample buffer.

For pull-down experiments, CHO cells transfected with the appropriate potassium channels were lysed in RIPA buffer containing 0.5 % Triton X-100 per 35 mm well. Debris was removed by centrifugation (15000 x g, 4°C, 10 min) and the supernatant was transferred in a new 1.5 ml Eppendorf tube. The supernatant was diluted with RIPA buffer  $\emptyset$  Triton X-100 to give final concentrations of Triton X-100 between 0.1 and 0.3 % of the cell lysate. Purified recombinant intracellular domains of NCAM140 and NCAM180 (1-10  $\mu$ g/ml) were added to the cell lysates and incubated with constant agitation at 4°C for 2 h. Intracellular domains were collected via their His-tag by addition of Ni-beads (30  $\mu$ l, 4°C, overnight) with constant agitation. Beads were washed twice with RIPA  $\emptyset$  Triton X-100 and proteins were eluted from the beads with SDS sample buffer. Precipitates were subjected to SDS-PAGE and Western blotting and investigated immunologically for the presence of NCAM or potassium channel, respectively.

### **3.5 Surface biotinylation and internalization measurements of transfected CHO cells.**

Surface biotinylation and internalization kinetics were essentially carried out as described by Schmidt et al. (1997). In brief, 48 h after transfection, cells were washed twice with ice-cold PBSCM. Surface proteins were biotinylated by incubating cells with 0.5 mg/ml Sulfo-NHS-SS-biotin (Pierce, Rockford, IL, USA) in PBSCM for 10 min at 4°C. Biotinylation was terminated by incubation with 20mM glycine in PBSCM at 4°C for 10 min followed by extensive washing with PBSCM. Biotinylated cells were then either returned to 37°C in GMEM, 10% FCS for 1h or were lysed directly in RIPA-buffer and centrifuged for 15 min at 4°C. To determine the amount of protein that was internalized after 1 h at 37°C from the cell surface, surface bound biotin was stripped off the surface proteins. Cells were washed twice with NT-buffer at 4°C and incubated twice for 10 min with NT-buffer containing 10 mM sodium-2-mercaptoethanesulfonate (MesNa) at 4°C. The reaction was terminated by excessive washing with NT-buffer. Finally, cells were lysed in RIPA buffer and centrifuged at 4°C for 15 min at 14,000xg. The supernatants were removed and protein concentrations were

determined using the BCA kit (Pierce). The amounts of surface-localized proteins and internalized proteins were determined by precipitating biotinylated proteins with streptavidin-coupled agarose beads (Pierce) at 4°C overnight. Agarose beads were pelleted by centrifugation and washed twice with RIPA-buffer. Precipitated proteins were solubilized by addition of 2X SDS-sample buffer to the agarose beads. Proteins were separated by SDS-PAGE and proteins were quantified by immunoblot analysis using polyclonal Kir3.1 (gift of R. Veh) and polyclonal NCAM antibodies.

### **3.6 Internalization assays with Tritc-transferrin and Tritc-dextran**

(Prekeris et al., 1998)

CHO cells were detached 24h after transfection with Versene and re-seeded on coverslips. 48h after transfection, cells were serum-starved for 2h in GMEM Ø FCS and antibiotics and placed on Parafilm (American National Can, Menasha, WI, USA) in a humid chamber. The coverslips were overlaid with 100 µl of GMEM Ø FCS containing either 1 mg/ml Tritc-labeled dextran (Sigma) or 60 µg/ml Tritc-labeled transferrin and incubated for 30 min and up to 1 h at 37°C. Finally, cells were washed with three times with GMEM Ø FCS, fixed and embedded with Aqua Poly-Mount medium (Polysciences Inc., Warrington, PA, USA).

### **3.7 NCAM-stimulation with polyclonal antibodies**

For NCAM stimulation of CHO cells and oocytes, cells were either transfected with the appropriate NCAM constructs or oocytes were injected with the indicated RNAs.

24h after transfection, CHO cells were seeded on 6well dishes with a confluency of ~ 30% so that they reach a density of about 60% on the next day. The next day, were washed once with 1 ml of serum free GMEM and then incubated with 1 ml of serum free media for either for six hours or overnight in the CO<sub>2</sub>-incubator.

NCAM antibodies were directly added to the cell culture media supernatant of the oocytes/CHO cells to yield a final concentration of 200µg/ml and incubated for the indicated time. After stimulation, CHO cells were once washed with 1 ml ice-cold PBS and then frozen within the plates using a mixture of dry ice and 70% ethanol or in some cases liquid nitrogen.

The 6 well plates were stored at  $-80^{\circ}\text{C}$  until cell extracts were prepared as described below. Recordings in oocytes were performed after the indicated stimulation periods.

### **3.8 Immunoprecipitation of tyrosine phosphorylated proteins**

Stored cell lysates (III 3.3) were adjusted to same volume ( $\sim 0.5$  ml) and protein concentration ( $\sim 500$   $\mu\text{g}/\text{ml}$ ). 4G10-agarose bead suspension (Upstate) was washed twice with RIPA buffer. 30  $\mu\text{l}$  4G10-agarose suspension were added to each sample and gently mixed for  $\sim 12$  hours (overnight) at  $4^{\circ}\text{C}$ . Agarose beads were pelleted by centrifugation ( $500 \times g$ , 2 min,  $4^{\circ}\text{C}$ ) and washed twice with cold RIPA buffer. Finally, RIPA supernatant was removed and agarose beads were resuspended in 50  $\mu\text{l}$  2x SDS sample buffer and heated for 10 minutes at  $95^{\circ}\text{C}$ . 20  $\mu\text{l}$  of each sample were loaded onto a SDS-PAGE gel. Electrophoresis, western blotting and immunodetection using polyclonal FAK antibodies were performed as described above (III 3.2 and 3.3).

### **3.9 Isolation of detergent-resistant membrane fractions**

Lipid rafts were isolated as previously described (Melkonian et al., 1999). In brief, monolayers of co-transfected CHO cells grown in  $150 \text{ cm}^2$  plates were detached using 4 ml Versene (Life Technologies) and pelleted by centrifugation for 5 min at  $500 \times g$  and  $4^{\circ}\text{C}$ . Pellets were homogenized in TNE buffer at  $4^{\circ}\text{C}$  using a Dounce homogenizer (Weaton). Lysates were centrifuged at  $500 \times g$  to remove unlysed cells and debris. A small fraction of the cleared cell lysate was used to determine the total Kir3.1/3.2 and NCAM expression. Membranes were collected by centrifugation at  $100,000 \times g$  for 1 h at  $4^{\circ}\text{C}$  and resuspended in 500  $\mu\text{l}$  TNE buffer, pH 11, containing 1% Triton X-100. Membranes were incubated for 30 min on ice, adjusted to 40% sucrose with 80% sucrose in TNE buffer and placed in an SW 55Ti ultracentrifuge tube. The 40% fraction was overlaid with 1.5 ml TNE 36% sucrose and 2 ml 10% sucrose. After centrifugation (16 h,  $100,000 \times g$ ,  $4^{\circ}\text{C}$ ), six 750  $\mu\text{l}$  fractions were collected from the top, diluted with 3 ml TNE buffer, pH 11, and centrifuged for 1.5 h at  $100,000 \times g$  at  $4^{\circ}\text{C}$ . This procedure permits isolation of only the Triton X-100 insoluble proteins in the pelleted fractions, whereas Triton X-100 soluble proteins remain in the

supernatant. Pellets were resuspended in 50  $\mu$ l 2xSDS sample buffer and subjected to SDS-PAGE. For preparation of lipid rafts from brain homogenates 10 forebrains from 2-day-old mice were homogenized in TNE buffer. Low-density fractions were prepared exactly as described for CHO cells.

### **3.10 Preparation of membrane and triton X-100-insoluble fractions of CHO cells**

Confluent CHO cells (140 cm<sup>2</sup> flask) detached with Versene and transferred to a 15 ml falcon tube. After centrifugation (200 x g, 3 min, 20°C), cells were washed with ice-cold PBSCM, resuspended in 1 ml hypotonic lysis buffer and incubated on ice for 10 min. Cells were homogenized using a Dounce homogenizer (Weaton). The lysate was centrifuged (2000xg, 10 min, 4°C) to remove unlysed cells and debris. The resulting post-nuclear supernatant was centrifuged again (100,000xg, 1h, 4°C) and after removal of the supernatant (S1) the membrane pellet was resuspended in 500  $\mu$ l TNE buffer, pH11 and incubated on ice for 30 min. The lysate was centrifuged again (100,000xg, 1h, 4°C), the supernatant containing the Triton X-100 soluble proteins (S2) removed and the pellet containing the Triton X-100 insoluble proteins was resuspended in 100  $\mu$ l 2xSDS sample buffer. Finally, the supernatants S1 and S2 were diluted with 5xSample buffer and applied to SDS-PAGE.

### **3.11 Endoglycosidase H digestion of CHO cell lysates**

Cell lysates of transfected CHO cells were diluted with 2x citrate buffer (150 mM sodium-citrate, pH 5,5) and after addition of 0.1 U endoglycosidase H (EndoH, Roche Diagnostics) lysates were incubated at 37°C overnight. Controls were treated identically without addition of EndoH. Lysates were subjected to SDS-PAGE and probed with Kir3.1 antibodies.

### **3.12 Incubation of CHO cells with lovastatin and mevalonate**

24h after transfection with the indicated cDNAs, CHO cells were seeded onto poly-L-lysine coated coverslips and recordings were performed 48 h after transfection. Where indicated, both 10  $\mu$ M lovastatin (Calbiochem) and 250  $\mu$ M mevalonate (Sigma) (48h prior to analysis) or 3 mM methyl- $\beta$ -cyclodextrin (MCD) (Sigma) (12 h prior to analysis) were added to the medium containing 10% FCS. Under these concentrations, cells remain viable and can fully recover in medium containing 10% FCS. Lovastatin was prepared in its open acid form (IV 2.6) and mevalonate was applied in its lactone form.

## **4 Immunocytochemistry**

### **4.1 Immunocytochemistry of living cells**

Coverslips with the attached cells were washed with GMEM  $\emptyset$  FCS and placed on Parafilm in a humid chamber. 100  $\mu$ l of GMEM  $\emptyset$  FCS containing the primary antibody in the appropriate dilution were added on the coverslips and incubated at RT for 20 min. Afterwards, coverslips were put into 12-well dishes and washed twice with GMEM  $\emptyset$  FCS. Then coverslips were put on Parafilm in the humid chamber again, covered with 100  $\mu$ l GMEM  $\emptyset$  FCS containing the fluorescent dye-coupled secondary antibody in a 1:200 dilution, and incubated at 37°C for 20 min in the dark. Finally, coverslips were washed twice with GMEM  $\emptyset$  FCS, fixed and mounted on objectives with Aqua Poly-Mount medium (Polysciences Inc)

### **4.2 Fixation of CHO cells**

The medium was removed from the coverslips and cells were fixed with 1 ml of 4% para-formaldehyde in PBS for 10 min at RT. Cells were washed twice with PBS and stored in PBS at 4°C.

### **4.3 Immunocytochemistry of fixed CHO cells and hippocampal neurons**

Coverslips were placed on Parafilm in a humid chamber and incubated with 100  $\mu$ l blocking buffer for 1 h at RT. The blocking buffer was removed by aspiration and the coverslips were covered with 100  $\mu$ l antibody solution containing the appropriate primary antibody and incubated overnight at 4°C in a humid chamber. Coverslips were washed three times with PBS and incubated with 100  $\mu$ l antibody solution containing the fluorescent dye-labeled secondary antibody (Cy3, Cy5, FITC) for 1 h at room temperature in the dark. Finally, cells were washed three times with PBS and mounted on objectives with Aqua Poly-Mount medium (Polysciences Inc). Coverslips were stored in the dark at 4°C.

### **4.4 Fluorescence measurements of *Xenopus laevis* oocytes**

Cell surface fluorescence in oocytes was measured with a Zeiss LSM510 argon-crypton laser-scanning microscope equipped with a 16x oil-immersion objective lens. For quantification of fluorescence intensity, confocal images were taken under constant parameters from ten average scans at different locations (n=5 cells). Fluorescence signal was quantified using the image processing software *Scion Image* (Scion Corporation).

### **4.5 Confocal laser-scanning microscopy**

All images of CHO cells and hippocampal neurons were obtained with a Zeiss LSM510 argon-crypton confocal laser-scanning microscope equipped with a 60x oil-immersion objective lens. Images were scanned with a resolution of 512x512. Detector gain and pinhole were adjusted to give an optimal signal to noise ratio.

## **5 Electrophysiology**

### **5.1 Heterologous expression in *Xenopus laevis* oocytes**

For heterologous expression of proteins in oocytes, the corresponding cDNAs of the proteins were cloned into the psGEM plasmid, which provides the  $\beta$ -globine gene at the 3' and 5' untranslated region of the plasmid. Capped run-off poly(A)<sup>+</sup> RNA transcripts were prepared as described and injected into oocytes. Injection of oocytes and electrophysiological recordings of oocytes were performed in cooperation with Dr. Erhard Wischmeyer in the group of Dr. Andreas Karschin, Göttingen.

### **5.2 Electrophysiological recordings from transfected CHO cells and hippocampal neurons**

Electrophysiological recordings were performed in cooperation with Dr. Alexander Dityatev in the group of Melitta Schachner.

## **6 Computer based sequence analysis**

Computer based sequence analysis and alignments of DNA sequences and protein sequences was performed using the Lasergene-programe (DNASTAR, *Inc.*, [www.dnastar.com](http://www.dnastar.com)). The following databases were used: Medline-, BLASTN- and BLASTP-Server of NCBI (National Center for Biotechnology Information, [www.ncbi.nlm.nih.gov](http://www.ncbi.nlm.nih.gov)).

## V Results

### 1 Kir3 inward currents are increased in hippocampal neurons of NCAM<sup>-/-</sup> mice.

To explore the interaction of NCAM and 5-HT<sub>1A</sub> receptor signaling, the Kir3-mediated currents were first investigated in hippocampal neurons cultured from wild-type NCAM<sup>+/+</sup> and NCAM<sup>-/-</sup> mice as a likely target for 5-HT<sub>1A</sub> receptor signaling (Lüscher et al., 1997). By this approach, it was tested whether the absence or presence of NCAM had any influence on the Kir3-mediated currents within the “natural environment” of the two molecules. Expression of Kir3 channels in pyramidal cell-like neurons could be demonstrated by both immunocytochemically (see V 8) and patch-clamp analysis (IV 5.2). Whole cell voltage-clamp experiments revealed several features typical of Kir3 currents: slow current activation (Fig. 4A), current potentiation by the 5-HT<sub>1A</sub> receptor agonist 8-OH DPAT (Fig. 4B), and the GABA<sub>B</sub> receptor agonist baclofen (Fig. 1C), complete current block by 1 mM Ba<sup>2+</sup> (Figs. 4B, C) and current dependence on extracellular [K<sup>+</sup>] (data not shown). When currents were compared in neurons from NCAM<sup>+/+</sup> and NCAM<sup>-/-</sup> mice, it was found that Kir3-like currents significantly increased to 238% in the absence of NCAM (Fig. 4E; -63±56 pA, n=30, in wild type neurons versus -150±95 pA, n=29, in mutant neurons at a holding potential of -130 mV). In contrast, transient and sustained outward K<sup>+</sup> currents remained unchanged between the two genotypes (Fig. 4D, E). These results indicated that the presence of NCAM somehow reduced Kir3-like currents in hippocampal neurons.

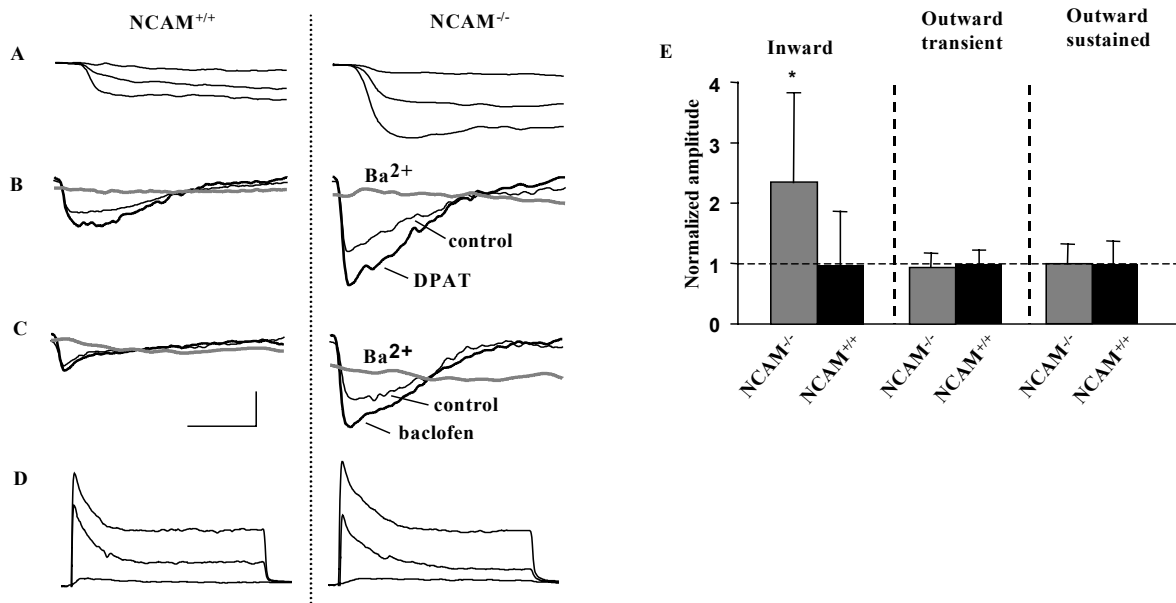


**Figure 4: Increased inward currents in NCAM deficient cultured hippocampal neurons.**

(A) Slowly activating inward currents were evoked in wild-type (NCAM<sup>+/+</sup>) and NCAM deficient (NCAM<sup>-/-</sup>) hippocampal neurons by voltage steps from -60 mV to -90, -110 and -130 mV. Inward currents activated in neurons by a voltage ramp from -130 mV to -40 mV were augmented by 30 μM 8-OH DPAT (B), and by 50 μM RS)-baclofen (C). These currents were blocked by addition of 1 mM Ba<sup>2+</sup> into the extracellular solution (B and C). (D) Transient and sustained K<sup>+</sup> outward currents were evoked in neurons by voltage steps from -60 mV to -30, -10 and +10 mV. (E) Cumulative data show a significant difference in inward currents recorded in neurons from NCAM deficient and wild type mice (\*p<0.01; Student's t-test). Bars represent mean values of currents recorded in NCAM<sup>-/-</sup> relative to NCAM<sup>+/+</sup> neurons. Error bars represent standard deviations. Absolute values corresponding to the bars are (number of cells) 64±56 pA (n=20), 150±95 pA (n=29), 3.61±0.25 nA (n=10), 3.41±0.27 nA (n=9), 1.76±0.22 nA (n=10), 1.75±0.19 nA (n=9). Scale bars, 100 pA and 50 ms (A), 100 pA and 200 ms (B), 50 pA and 200 ms (B), 1 nA and 50 ms (D).

## 2 NCAM140 and NCAM180 reduce neuronal Kir3 currents in *Xenopus* oocytes and CHO cells

To determine the functional relationship between NCAM and Kir3 channels, *Xenopus* oocytes (IV 5.1) were co-injected with equimolar RNA concentrations (IV 1.10.1) of NCAM isoforms and concatenated pairs of Kir3 channel subunits (IX 3.1 and IX 3.2), which mimic the Kir3 subunit composition in native cells (Wischmeyer et al., 1997) (see Fig. 5).

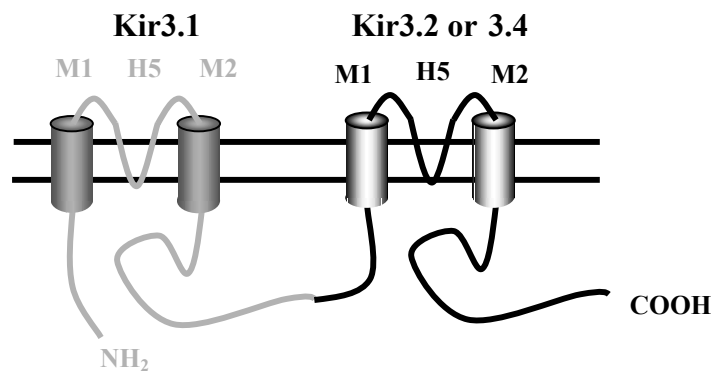


**Figure 5: Schematic drawing of the Kir3.1/3.X concatamers.**

The NH<sub>2</sub>-termini of the Kir3.2, 3.3 or 3.4 subunit were fused in frame to the COOH-terminus of the Kir3.1 subunit. This construct provides the advantage that the stoichiometry between Kir3.1 and the second subunit is fixed with respect to channel composition, hence resulting in more reproducible channel expression.

For control, 5-HT<sub>1A</sub> receptor RNA was co-injected to quantify receptor-activated Kir3 currents with ramp and voltage-step protocols. With 96 mM K<sup>+</sup> and 10 μM 5-HT in the bath solution, the Kir3.1/3.2 combination gave rise to robust inwardly rectifying K<sup>+</sup> currents, which averaged  $-23.1 \pm 7.1$  μA (n=10) at a holding potential of  $-100$  mV. Independent of the presence of NCAM isoforms both basal and ligand-activated macroscopic Kir3.1/3.2 currents exhibited biophysical properties, e.g. slow current activation (Fig. 6A), K<sup>+</sup> permeability, dependence of conductance on extracellular K<sup>+</sup> or block by Ba<sup>2+</sup> and Cs<sup>+</sup>, typical of native G protein-activated Kir3 channels (data not shown). When co-expressed with NCAM180 or NCAM140 (IX 4.2.2), total current amplitudes of Kir3.1/3.2 were strikingly reduced to  $36 \pm 14\%$  (n=10) and  $25 \pm 12\%$  (n=10), respectively (Fig. 6A, B). These values are in similar magnitude to the reduction of Kir3-like currents in NCAM<sup>+/+</sup> mice (42% reduction) compared to NCAM<sup>-/-</sup> mice. However, co-expression of NCAM120 (IX 4.2.1), which is devoid of an intracellular domain, and a receptor tyrosine kinase of the Ig-superfamily (e.g. the trkB receptor), had no significant effect on Kir3.1/3.2 currents. When probed in Chinese hamster ovary (CHO) cells (IV 3.2), co-transfected NCAM120, NCAM140 and NCAM180 isoforms suppressed Kir3.1/3.2 channel activity in a quantitatively similar manner (Fig. 6C).

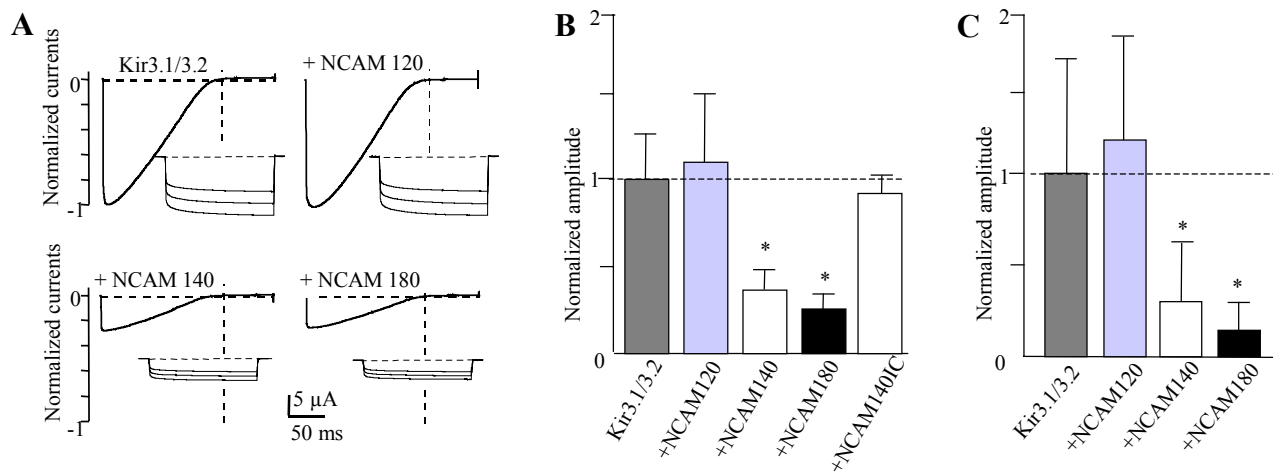


**Figure 6: Suppression of Kir3.1/3.2 channels by NCAM180 and NCAM140 in *Xenopus* oocytes and CHO cells.**

Whole cell currents of *Xenopus* oocytes injected with cRNAs encoding Kir3.1/3.2 channel subunits, 5-HT<sub>1A</sub> receptor and one of the indicated NCAM isoforms. (A) Currents are responses to 2 s voltage ramps between –150 mV and +60 mV and 500 ms voltage jumps to –80, –100, –120 mV, respectively, in the presence of 10 μM 5-HT and 96 mM K<sup>+</sup>. Activation time constants at 0 mV were 20.3 ms in the absence and 19.7 ms in the presence of NCAM140. (B) Bar graph showing the relative modulation of Kir3.1/3.2 currents by NCAM120 (1.1±0.43; amplitude relative to control), NCAM140 (0.36±0.14), NCAM180 (0.25±0.12) and NCAM140IC (0.9±0.18) in oocytes. (C) Bar graph showing the relative modulation of Kir3.1/3.2 currents by NCAM120 (1.24±0.67, n=10), NCAM140 (0.29±0.33, n=13) and NCAM180 (0.17±0.09, n=11) in transfected CHO cells. Error bars represent standard deviations; asterisks denote statistical significance (Student's t-test; p<0.01).

To investigate the specificity of the current reduction by NCAM isoforms other Kir3 channel combinations were also tested. The Kir3.1/3.3 subunit (IX 3) combination expressed in neurons was also severely suppressed by NCAM180 to 18±12% (n=10). In contrast, both a Kir3.1/3.4 subunit (IX 3) combination, constituting the cardiac K<sub>ACH</sub> channel, as well as other neuronal, constitutively active Kir channels (e.g. Kir2.1) were not significantly affected (Fig. 7A, B). These results are quite surprising, since the homology between the Kir3.2 and Kir3.4 subunit is approximately 70% on amino acid level (see also Fig. 9).

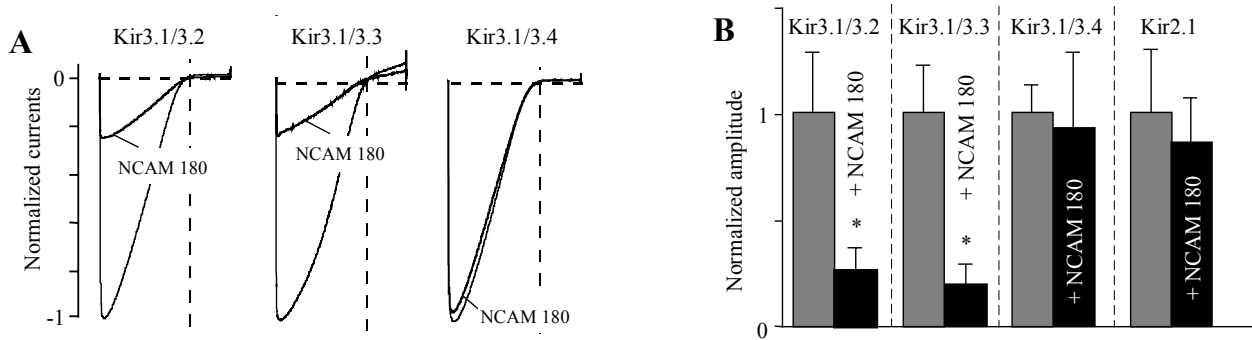


**Figure 7: Neuronal Kir3 channels are inhibited by NCAM.**

(A) Macroscopic current responses to 2 s voltage ramps between  $-150$  mV and  $+60$  mV of oocytes injected with NCAM180,  $5\text{-HT}_{1A}$  receptor and different combinations of Kir3 subunits with Kir3.1. (B) Bar graph showing the relative inhibition by NCAM180 of Kir3.1/3.2 channels ( $0.25 \pm 0.12$  amplitude relative to control in the absence of NCAM), Kir3.1/3.3 ( $0.18 \pm 0.12$ ), Kir3.1/3.4 ( $0.92 \pm 0.38$ ), and Kir2.1 ( $0.86 \pm 0.26$ ). Error bars represent standard deviations; asterisks denote statistical significance (Student's t-test;  $p < 0.01$ ).

### 3 NCAM140 reduces surface localization of EGFP-tagged Kir3.2 channels in *Xenopus* oocytes

To visualize channel targeting to the cell surface of *Xenopus* oocytes, Kir3.2 and Kir3.4 channel subunits were tagged with enhanced green fluorescent protein (EGFP) at their COOH-termini (IX 3.1.3). RNAs were injected with or without NCAM120, NCAM140 and NCAM180, and membrane fluorescence was inspected by confocal microscopy 48 h after RNA injection (IV 4.4). While un-injected oocytes showed no background fluorescence, injection of Kir3.1/3.2-EGFP and Kir3.1/Kir3.4-EGFP constructs resulted in strong signals at the cell surface, which were quantified by line-scan luminometry using a photomultiplier (Fig. 8). Co-expression of NCAM140 caused a prominent decrease by  $\sim 58\%$  of Kir3.1/3.2-EGFP fluorescence in the membrane (Fig. 8A, B), whereas the Kir3.1/3.4-EGFP signal remained unaffected by co-expressed NCAM140 (Fig. 8C, D). Co-injection of NCAM120, however, did not alter Kir3.1/3.2-EGFP fluorescence levels.

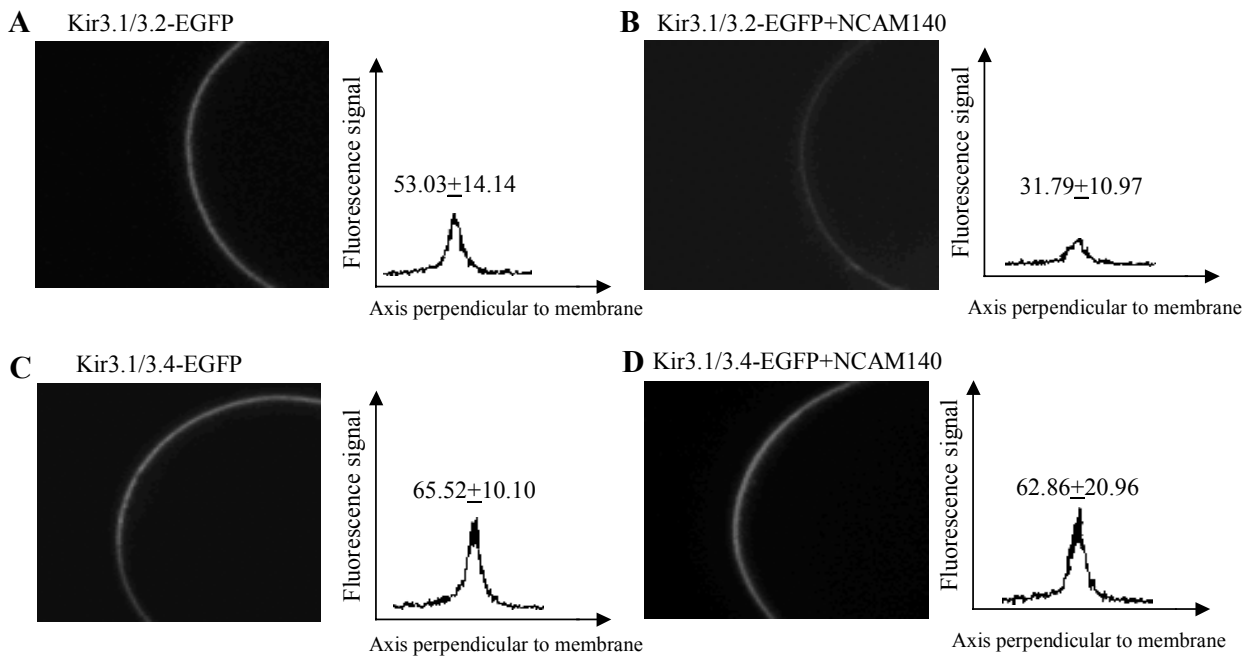


**Figure 8: Plasma membrane localization of Kir3 channels is altered by NCAM.**

Shown are representative confocal images of oocytes injected with cRNAs of EGFP-tagged Kir3.1/3.2 (A, B), and Kir3.1/3.4 (C, D), respectively, in the absence (A, C) and presence (B, D) of NCAM140 as indicated. Graphs show average fluorescence measurements of 10 line scanings perpendicular to the cell surface representative for 5 oocytes measured. Data represent mean  $\pm$  SD of fluorescent signal.

#### 4 The NH<sub>2</sub>-terminus of Kir3.2 is the major structural determinant for NCAM-sensitivity

The differential sensitivity of Kir3 channels to NCAM inhibition opened up the possibility to decipher the structural determinants for the reduced Kir3 channel membrane localization. Since it was unlikely that Kir3.1 subunits, present in all tested combinations, conferred the sensitivity for NCAM, hybrid channels were analyzed in which the NH<sub>2</sub>- or COOH- termini of the Kir3.2 and Kir3.4 subunits were exchanged (IX 3.1.1). As shown in Figure 9, the identity between Kir3.2, Kir3.3 and Kir3.4 is ~70% on amino acid level. Hence, the Kir3.2 and Kir3.3 subunits might have some structural features in common that are different from Kir3.4 subunit. Since only those NCAM isoforms with an intracellular domain inhibited Kir3 currents, the intracellular domains of the Kir3 channels were a likely target to determine the NCAM sensitivity.

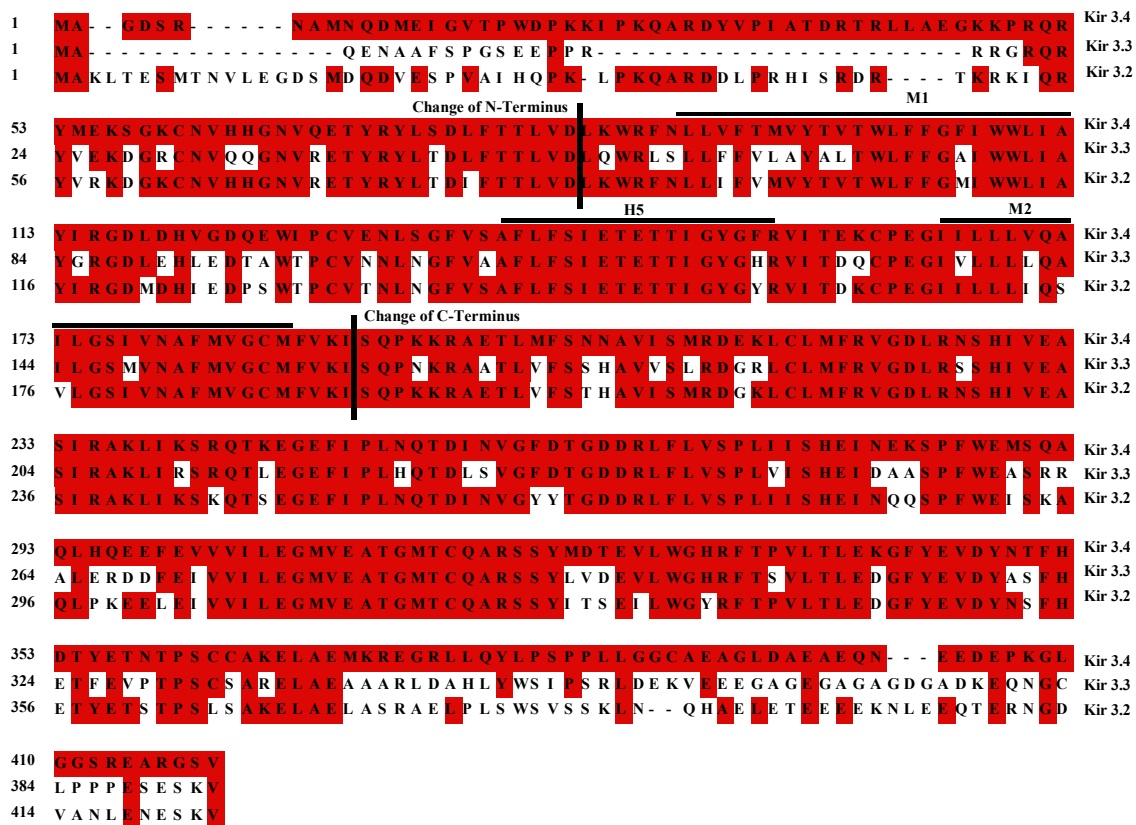


**Figure 9: Alignment of the amino acids of the Kir3.2, Kir3.3 and Kir3.4 subunits.**

Amino acids in Kir3.2 and Kir3.3 that are identical to Kir3.4 are underlined in gray. The identity between the Kir3 family members is 60-80%. Positions where the amino acids were exchanged between Kir3.2 and Kir3.4 are marked with a vertical line. M1, M2: membrane-spanning region; H5: pore-forming region.

When the COOH-termini were exchanged, the hybrid channels maintained the NCAM sensitivity of the core channel (Fig. 10A, B), whereas exchange of the NH<sub>2</sub>-termini reverted the sensitivity of the core channel towards NCAM140 (Fig. 10C, D). Thus, Kir3.1/3.4 channels were suppressed by NCAM140 when the NH<sub>2</sub>-terminus of Kir3.4 was substituted by the NH<sub>2</sub>-terminus of Kir3.2. Although current suppression of hybrid channels was not as pronounced as in Kir3.1/3.2 wild type channels, the NH<sub>2</sub>-termini of Kir3.2/3.3 channels harbor the major structural determinants for NCAM inhibition.

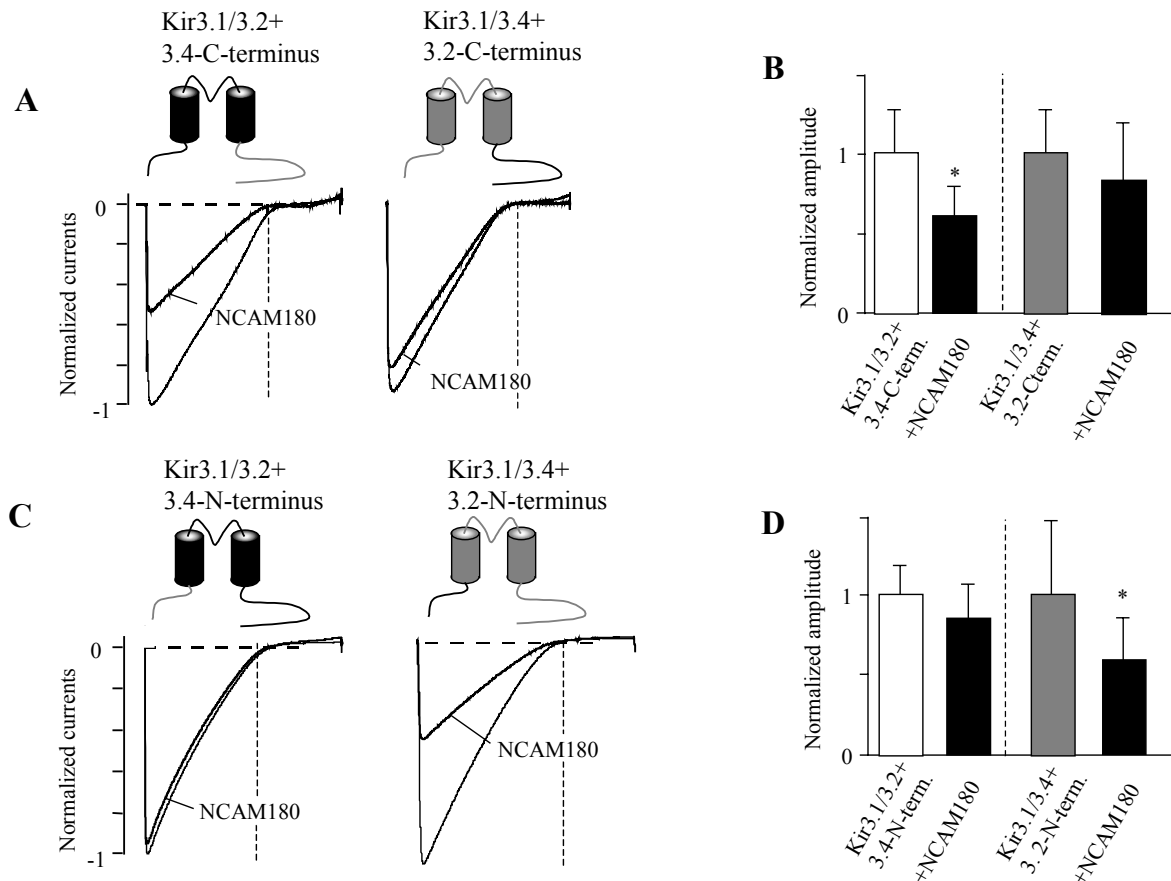


**Figure 10: Kir3 subunits NH<sub>2</sub>-termini determine sensitivity to NCAM.**

(A, C) Macroscopic current responses to 2 s voltage ramps between  $-150$  mV and  $+60$  mV of oocytes injected with NCAM180, 5-HT<sub>1A</sub> receptor and different combinations of hybrid Kir3.2/Kir3.4 subunits connected to Kir3.1 subunits. NH<sub>2</sub>- and COOH-termini of injected Kir3 channel subunits were exchanged as shown in the cartoons with Kir3.2 components in grey and Kir3.4 in black. (B) Bar graph showing the relative inhibition by NCAM180 of Kir3.1/3.2 and Kir3.1/3.4 with the COOH-terminus exchanged, Kir3.1/3.2C4 ( $0.6 \pm 0.26$ ), Kir3.1/3.4C2 ( $0.82 \pm 0.39$ ) (D) Relative inhibition by NCAM180 of Kir3.1/3.2 and Kir3.1/3.4 with the N-terminus exchanged Kir3.1/3.2N4 ( $0.84 \pm 0.2$ ), and Kir3.1/3.4N2 ( $0.56 \pm 0.27$ ;  $n=10$  each). Error bars represent standard deviations; asterisks denote statistical significance (Student's t-test;  $p < 0.01$ ).

For further insight at the primary amino acid level, sub-domains and single amino acid residues that differ between the NH<sub>2</sub>-termini of Kir3.2 and Kir3.4 were also exchanged (IX 3.1.1.1 and IX 3.1.1.2). As shown in Figure 11, the following mutants were constructed: (i) exchange of amino acids 1-35 in the NH<sub>2</sub>-terminus; (ii) exchange of amino acids 1-54 in the NH<sub>2</sub>-terminus; (iii) exchange of amino acids at positions 58, 61, 72; and (iv) exchange of amino acids at position 58, 61, 72, 79, 98 of Kir3.2. However, in none of these mutants was the inhibitory effect of NCAM140 reversed (data not shown), suggesting that multiple

allosteric effects are involved in the NCAM-mediated Kir3 inhibition. Furthermore, the N-terminus of the Kir3.4 subunit contains two clathrin-dependent endocytosis signals, namely the YXXI-motif and the LL-motif (see Ochsenbauer et al., 2000 and references herein), which are absent in Kir3.2 and Kir3.3 subunits. Since these motifs are the only ones with a known function in the NH<sub>2</sub>-termini of the Kir3 subunits, these amino acids were also mutated in the Kir3.4 subunit to check whether the absence of certain endocytosis motifs in case of Kir3.2 is responsible for the NCAM-mediated inhibition (IX 4.1.1.2). However, this Kir3.1/3.4 mutant (called Kir3.1/3.4  $\Delta$  endocytosis signals) still exhibited no NCAM-sensitivity, indicating that these endocytosis signals are not involved (data not shown).

1	<u>M</u> <u>A</u> - - <u>G</u> <u>D</u> <u>S</u> <u>R</u> - - - - - <u>N</u> <u>A</u> <u>M</u> <u>N</u> <u>Q</u> <u>D</u>	Kir3.4
1	<u>M</u> <u>A</u> - - - - - - - - - - - - - - - <u>Q</u> <u>E</u> <u>N</u>	Kir3.3
1	<u>M</u> <u>A</u> <u>K</u> <u>L</u> <u>T</u> <u>E</u> <u>S</u> <u>M</u> <u>T</u> <u>N</u> <u>V</u> <u>L</u> <u>E</u> <u>G</u> <u>D</u> <u>S</u> <u>M</u> <u>D</u> <u>Q</u> <u>D</u>	Kir3.2
Kir3.4/3.2 pos23		
13	<u>M</u> <u>E</u> <u>I</u> <u>G</u> <u>V</u> <u>T</u> <u>P</u> <u>W</u> <u>D</u> <u>P</u> <u>K</u>   <u>K</u> <u>I</u> <u>P</u> <u>K</u> <u>Q</u> <u>A</u> <u>R</u> <u>D</u> <u>Y</u>	Kir3.4
6	<u>A</u> <u>A</u> <u>F</u> <u>S</u> <u>P</u> <u>G</u> <u>S</u> <u>E</u> <u>E</u> <u>P</u> <u>P</u> <u>R</u> - - - - - - - - -	Kir3.3
21	<u>V</u> <u>E</u> <u>S</u> <u>P</u> <u>V</u> <u>A</u> <u>I</u> <u>H</u> <u>Q</u> <u>P</u> <u>K</u> - <u>L</u> <u>P</u> <u>K</u> <u>Q</u> <u>A</u> <u>R</u> <u>D</u> <u>D</u>	Kir3.2
Kir3.4/3.2 pos50		
33	<u>V</u> <u>P</u> <u>I</u> <u>A</u> <u>T</u> <u>D</u> <u>R</u> <u>T</u> <u>R</u> <u>L</u> <u>L</u> <u>A</u> <u>E</u> <u>G</u> <u>K</u> <u>K</u> <u>P</u> <u>R</u>   <u>Q</u> <u>R</u>	Kir3.4
18	- - - - - - - - - - - - - - - <u>R</u> <u>R</u> <u>G</u> <u>R</u>   <u>Q</u> <u>R</u>	Kir3.3
40	<u>L</u> <u>P</u> <u>R</u> <u>H</u> <u>I</u> <u>S</u> <u>R</u> <u>D</u> <u>R</u> - - - - - <u>T</u> <u>K</u> <u>R</u> <u>K</u> <u>I</u>   <u>Q</u> <u>R</u>	Kir3.2
53	<u>Y</u> <u>M</u> <u>E</u> <u>K</u> <u>S</u> <u>G</u> <u>K</u> <u>C</u> <u>N</u> <u>V</u> <u>H</u> <u>H</u> <u>G</u> <u>N</u> <u>V</u> <u>Q</u> <u>E</u> <u>T</u> <u>Y</u> <u>R</u>	Kir3.4
24	<u>Y</u> <u>V</u> <u>E</u> <u>K</u> <u>D</u> <u>G</u> <u>R</u> <u>C</u> <u>N</u> <u>V</u> <u>Q</u> <u>Q</u> <u>G</u> <u>N</u> <u>V</u> <u>R</u> <u>E</u> <u>T</u> <u>Y</u> <u>R</u>	Kir3.3
56	<u>Y</u> <u>V</u> <u>R</u> <u>K</u> <u>D</u> <u>G</u> <u>K</u> <u>C</u> <u>N</u> <u>V</u> <u>H</u> <u>H</u> <u>G</u> <u>N</u> <u>V</u> <u>R</u> <u>E</u> <u>T</u> <u>Y</u> <u>R</u>	Kir3.2
73	<u>Y</u> <u>L</u> <u>S</u> <u>D</u> <u>L</u> <u>F</u> <u>T</u> <u>T</u> <u>L</u> <u>V</u> <u>D</u>	Kir3.4
44	<u>Y</u> <u>L</u> <u>T</u> <u>D</u> <u>L</u> <u>F</u> <u>T</u> <u>T</u> <u>L</u> <u>V</u> <u>D</u>	Kir3.3
76	<u>Y</u> <u>L</u> <u>T</u> <u>D</u> <u>I</u> <u>F</u> <u>T</u> <u>T</u> <u>L</u> <u>V</u> <u>D</u>	Kir3.2

**Figure 11: Alignment of the NH<sub>2</sub>-termini of the Kir3.2, Kir3.3 and Kir3.4 subunits.**

Amino acids in Kir3.2 and Kir3.3 that are identical to Kir3.4 are underlined in dark gray. The positions where the amino acids were exchanged between Kir3.2 and Kir3.4 are marked with a vertical line. Single amino acids that were mutated in the Kir3.4 or Kir3.2 subunit are underlined in light gray.

## 5 The intracellular domain of NCAM140 is not sufficient to inhibit Kir3-mediated currents

Since cell surface localization of Kir3 channels is specifically reduced by the NCAM140 and NCAM180 isoforms that harbor an intracellular domain, the intracellular domain of NCAM140 itself was tested to cause Kir3.1/3.2 inhibition. As shown in Figure 12, transfected intracellular domains of NCAM140 and NCAM180 (IX 4.2.5) are membrane associated due to the palmitoylation of cysteines, as has also been previously reported (Little et al., 1998). However, when co-injected with Kir3.1/3.2 subunits, the intracellular domain of NCAM140 (called NCAM140IC) neither suppressed Kir3 channel surface localization nor Kir3 inward currents ( $90\pm 18\%$  of control; see Fig 6B). Hence, the presence of the intracellular domains alone is not sufficient to impair surface localization of the Kir3 channels.

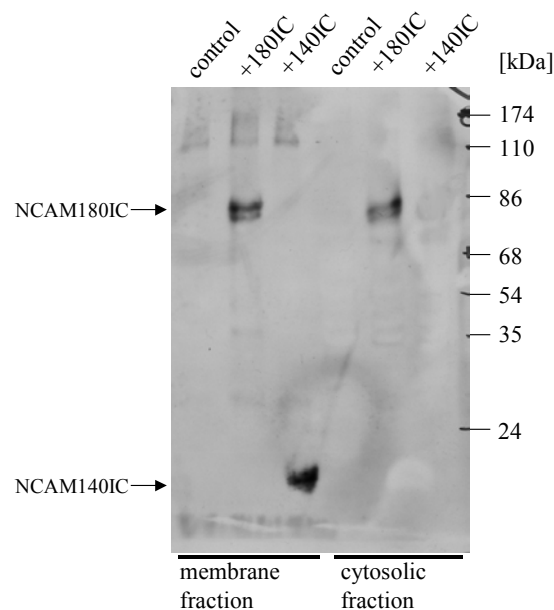


**Figure 12: NCAM140IC and NCAM180IC are membrane associated.**

Sub-cellular fractionation of NCAM140IC- and NCAM180IC-transfected CHO cells revealed that both proteins are present in the membrane fraction, indicating an association with the membrane. However, while NCAM140IC is completely membrane associated, NCAM180IC can also be detected in the cytosolic fraction, indicating that either the protein is incompletely palmitoylated or that the protein is not as tightly membrane associated as NCAM140IC, probably due to the higher molecular mass of NCAM180IC (see Fig. 17A).

## 6 Stimulation of NCAM140 or NCAM180 associated signal transduction pathways did not alter surface localization of Kir3.1/3.2

As a next step, the possible signaling mechanisms were investigated that could account for the reduced surface expression of neuronal Kir3 channels in the presence of NCAM140 or NCAM180. First, acute or prolonged stimulation of the different NCAM-isoforms by NCAM-specific antibodies was without effect on the activity of Kir3.1/3.2 channels in *Xenopus* oocytes (IV 3.7). Under the recording conditions, no significant differences in Kir3.1/3.2 current amplitudes were measured for either NCAM140 or NCAM180 after application of polyclonal NCAM antibodies (200  $\mu\text{g/ml}$ ) for 30 min and 48 h, respectively. Secondly, suppression was unaltered when assayed for known mediators of NCAM signaling, i.e. incubation of oocytes for 48 h with 50  $\mu\text{M}$  PD98059 (2'-amino-3'-methoxyflavone), a selective inhibitor of MAP kinase kinases (MEK; (Kolkova et al., 2000), or PD173074, a specific inhibitor of the FGF receptor (Mohammadi et al., 1998). Thirdly, single-channel measurements in the cell-attached configuration provided evidence that unitary channel properties of Kir3.1/3.2 channels remained unchanged in the presence of NCAM180 (Fig. 13). Both the elementary conductance ( $\gamma = 36$  pS), and the open probability ( $p_o = 0.71 \pm 0.02$  versus  $p_{o\text{NCAM}} = 0.67 \pm 0.02$ ) were not significantly altered. Hence, it is unlikely that NCAM140 or NCAM180 modulate the channel such that it is more in the closed state, either by direct association of the intracellular domains of NCAM and Kir3.1/3.2 or by NCAM-mediated phosphorylation of the channel (see I 1.3).

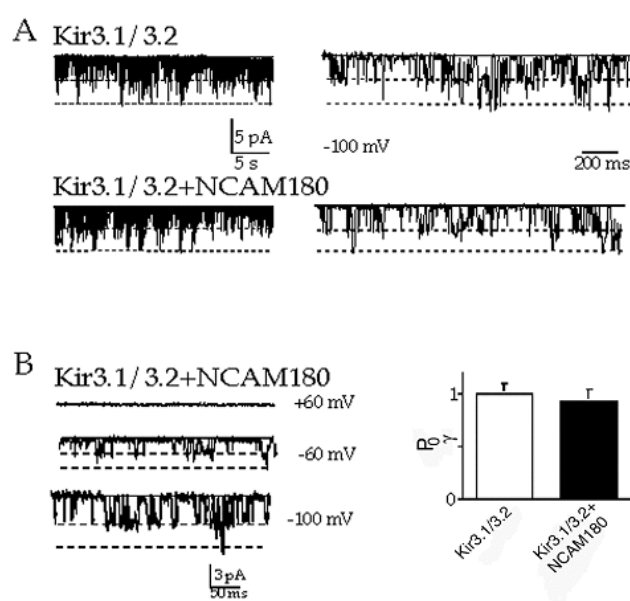


**Figure 13: NCAM180 does not affect Kir3.1/3.2 single channel properties.**

Cell-attached single channel recordings from oocytes injected with Kir3.1/3.2 RNA in the absence and presence of NCAM180 as indicated. (A) Shown are original current recordings with a filter setting of 1 kHz at the pipette potential. (B) Bar graph comparing the product of single channel open probability and unitary conductance ( $p_o \times \gamma$ ) of the Kir3.1/3.2 channels recorded in (A) at  $-100$  mV in the absence (white bar; normalized to unity $\pm$ 0.1) and presence of NCAM (black bar; 0.94 $\pm$ 0.1 of unity).

**7 NCAM140 does not interact physically with the Kir3 channels**

It was also tested whether any parallels can be drawn to the interaction of FasII and shaker  $K^+$  channels (see I 1.3). It was therefore investigated if any of the Kir3 channels interact physically with the transmembranous NCAM isoforms, which might cause the reduced surface delivery by yet unknown mechanisms. However, it was impossible to demonstrate any direct physical interaction of Kir3.1/3.2 channels and NCAM140 by co-capping and co-immunoprecipitation assays (IV 3.4). First, the interaction of both molecules in their “natural” environment of the cell membrane of hippocampal neurons or CHO cells was investigated. Since NCAM-mediated current reduction can also be observed in CHO cells, a physical interaction as a putative mechanism should be observable in these cells, even if linker proteins are involved. Antibody-induced clustering (IV 4.1) of NCAM140 in the cell membrane of Kir3.1/3.2 or Kir3.1/3.4 co-transfected CHO cells showed that the potassium channel did not co-cluster (IV 4.3) in the NCAM patches on the cell surface, indicating that NCAM140 and neither of the Kir3 channels are physically associated in the cell membrane of CHO cells (Fig. 14 A). In hippocampal neurons virtually the same results were obtained: incubation of wild type neurons with polyclonal NCAM antibodies induced clustering of NCAM on the neurites, but the Kir3.1 subunit was not enriched in these NCAM clusters. Note that NCAM is predominantly present on neurites, whereas the potassium channel is present both on neurites and on the somata of the cell (Fig. 14 B). Within the somata of the cell, a large fraction of the Kir3.1 subunits seems to be localized intracellularly.

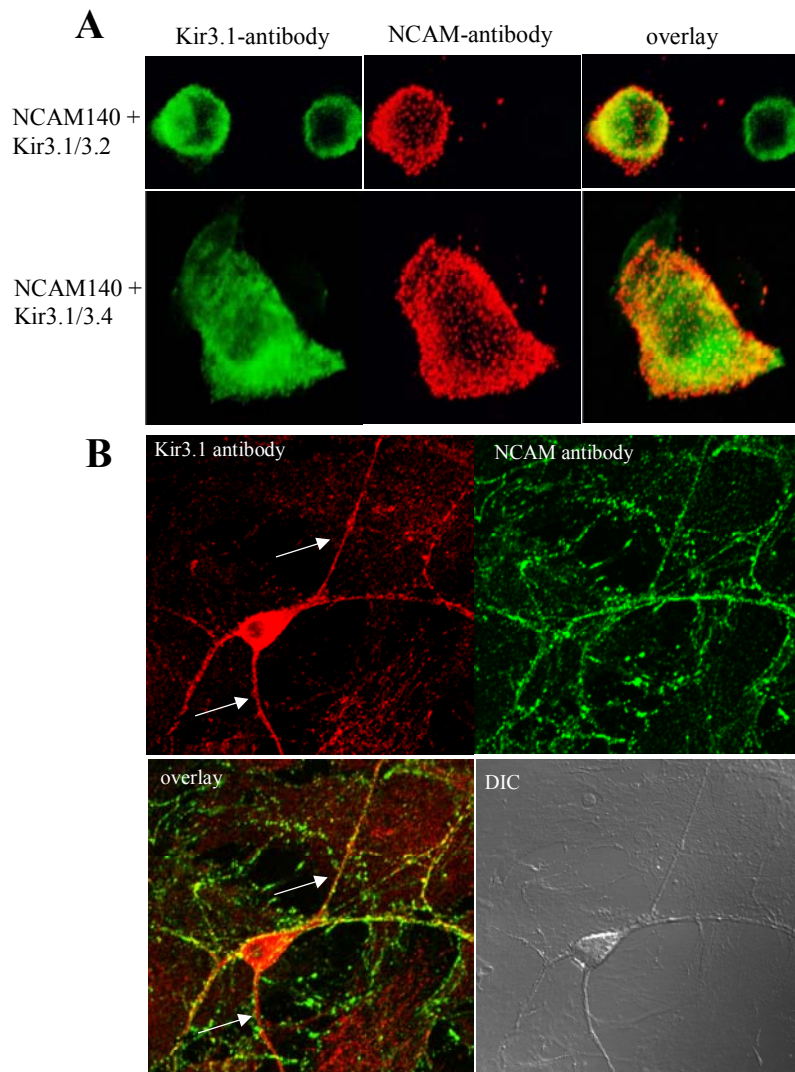


**Figure 14: Clustering of NCAM140 does not result in a redistribution of the Kir3 potassium channels in transfected CHO cells or hippocampal neurons.**

(A) A representative confocal image of transfected CHO cells. Kir3.1/3.2 or Kir3.1/3.4 channels were co-transfected with NCAM140 and NCAM140 was clustered on the cell surface by incubation with polyclonal NCAM-antibodies (red). Cells were fixed, permeabilized and stained for the Kir3.1 subunit (green). Neither Kir3.1/3.2 nor Kir3.1/3.4 co-distributed with NCAM140 in the patches in the cell surface. Note that the majority of the Kir3 channels are located intracellularly. (B) A representative confocal image of a wild type hippocampal neuron. Neurons were kept 9 days in culture and NCAM was clustered on the cell surface by incubation with polyclonal NCAM-antibodies (green). Cells were fixed, permeabilized and stained for the Kir3.1 subunit (red). NCAM clusters are mainly present on the neurites of the cell with only little cell body staining. Kir3.1 staining is predominantly in the cell body, but also present in the neurites. In parallel to CHO cells, Kir3.1 subunits did not accumulate in the NCAM clusters on neurites. Arrows indicate areas where essentially no overlap of the staining for NCAM and Kir3.1 can be observed.

Finally, two biochemical approaches were used to further investigate a putative physical interaction of the Kir3 channels and NCAM: On the one hand it was tested whether any of the NCAM isoforms co-immunoprecipitate with the Kir3 channels or pull-down assays were used by incubating cell lysates containing the Kir3 channels with recombinantly expressed NCAM140IC and NCAM180IC proteins and then subsequently precipitating the intracellular domains from the cell lysate (IV 3.4). For immunoprecipitation, His-tagged Kir3 channels (IX 4.1.2) were used which provided the advantage that immunoprecipitation could be carried out with Ni-beads and not with antibodies that might interfere with subsequent detection of precipitated proteins. However, these approaches confirmed the results obtained from the co-clustering experiments: neither did any of the NCAM isoforms co-precipitated with the Kir3 channels under various detergent concentrations (Fig. 12) nor did the recombinantly expressed proteins NCAM140IC or NCAM180IC pulled down the Kir3 channels (not shown). Taken together, it is therefore unlikely that a direct interaction of NCAM140 and the Kir3.1/3.2 channel is responsible for the surface reduction of Kir3 channels.

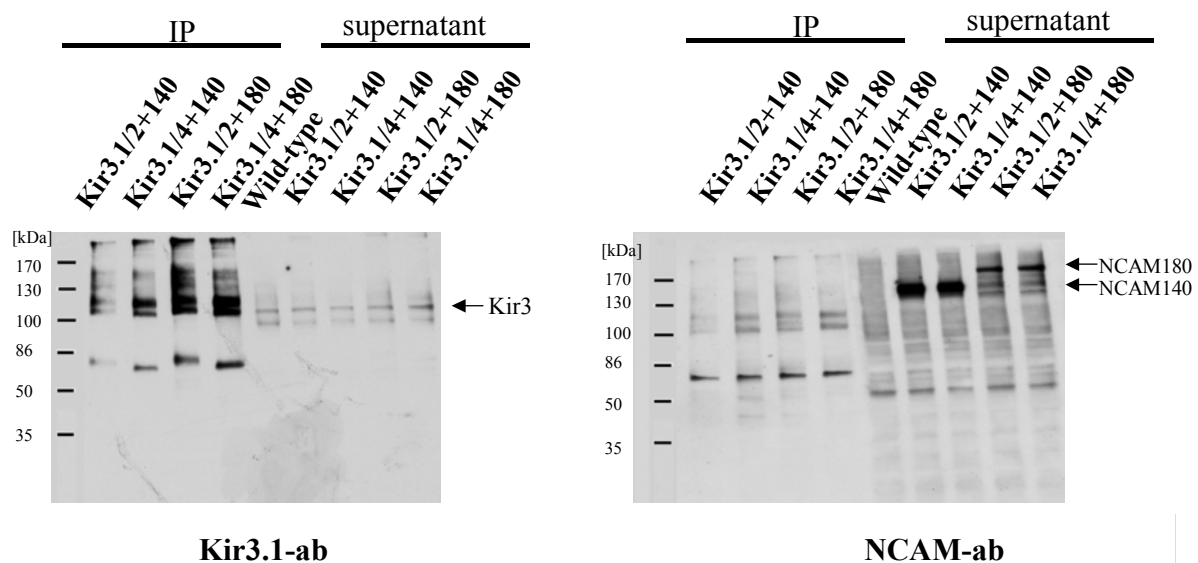


**Figure 15: NCAM did not co-precipitate with Kir3.1/3.2 or Kir3.1/3.4 His-tag channels**

CHO cells were co-transfected with combinations of NCAM140 or NCAM180 and Kir3.1/3.2 or Kir3.1/3.4 and cell lysates were subjected to immunoprecipitation using Ni-beads. Precipitates and supernatants were subjected to SDS-PAGE and probed with NCAM antibody. To confirm precipitation of Kir3 channels, the blot was stripped and re-probed with Kir3.1 antibodies. While most of the Kir3.1/3.2 and Kir3.1/3.4 channels were precipitated and virtually no  $K^+$  channel could be detected in the supernatant, the NCAM immunoreactivity remained solely in the supernatant.

## 8 All NCAM isoforms are present in lipid raft microdomains

Based on the observation that the intracellular domains of NCAM140 and NCAM180 can be palmitoylated at four cysteine residues adjacent to the transmembrane domain (Little et al., 1998) it was investigated by this study whether localization to cholesterol-rich membrane microdomains, the so-called lipid rafts or detergent resistant microdomains (DRMs), could play a major role in signal transduction mediated by NCAM. These lipid rafts reveal high concentrations of cholesterol and sphingoglycolipids and thereby a higher resistance towards non-ionic detergents such as Triton X-100 than other membrane compartments. Several studies have illuminated the involvement of lipid rafts in signaling of hematopoietic cells (Brown and London, 1998) and there is growing evidence that transition of cellular receptors into rafts can enhance downstream signaling (Cinek and Horejsi, 1992; Stefanova et al., 1991; Tansey et al., 2000). Since these microdomains are enriched in potent effectors of signal transduction (e.g. src-family kinases and the growth-associated protein 43 (GAP-43)) (Aarts et al., 1999; Simons and Ikonen, 1997), the accumulation of NCAM receptors in these microdomains might regulate downstream signaling in a particular manner. Therefore, the question arose whether raft localization of particular NCAM isoforms was essential for downstream signaling such as activation of the fyn pathway and for inhibition of Kir3.1/3.2 surface localization.

For the determination of NCAM140 and 180 in lipid rafts, brain homogenate and two cell lines were used, namely neuroblastoma cells (Neuro2A) expressing the three major isoforms of NCAM endogenously and NCAM negative CHO cells, which were used for transfection with the NCAM isoforms. Insolubility in cold non-ionic detergents and flotation on sucrose density gradients are the well-established criteria for identification of lipid raft-associated proteins (Hooper, 1997). Using these flotation gradients, the NCAM localization in the detergent insoluble, low-density membrane fractions (raft-associated proteins) and in the insoluble high-density fraction (IV 3.9) was determined.

In the homogenate of the forebrain of 2-day-old mice, all three main NCAM-isoforms could be detected in the top fractions of the flotation gradient (Figure 16A, upper panel, lanes 3 and 4), confirming an association of the NCAM isoforms with low-density lipids in raft microdomains. A large fraction of NCAM molecules in the raft fractions appeared to be polysialylated, since a broad band could be detected as a smear extending from 180 kDa to higher apparent molecular weights, indicating a high degree of glycosylation. Furthermore, the non-receptor tyrosine kinase fyn (Fig. 16A, middle panel), which has been described as

raft associated (van't Hof and Resh, 1997) and the focal adhesion kinase (FAK) (Fig. 16A, lower panel) were also found to be present in the low-density fractions of the gradient, thus co-localizing NCAM with its potential signaling effectors in the lipid raft fractions.

In neuroblastoma cells, all isoforms were also present in the top fractions of the flotation gradient, confirming the association of the NCAM isoforms with lipids rafts (Figure 16B, lanes 2-4) in cell lines. The non-receptor tyrosine kinase fyn also co-localized in these cells with NCAM in the upper fractions. However, while NCAM120 was mainly raft-associated (see also Kramer et al., 1999), high amounts of NCAM140 and 180 remained in the Triton X-100 insoluble bottom fractions (Figure 16B, lanes 8 and 9) of the flotation gradient, probably associated with cytoskeletal proteins (Montixi et al., 1998).

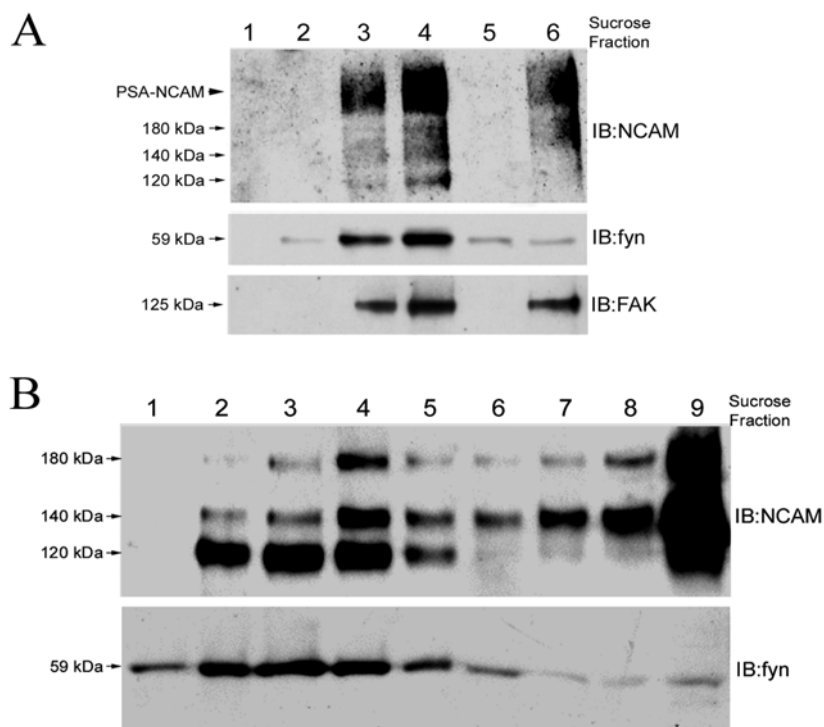


**Figure 16: NCAM is present in detergent resistant membrane fractions.**

(A) In homogenates of forebrain, all NCAM isoforms are present in the low-density fractions (lanes 3 and 4) representing the lipid raft fraction and in the high-density Triton X-100 insoluble fraction (lane 6) possibly containing cytoskeleton-associated proteins (upper panel). The raft-associated non-receptor tyrosine kinase fyn (middle panel) and the focal adhesion kinase FAK (lower panel) co-localize with NCAM in the low-density lipid raft fractions.

(B) In the neuroblastoma cell lysate, NCAM140 and NCAM180 are present in the low-density fractions (lanes 2-4) representing the lipid raft fraction and in the high-density Triton X-100 insoluble fraction (lane 9) possibly containing cytoskeleton-associated proteins. In contrast, the GPI-linked NCAM120 is mainly present in the raft fractions (lane 2-4) with only small amounts in the high-density Triton X-100 insoluble fractions (lanes 9). The raft associated non-receptor tyrosine kinase fyn is also exclusively present in the low-density fraction. Similar results were obtained in three independent experiments.

## 9 Mutation of palmitoylation sites abolishes the presence of NCAM140 in lipid rafts

To investigate the importance of intracellular palmitoylation sites of NCAM140 and NCAM180 (Fig. 17A) for the association of NCAM with rafts, a NCAM140 mutant was constructed (IX 4.2.3) which lacks its four palmitoylation sites by mutating the four intracellular cysteine residues to serine residues (NCAM140 $\Delta$ , Figure 17 B). Analysis of the subcellular distribution of NCAM140 in transfected CHO cells revealed an association of NCAM140 with lipid rafts as in neuroblastoma cells (Figure 17 D, left, lanes 2 and 3). In contrast, NCAM140 $\Delta$  distribution showed a drastic reduction in lipid rafts when compared to NCAM140 (Figure 17 D, right, lanes 2 and 3), indicating that palmitoylation is a major determinant in the localization of NCAM140 to lipid rafts. Mutation of NCAM140 palmitoylation sites neither significantly influenced the overall expression of the protein (Figure 17 C) nor its surface expression (see Fig. 21 A). The amount of NCAM140 $\Delta$  was also reduced in the bottom fraction of the sucrose gradient, indicating an overall reduced Triton X-100 insolubility (Figure 17 D, right, lane 6).

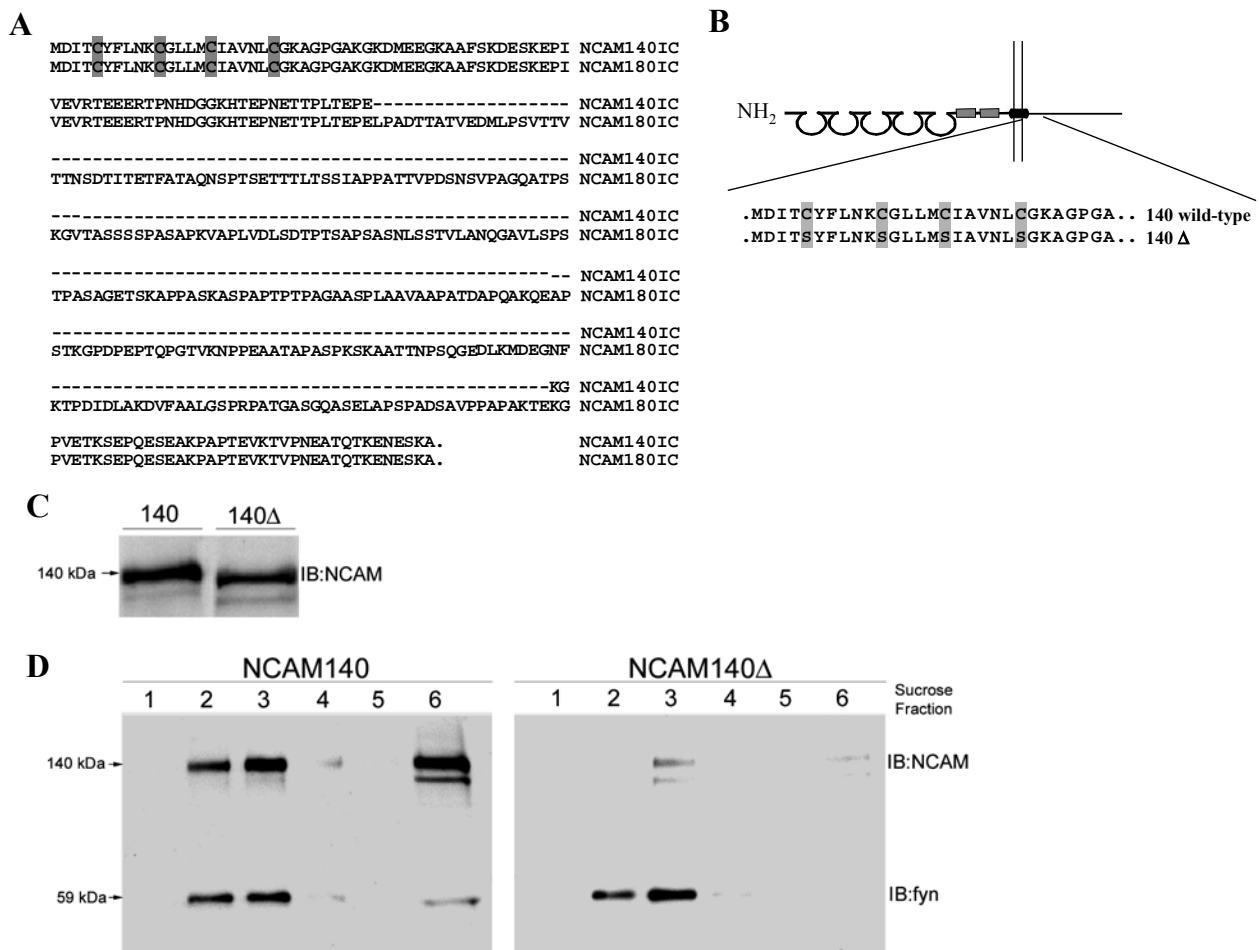


**Figure 17: Mutation of NCAM140 palmitoylation sites abolishes NCAM140 raft association.**

(A) Alignment of the intracellular domains of NCAM140 and NCAM180. The NH<sub>2</sub>-terminus and the COOH terminus are identical between both intracellular domains, but NCAM180IC has additionally an insert of 261 aa, also called exon18. Both isoforms possess four intracellular cysteines for palmitoylation (underlined in gray).

(B) Schematic diagram of the structure of NCAM140 and NCAM140Δ. The plasma membrane is indicated by the pair of vertical lines. The semi-circles represent the five Ig-like domains. The two fibronectin type III-like domains are shown as black boxes. The expanded segment shows the N-terminal sequence of the cytoplasmic domain and the four cysteines that were mutated to serines in the NCAM140Δ construct to remove all sites for palmitoylation.

(C) Western blot analysis of the total cell lysate of NCAM140 and NCAM140Δ transfected CHO cells using a polyclonal NCAM antibody. Comparison of expression levels in CHO cells transfected with both constructs indicate that mutation of the four cysteines did not significantly alter protein expression. Similar results were obtained in three independent experiments.

(D) Western blot analysis of sucrose gradient fractions of NCAM140 (left) and NCAM140Δ (right) transfected CHO cells. NCAM140 is present both in the low-density raft fractions (lanes 2 and 3) and in the high-density fraction (lane 6). To estimate the percentage of raft-associated NCAM140 versus total NCAM140, the densitometrically determined immunoblot intensities of the NCAM140 bands in the total cell lysate (Figure 17C) and in the raft fractions (Figure 17B, left, lanes 2 and 3) were normalized to the total protein subjected to SDS-PAGE. Relating the amount of NCAM140 present in lipid rafts by the total amount of NCAM140 revealed that approximately 2% of the total NCAM140 protein is present in the lipid raft fractions under these artificial raft isolation procedures. Analysis of the sucrose gradient fractions of NCAM140Δ transfected cells shows a drastically reduced amount of NCAM in the low-density fractions (lanes 2 and 3) and the high-density bottom fraction (lane 6), indicating that palmitoylation is essential for NCAM140 to be present in lipid rafts and in the Triton X-100 insoluble fraction. The blots of the NCAM140 and NCAM140Δ gradient fractions were reprobed with p59fyn antibody to confirm equal protein loading and isolation of the lipid raft fractions. Similar results were obtained in three independent experiments.

As a next step, the question was addressed as to the physiological relevance of the raft localization of NCAM isoforms for activation of the fyn-FAK pathway. However, it is unlikely that activation of the fyn-FAK pathway is involved in the surface delivery of the Kir3.1/3.2 channels, since it has been reported that only NCAM140 but not NCAM180 can activate this pathway (Beggs et al., 1994). Since both NCAM140 and NCAM180 are capable to reduce surface delivery of Kir3.1/3.2, there might be other yet unknown raft-associated signaling pathways that could be activated by both NCAM isoforms. Nevertheless, the fyn-FAK pathway was first used as a convenient read-out system to monitor the effects of NCAM exclusion from lipid-rafts on its signaling capability.

## **10 Activation of the focal adhesion kinase FAK by NCAM140 is impaired when NCAM140 is excluded from lipid rafts**

The non-receptor tyrosine kinase fyn and the focal adhesion kinase FAK have been implicated in NCAM-mediated signaling using dominant-negative approaches (Kolkova et al., 2000). This FGF receptor-independent signaling of NCAM140 could be linked to raft-associated kinases, such as fyn, and phosphorylation of downstream effectors of fyn, namely FAK. Given that FAK can activate the ERK1/2 pathway (Chen et al., 1998) and that it plays a pivotal role in NCAM signaling, alterations of FAK phosphorylation were investigated either when the NCAM molecule was excluded from lipid rafts or when palmitoylation sites were mutated (transfection with NCAM140 $\Delta$ ). The importance of lipid rafts for NCAM140 signaling was further characterized by treatment of NCAM140-expressing CHO cells with methyl- $\beta$ -cyclodextrin (MCD) that binds to cholesterol thereby destroying the integrity of lipid rafts. It has been reported that this treatment inhibits signaling of receptor complexes that contain GPI-linked components (Bruckner et al., 1999; Xavier et al., 1998) but does not impair signaling of non-raft associated receptors (Peiro et al., 2000). Hence, two approaches were used to document the involvement of lipid rafts in NCAM140 signaling: Change of the intrinsic property of NCAM140 to be raft-associated by mutation of palmitoylation sites or disruption of lipid rafts themselves by cholesterol-depletion of the cell membrane.

Tyrosine phosphorylated proteins were immunoprecipitated from lysates of control or NCAM stimulated cells transfected with NCAM140 or NCAM140 $\Delta$  (IV 3.8). Immune complexes were subjected to immunoblot analysis with FAK antibody. Up-regulation of FAK phosphorylation was readily detectable after stimulation of NCAM140 transfected CHO cells with polyclonal NCAM antibodies (see Figure 18). In contrast, only low levels of FAK immunoreactivity could be detected in immunoprecipitates of NCAM140 $\Delta$ -transfected cells or in cholesterol-depleted NCAM140-transfected cells. These observations provide evidence that NCAM140-mediated signaling via FAK depends on the presence of NCAM140 in lipid rafts. Disruption of the integrity of the lipid raft matrix or exclusion of NCAM140 from lipid rafts impairs the ability of NCAM140 to activate the FAK kinase.

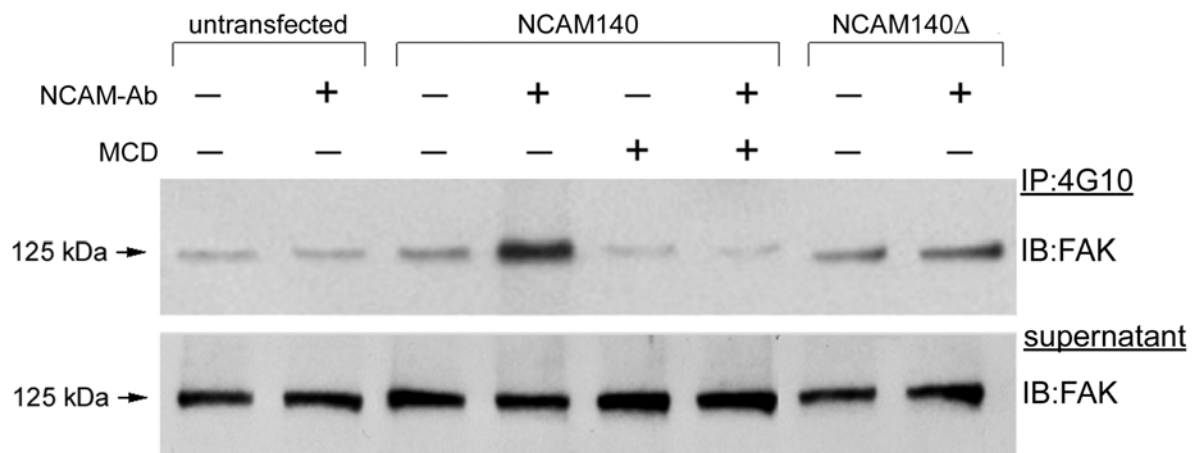


**Figure 18: Lipid raft integrity is critical for NCAM140-mediated signal transduction.**

NCAM140-transfected CHO cells were treated with 10 mM methyl- $\beta$ -cyclodextrin (MCD) to disperse lipid rafts 20 min prior to NCAM stimulation with polyclonal antibodies.

NCAM140- and NCAM140 $\Delta$ -transfected CHO cells were stimulated with polyclonal NCAM antibodies and tyrosine-phosphorylated proteins were immunoprecipitated (IP) from the cell lysates. Western blot analysis with a FAK antibody detected tyrosine-phosphorylated FAK in immunoprecipitates. NCAM140 stimulation induces phosphorylation of FAK in control (-MCD) cells. Exclusion of NCAM140 from lipid rafts either by cholesterol depletion (+MCD) or by mutation of NCAM140 palmitoylation sites (NCAM140 $\Delta$ ) attenuates phosphorylation of FAK. Similar results were obtained in two independent experiments. IB: immunoblot for the molecules indicated.

## 11 Impairment of NCAM140 raft association or disruption of intracellular rafts in CHO cells revert the inhibitory effect of NCAM140 on Kir3.1/3.2 surface localization

As a next step it was investigated whether NCAM140 $\Delta$  is still capable to inhibit surface delivery of Kir3.1/3.2 channels. This approach was supported by the observation that the Kir3.1/3.2 channel is partly associated with lipid rafts in transfected CHO cells and brain homogenates. As shown in Figures 19A and 19B, Kir3.1 immunoreactivity is prominent in the upper fractions (lanes 3 and 4) of a sucrose density gradient of Triton X-100 insoluble protein fractions of transfected CHO cell lysate and mouse forebrain homogenates, indicating an association with lipid rafts in CHO cells and mouse brains. Kir3.1 subunits were also present in the Triton X-100 insoluble bottom fraction of the gradient (Fig. 19A, B lane 6), which is likely to contain cytoskeleton-associated Kir3.1 subunits (Kennedy et al., 1999). Therefore, lipid rafts may function as a platform from which NCAM controls the surface localization of Kir3.1/3.2 channels. It should be noted that the amount of Kir3.1/3.2 in the

lipid raft fractions is virtually identical in the presence of NCAM140 and NCAM140 $\Delta$ , and thus independent of the lipid raft association of NCAM140 (Fig. 19B). However, the surface localization of Kir3.1/3.2 channels in CHO cells and oocytes (as measured by voltage clamp analysis) was comparable in the presence of NCAM140 $\Delta$  and NCAM120, (Fig. 19C), demonstrating that inhibition by NCAM140 is completely abolished when lipid raft association is disrupted.

To further document the involvement of lipid rafts in the NCAM-mediated surface localization of Kir3.1/3.2, lipid rafts were disrupted in CHO cells by depletion of cholesterol using either MCD (see V. 10) or lovastatin, a blocker of the 3-HMG CoA reductase and thus of cholesterol biosynthesis (IV 3.12 and IV 2.6). The latter treatment not only disperses lipid rafts in the plasma membrane, but also affects intracellular organelles such as the trans-Golgi network. As shown in Figure 19C, disruption of lipid rafts by MCD did not affect the inhibition Kir3 channel cell surface localization by NCAM140, indicating that plasma membrane lipid raft-associated NCAM140 is not involved in the regulation of membrane localization. Furthermore, treatment of transfected CHO cells with MCD per se did not impair surface localization of Kir3.1/3.2, since currents of MCD-treated and untreated Kir3.1/3.2-NCAM120 co-transfected cells were essentially the same.

In contrast, treatment of Kir3.1/3.2-NCAM140 co-transfected cells with lovastatin and mevalonate resulted in a partial rescue of Kir3.1/3.2 surface localization (50% reduction in the presence versus 80% reduction in the absence of lovastatin/mevalonate compared to Kir3.1/3.2-NCAM120 transfected CHO cells). Lovastatin/mevalonate treatment had no significant influence on Kir3.1/3.2-NCAM120 co-transfected cells, indicating that reduction of cholesterol did not affect surface localization of the Kir3 channel. This partial rescue is probably due to the incomplete block of cholesterol biosynthesis by lovastatin/mevalonate (Keller and Simons, 1998).

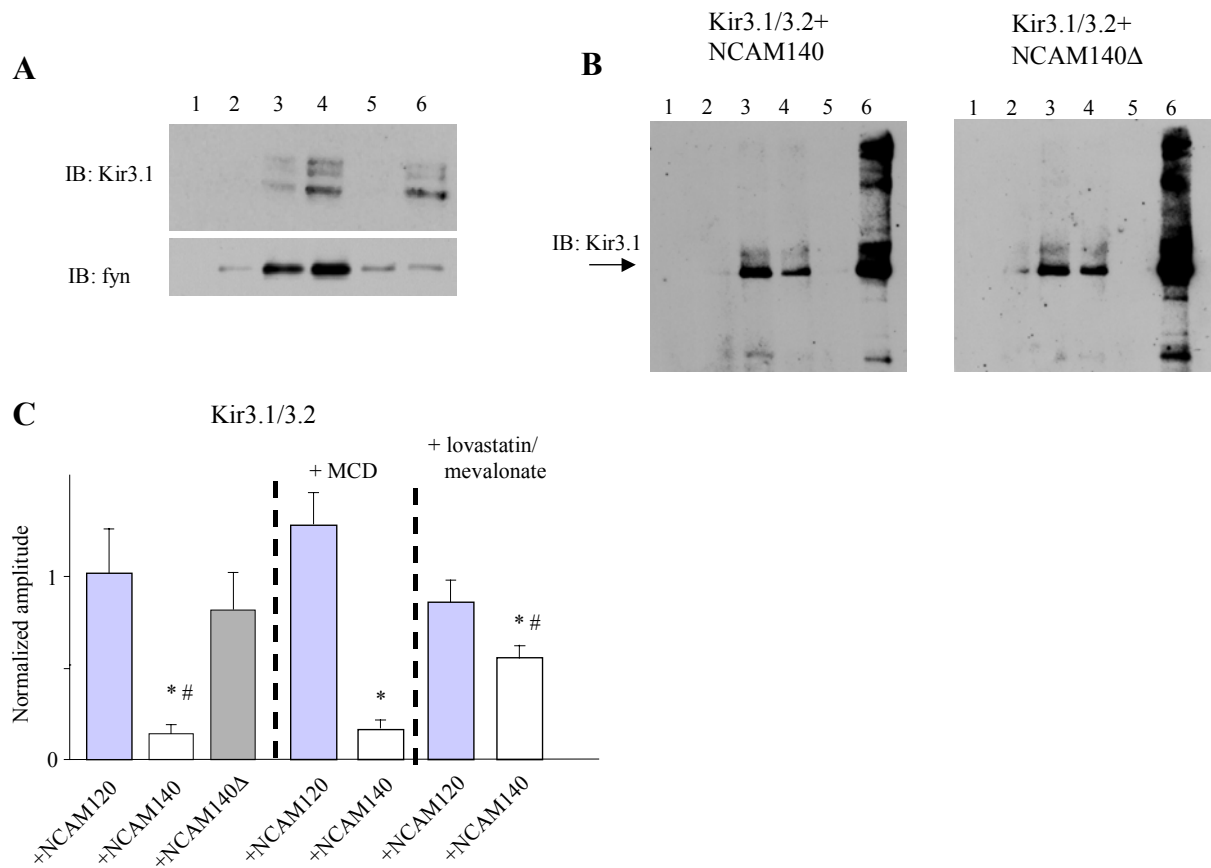


**Figure 19: Exclusion of NCAM140 from lipid rafts or depletion of cholesterol neutralizes the inhibitory effect of NCAM140.**

(A) Western blot analysis of sucrose gradient fractions of Kir3.1/3.2 and NCAM140 (left) or NCAM140Δ (right) co-transfected CHO cells. Kir3.1/3.2 is present both in the low-density raft fractions (lanes 3 and 4) and in the high-density fraction (lane 6). Analysis of the low-density sucrose gradient fractions shows that the amount of Kir3.1/3.2 is not altered in lipid rafts by NCAM140. (B) In forebrain homogenates, the Kir3.1 subunit is present in the low-density fractions (lanes 3 and 4) representing the lipid raft fraction and in the high-density Triton X-100 insoluble fraction (lane 6) possibly containing cytoskeleton-associated proteins (upper panel). The blot was reprobbed with an antibody for the raft-associated non-receptor tyrosine kinase fyn (lower panel) to confirm isolation of lipid rafts. IB: Immunoblot for the molecules indicated.

(C) Bar graph showing the relative inhibition of Kir3.1/3.2 currents in CHO cells mediated by NCAM140 ( $0.14 \pm 0.04$ ), NCAM140Δ ( $0.79 \pm 0.19$ ) and NCAM120 ( $1.00 \pm 0.23$ ). Methyl-β-cyclodextrin treatment did not change NCAM120 ( $1.38 \pm 0.18$ ) and NCAM140 ( $0.17 \pm 0.13$ ) mediated inhibition, while lovastatin/mevalonate treatment rescued NCAM140-mediated inhibition ( $0.47 \pm 0.07$ ), leaving NCAM120-mediated inhibition unchanged ( $0.86 \pm 0.14$ ). Shown are amplitudes relative to Kir3.1/3.2-NCAM120 co-transfected cells. Asterisks indicate statistical significance from control, # represents statistical significance between Kir3.1/3.2+NCAM140 with and without lovastatin/mevalonate (Student's t-test;  $p < 0.01$ ). Error bars represent S.E.M.

## 12 Kir3 channel reduction by NCAM140 - altered delivery to or internalization from the plasma membrane?

To investigate how the lovastatin/mevalonate treatment rescues the inhibitory effect of NCAM140 and whether reduced surface localization of the Kir3.1/3.2 channel correlates with reduced currents also in CHO cells, the cell surface localization of Kir3.1/3.2 and Kir3.1/3.4 was analyzed by surface biotinylation (IV 3.5). A flag-epitope tag providing two lysine residues with primary NH<sub>2</sub>-groups for biotinylation was introduced in the extracellular loop of Kir3.1 (Kennedy et al., 1999) (IX 4.1.3). Single channel properties of the Kir3.1/3.2 and Kir3.1/3.4 channels and inhibition by NCAM140 were unaffected by the flag epitope (data not shown), but the flag epitope was accessible on the cell surface for  $\alpha$ -flag antibodies in Kir3.1/3.2 channels (Fig. 20).

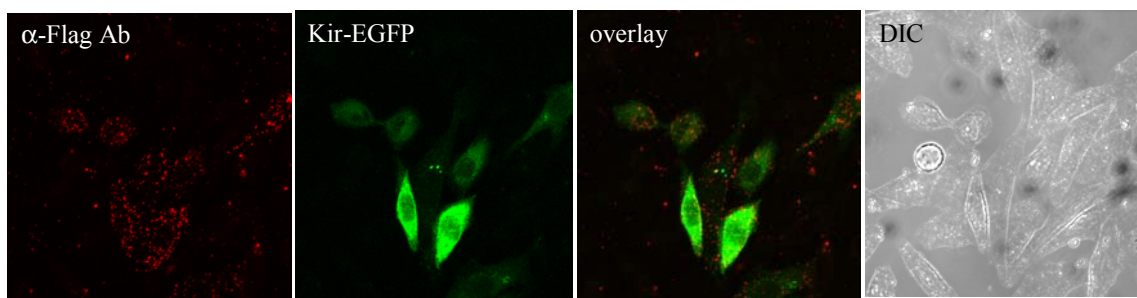


**Figure 20: The flag epitope of Kir3.1flag/3.2-EGFP channels is recognized by a  $\alpha$ -flag antibody on living cells.**

To document the accessibility of the flag epitope in Kir3.1flag/3.2 channels on the cell surface, CHO cells were transfected with Kir3.1flag/3.2-EGFP channels. Cells were incubated with monoclonal flag antibodies (IV 4.1), fixed and inspected with a confocal microscope. Only those cells that express the channel and thus appear green were stained by the antibody. However, surface staining is rather weak indicating that most of the channel is located intracellularly.

While the protein expression of Kir3.1 flag/3.2 was not modulated by NCAM140 (Fig. 21A, lanes 10-13), quantification of Kir3.1flag/3.2 and Kir3.1flag/3.4 surface localization revealed that NCAM140 (but not NCAM140 $\Delta$ ) reduced the amount of Kir3.1flag/3.2 protein (but not Kir3.1flag/3.4) in the plasma membrane by  $\sim$ 50% (n=3) (Fig. 21A lanes 8 versus 7 and 9), showing that current suppression in CHO cells by NCAM140 is due to reduction of Kir3.1flag/3.2 surface localization. Furthermore, lovastatin/mevalonate treatment did also not

alter the overall protein expression of Kir3.1/3.2 and of NCAM140 (Fig. 21A, lanes 4-6 versus 10-12), but increased the cell surface localization of Kir3.1/3.2 (lane 2 versus lanes 1 and 3). By this approach, the percentage of NCAM and Kir3.1/3.2 protein present on the cell surface could be estimated. By dividing the amount of protein which is accessible for the biotinylation reagent (lanes 9-11) by the total amount of protein present in the cell (lanes 10-12), it was estimated that only approximately 4% of the Kir3 channel is present on the cell surface, while approximately 20% of the NCAM protein are surface localized. These data support the immunohistochemical data obtained from transfected CHO cells and hippocampal neurons, where large amount of Kir3 protein could be detected intracellularly.

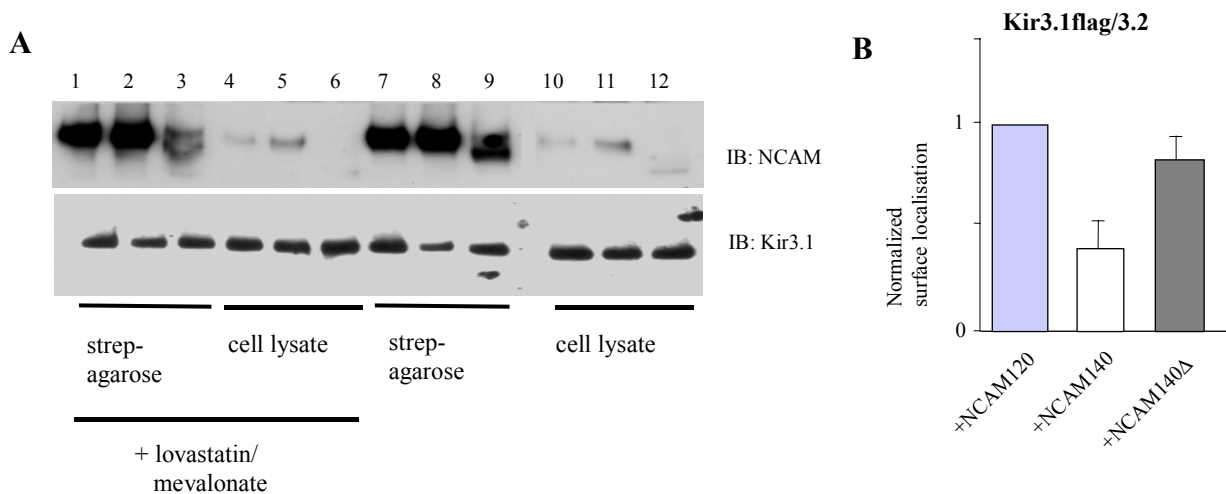


**Figure 21: NCAM140 reduces cell surface localization of Kir3.1/3.2 in CHO cells.**

(A) Western blot analysis of NCAM and Kir3.1/3.2 surface expression in CHO cells. CHO cells were co-transfected with Kir3.1/3.2 and either NCAM120 (lane 3, 6, 9, 12), NCAM140 (lane 2, 5, 8, 11) or NCAM140Δ (lane 1, 4, 7, 10). Cell lysates (lanes 4-6, 10-12) and proteins bound to streptavidin-agarose (lanes 1-3 and 7-9) were separated by SDS-PAGE and the amount of Kir3.1/3.2 or NCAM was quantified by immunoblot analysis using polyclonal NCAM antibodies (upper panels) or polyclonal Kir3.1 antibodies (lower panels). NCAM140 reduces surface localization of Kir3.1/3.2 compared to NCAM120 and NCAM140Δ co-transfected cells (lane 8 versus lanes 7 and 9), while overall intensity of Kir3.1/3.2 immunoreactive bands in the cell lysate is not altered by NCAM140 (lane 11 versus lanes 10 and 12). Incubation with lovastatin/mevalonate does not influence Kir3.1/3.2 expression (lanes 4-6 versus 10-12), but enhances surface localization of Kir3.1/3.2 (lane 2 versus lanes 1 and 3). Comparison of NCAM140 and NCAM140Δ surface expression shows that both isoforms are delivered to the surface in approximately the same amounts (lane 1 versus lane 2 and lane 7 versus lane 8). (B) Relative surface localization of Kir3.1/3.2 in the presence of NCAM140 ( $0.48 \pm 0.03$ ) and NCAM140Δ ( $0.84 \pm 0.09$ ) in comparison to NCAM120. Immunoreactive bands were quantified by densitometric analysis and expressed relative to NCAM120 (100%). Each bar represents the mean  $\pm$  SEM of 3 independent experiments.

The surface biotinylation assay also allowed the measurement of internalization rates of the Kir3.1/3.2 channel (IV 3.5). Reduced surface localization of the Kir3.1/3.2 channel by NCAM140 and NCAM180 could on the one hand result from enhanced internalization of the  $K^+$  channel while insertion into the surface membrane remains unaltered or could be, on the other hand, due to a reduced insertion into or impaired transport to the plasma membrane (see Fig. 22 for a schematic drawing).

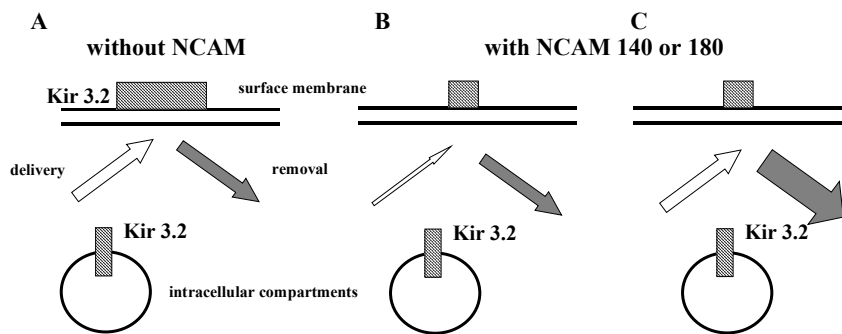


**Figure 22: Schematic drawing of the possible mechanisms of a reduced Kir3.1/3.2 surface localization.**

(A) The Kir3.1/3.2 channel is delivered to the surface from intracellular compartments and removed from the membrane with certain kinetics. Thus a steady state occurs, in which the amount of Kir3 is constant on the cell surface. Reduction of Kir3.1/3.2 surface localization by NCAM140 can either be achieved by a reduction of cell surface transport (B), leaving the internalization rate constant or enhancing internalization rates while leaving surface delivery unaltered (C).

Determination of internalized Kir3.1/3.2 channels in transfected CHO cells showed that after 1h at 37°C, less Kir3 channels were internalized in the presence of NCAM140 (Fig. 20A, lane 5) compared to NCAM120 and NCAM140Δ (Fig. 20A, lanes 4 and 6). Since also less Kir3 channels were initially surface localized in the presence of NCAM140 (Fig. 21A, lane 2 versus lanes 1 and 3), the ratio between the initial amount of Kir3.1/3.2 present at the cell surface (lanes 1-3) and the amount internalized after 1 hour (lanes 4-6) turned out to be independent of the individual NCAM isoforms (Fig. 23B). Therefore, these data show that NCAM140 does not alter the internalization rates of Kir3.1/3.2 channels, indicating that NCAM140 and NCAM180 reduce the delivery of Kir3.1/3.2 to the plasma membrane.

Kir channels have recently been shown to contain ER export/retention signals in their cytoplasmic domains, which control the number of channels in the plasma membrane (Ma et al., 2001). To determine whether on their way to the cell surface Kir3.1/3.2 channels remain to a higher degree in the endoplasmic reticulum (ER) in the presence of NCAM140 the EndoglycosidaseH (EndoH) sensitivity of Kir3.1/3.2 was measured in the presence of

NCAM140 and NCAM140 $\Delta$  (IV 3.11). Glycosylation of the core carbohydrates, which are attached to the protein in the ER, by enzymes in the Golgi apparatus confer a resistance of the carbohydrate chains towards EndoH. Hence, molecules that have entered the Golgi apparatus do not change their apparent molecular weight upon EndoH digestion. The results show that NCAM140 does not confer EndoH sensitivity to the Kir3.1/3.2 channel compared to NCAM140 $\Delta$ , indicating that the channels were not retained in the ER when NCAM140 was present (Fig. 23C). However, while the Kir3.1 immunoreactive bands do not change their apparent molecular weight at all, a small fraction of the NCAM-immunoreactive band is shifted towards lower molecular weight (Fig. 23C, lower panel). In summary, the control of the number of Kir3.1/3.2 channels in the cell surface membrane by NCAM140 is likely to occur at later stages *en route* to the membrane, presumably at the level of the trans-Golgi network due to the dependence on lipid rafts.

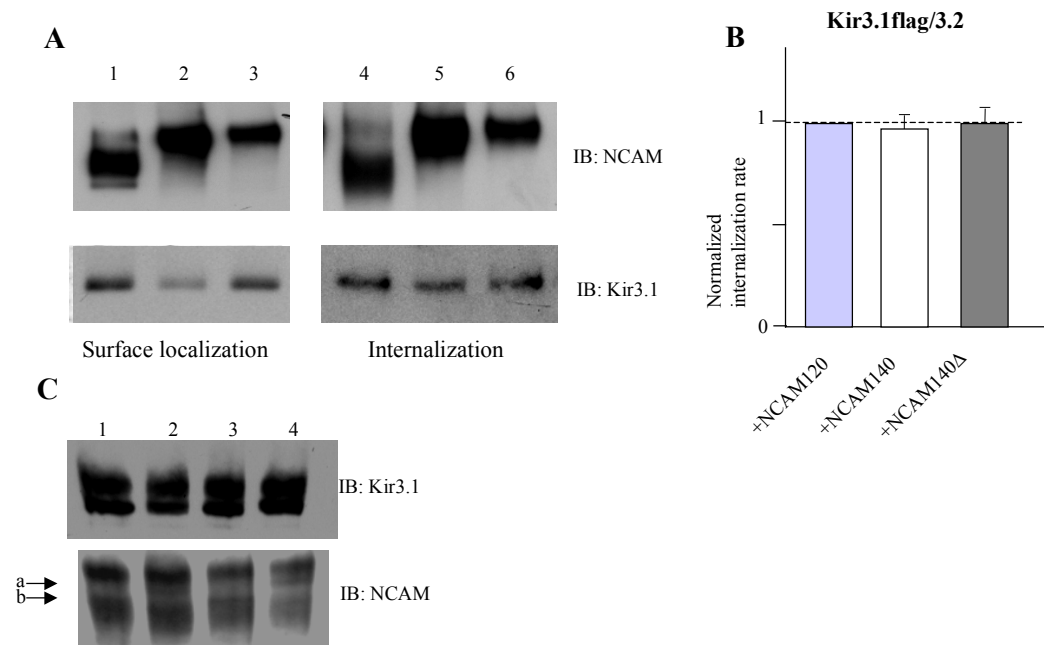


**Figure 23: NCAM did not alter internalization rates of Kir3.1/3.2 in CHO cells.**

(A) Internalization kinetics of Kir3.1/3.2 in the presence of NCAM120 (lanes 1, 4), NCAM140 (lanes 2, 5) and NCAM140 $\Delta$  (lanes 3, 6). Lanes 1-3 show the initial amount of Kir3.1/3.2 channels (upper panel) and NCAM isoforms (lower panel) present at the cell surface at 0 min. Lanes 4-6 show the amount of Kir3.1/3.2 and the individual NCAM isoforms internalized after 60 min at 37°C. Compared to NCAM, the Kir3 channel is internalized in only small amounts. (B) Internalization rates were calculated by dividing the relative intensities of Kir3.1 immunoreactive bands (normalized to co-transfection with NCAM120) after cells had been exposed to 60 min at 37°C (lanes 4 to 6) by the band intensities at 0 min (lanes 1 to 3). Kir3.1/3.2 channels are internalized with the same kinetics when co-transfected with NCAM140 (0.97±0.04) or NCAM140 $\Delta$  (1.00±0.05) compared to co-transfection with NCAM120. Bar graphs show internalization relative to NCAM120 (100%). Each bar represents the mean±S.E.M. of 2 independent experiments. IB: Immunoblot for the molecules indicated. (C)

EndoH digestion of CHO cell lysates transfected with Kir3.1/3.2 and NCAM140 $\Delta$  (lanes 1 and 2) or NCAM140 (lanes 3 and 4). Cell lysates were either treated with EndoH (lanes 1 and 3) or under the same conditions without EndoH (lanes 2 and 4). EndoH digestion does not result in a shift of the Kir3.1 immunoreactive bands (upper panel) in their apparent molecular weights, indicating that the Kir3.1/3.2 channel does not acquire an increased EndoH sensitivity in the presence of NCAM 140. In contrast, a faint band within the immunoreactive band (a) of NCAM140 and NCAM140 $\Delta$  is shifted to lower molecular weights by EndoH (b), indicating that a small fraction of NCAM140 and NCAM140 $\Delta$  is present in the ER. IB: Immunoblot for the molecules indicated. The Western blot is representative of two independent experiments.

To further support the idea that NCAM did not alter internalization rates of the Kir3.1/3.2 or Kir3.1/3.4 channels, the possible endocytosis mechanisms of the Kir3 channels were investigated. In principle, two internalization mechanisms can be defined: one is characterized by the receptor-mediated internalization such as the uptake of transferrin by the transferrin receptor. The other pathway is rather unspecific with respect to surface receptors and is therefore called fluid phase endocytosis. One prominent example is the uptake of dextran beads into the cell. It was further investigated, whether any of the channels accumulates with the fluorescent-labeled endocytosis markers intracellularly, thus providing evidences for the underlying endocytosis mechanisms of the Kir3 channels (Prekeris et al., 1998). CHO cells were transfected with the EGFP-tagged Kir3 channels and incubated with Tritc-labeled transferrin and dextran for 30 min at 37°C (IV 3.6). Since the endocytosis markers cannot be further processed, they accumulate intracellularly in late endosomes. As shown in Fig. 24, both markers are readily internalized and accumulate in intracellular organelles. However, both Kir3 channels did not co-localize with transferrin or dextran intracellularly, indicating that they are not co-internalized via these pathways. These observations support the observations that Kir3 channels are internalized slowly (see Fig. 23) and that internalization does not occur via the transferrin pathway or dextran pathway.

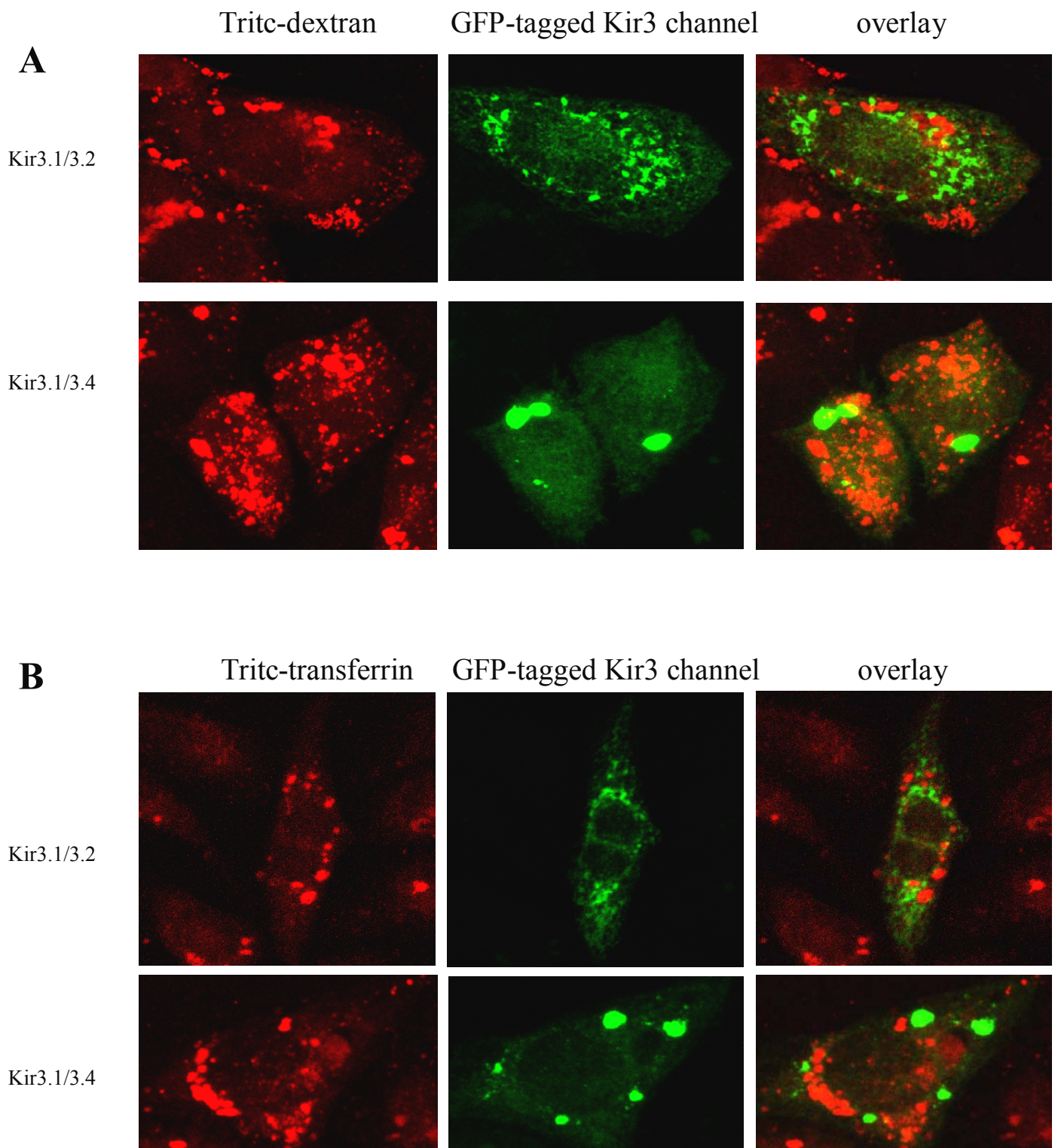


**Figure 24: Kir3.1/3.2- and Kir3.1/3.4-EGFP channels do not co-localize with the Tritc-labeled endocytosis markers transferrin and dextran.**

Representative confocal images of CHO cells transfected with Kir3.1/3.2- and Kir3.1/3.4-EGFP channels. Cells were incubated with the endocytosis markers transferrin and dextran for 30 min at 37°C, fixed and inspected by confocal microscopy. Internalized dextran (A) and transferrin (B) can readily be observed in intracellular compartments of the cells. Neither Kir3.1/3.2 nor Kir3.1/3.4 do accumulate in these compartments, indicating that the channels are not co-internalized.

### **13 Kir3.1/3.2 or Kir3.1/3.4 do not shift to a certain intracellular compartment after co-transfection with NCAM140 or NCAM180**

In order to characterize the fate of the Kir3.1/3.2 channels in the presence of NCAM140, the subcellular localization of the K<sup>+</sup> channels was investigated in the presence of the different NCAM isoforms. Since no change in the protein expression of Kir3.1/3.2 channels in the presence of NCAM140 (see V. 12) could be observed, a reduction of Kir3 surface localization might result in an accumulation of the channel in intracellular compartments. The Kir3.1/3.2- and Kir3.1/3.4-EGFP constructs were co-transfected with the individual NCAM isoforms into CHO cells and the transfected cells were stained with intracellular markers for the endoplasmatic reticulum and Golgi apparatus (IV 4.3). Although it was shown that Kir3 channels do not gain EndoH sensitivity in the presence of NCAM 140 (Fig. 23), these results were confirmed immunohistochemically by co-staining with the ER localized protein-disulfide isomerase (PDI). A co-localization of Kir3 channels with the Golgi marker adaptin was also investigated .

As shown in Fig. 25, a fraction of Kir3.1/3.2- and Kir3.1/3.4-EGFP channels co-localized with the ER marker PDI, which is not unusual for a protein that is overexpressed in a cell and thus large amounts of protein are produced and are on their way to later compartments such as Golgi. However, although difficult to quantify, no apparent redistributions could be observed of the Kir3.1/3.2- and Kir3.1/3.4-EGFP channels in the presence of NCAM140, supporting the EndoH digestion results that the Kir3.1/3.2 channel was not retained to a higher degree in the ER in the presence of NCAM140.

Additionally the co-localization of Kir3.1/3.2- and Kir3.1/3.4-EGFP channels with the Golgi apparatus was also investigated. As shown in Fig. 26, only small amounts of the Kir3.1/3.2- and Kir3.1/3.4-EGFP signal overlapped with the staining for adaptin. Moreover, this co-localization proved to be independent of the presence of NCAM isoforms. To conclude these results, it was impossible to identify a distinct intracellular compartment in which the K<sup>+</sup> channel accumulates in the presence of NCAM140.

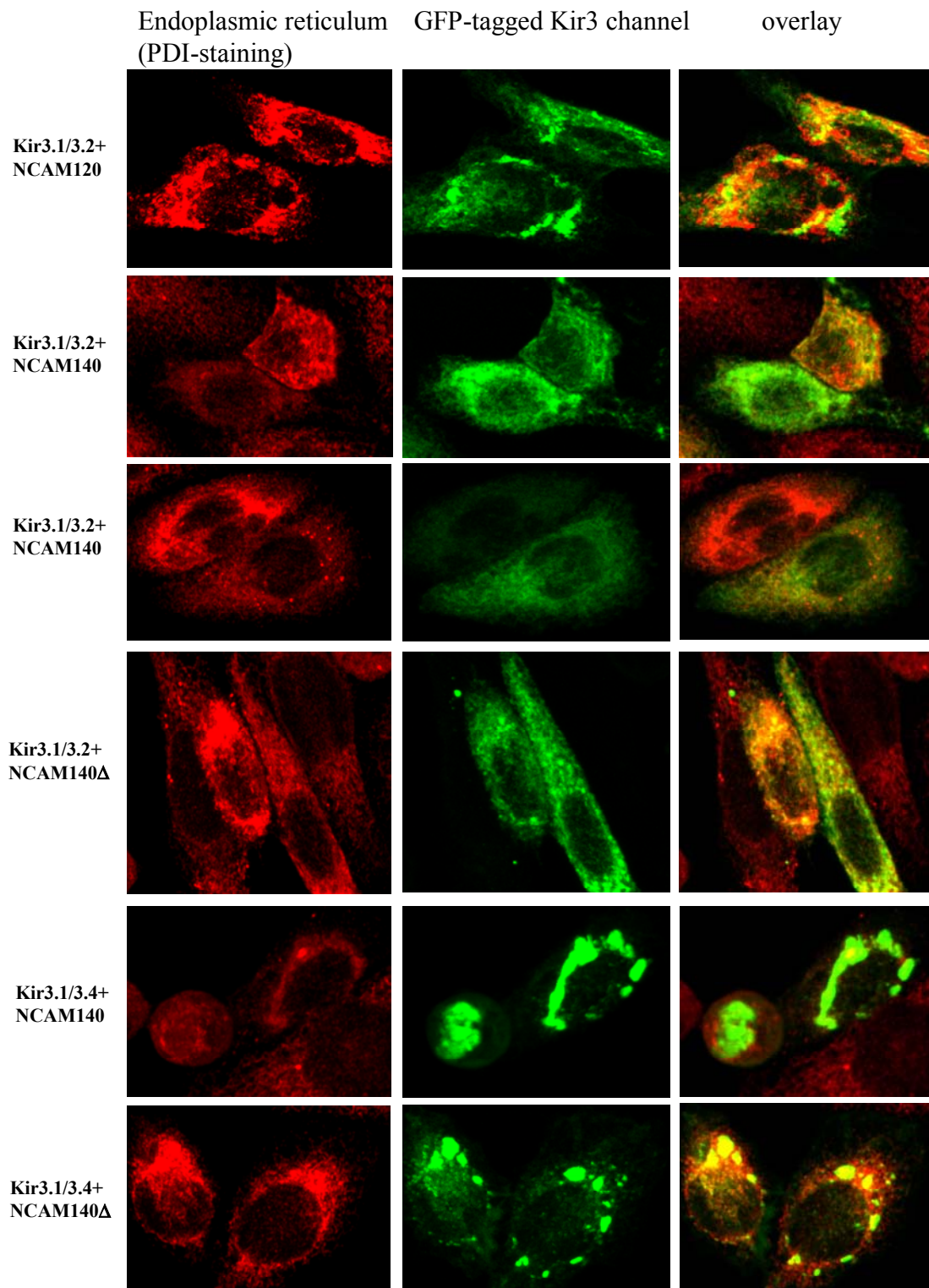


**Figure 25: Kir3.1/3.2- and Kir3.1/3.4-EGFP channels are not enriched in the endoplasmic reticulum in the presence of NCAM140.**

Representative confocal images of CHO cells co-transfected with Kir3.1/3.2- or Kir3.1/3.4-EGFP channels and the indicated NCAM isoform. Cells were fixed, stained for PDI and inspected by confocal microscopy. Although there is a partial overlap of the fluorescent signals, neither Kir3.1/3.2 nor Kir3.1/3.4 do accumulate in the ER in the presence of NCAM140, indicating that Kir3.1/3.2 is not retained in the ER by NCAM140.

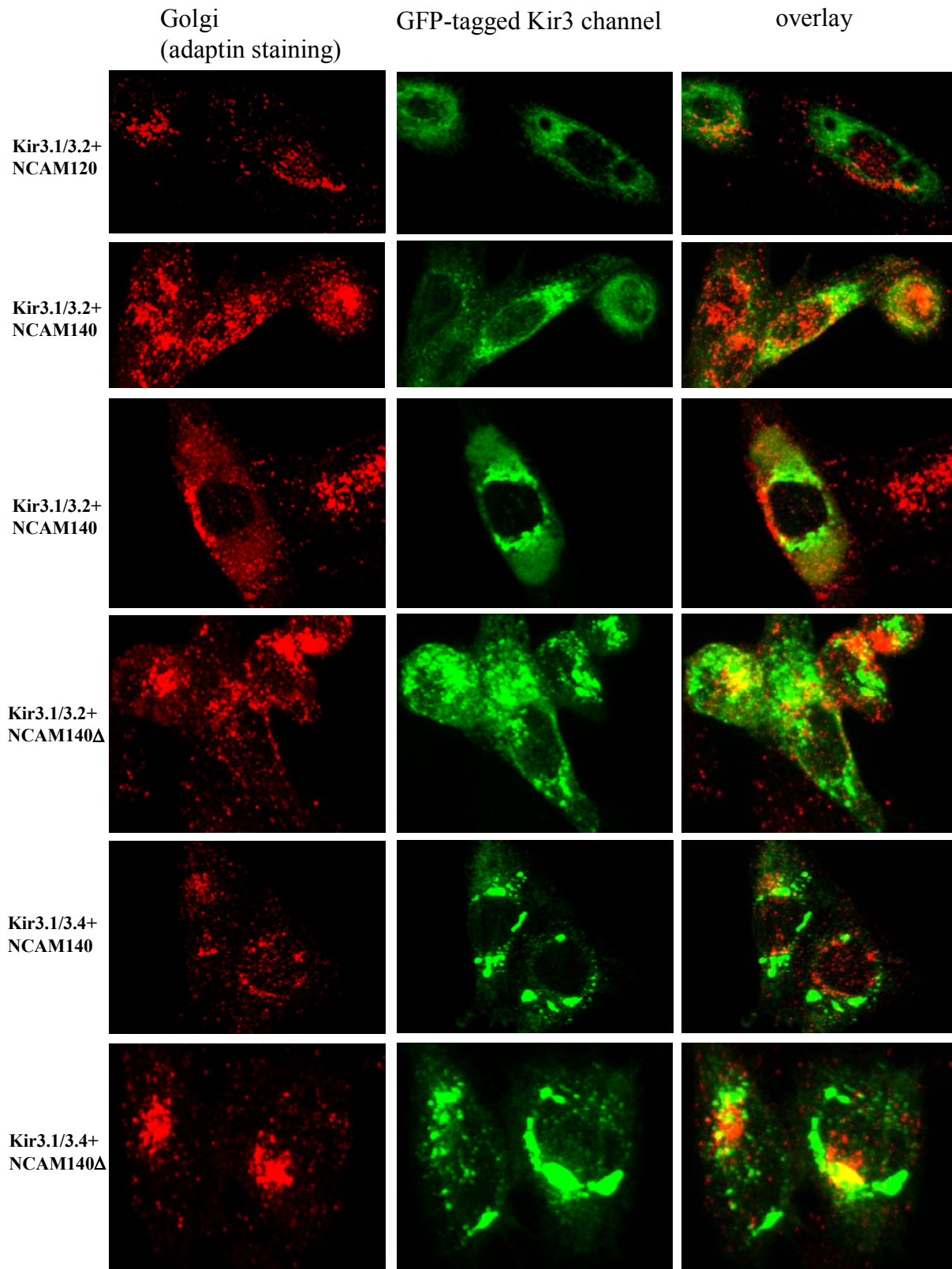


**Figure 26: Kir3.1/3.2- and Kir3.1/3.4-EGFP channels do not co-localize with the Golgi marker adaplin.**

Representative confocal images of CHO cells co-transfected with Kir3.1/3.2- or Kir3.1/3.4-EGFP channels and the indicated NCAM isoform. Cells were fixed, stained for adaplin and inspected by confocal microscopy.

Neither Kir3.1/3.2 nor Kir3.1/3.4 are retained in the Golgi when NCAM140 is present.

## VI Discussion

In the present study, the putative interplay of the neural cell adhesion molecule NCAM and the potassium channels of the Kir3 family was investigated. This study was instigated by the previous study on 5-HT<sub>1A</sub> receptor signaling in NCAM-deficient mice, where the 5-HT<sub>1A</sub> receptor had been identified to be hyper-sensitized to the receptor agonists 8-OH DPAT and buspirone (Stork et al., 1999). The 5-HT<sub>1A</sub> receptor itself, however, was unlikely to be altered, since receptor distribution and affinity in the different brain regions of NCAM deficient and wild type mice proved to be independent of the genotype. Based on these observations the option was pursued that NCAM influences Kir3 channels as the main downstream effector of 5-HT<sub>1A</sub> receptors.

### 1 NCAM140 and NCAM180 reduce plasma membrane localization of Kir3 channels

It was shown in cultured hippocampal neurons of wild type and NCAM-deficient mice and in heterologous expression systems that Kir3 currents (Kir3.1/3.2 or 3.1/3.3) are suppressed by ~60% by either NCAM140 or NCAM180. The reduction of Kir3 current by NCAM is a likely consequence of an impaired channel transport to the cell surface rather than increased internalization. In a previous study, Kir3.1 subunits in the CA1 region of the hippocampus were not only detectable on dendritic spine membranes, but also to a large extent in intracellular compartments of the cell somata. These intracellular compartments were identified as trans-Golgi network compartments and other, not fully characterized small vesicles (Drake et al., 1997). In primary thyrotroph cells, the Kir3.1 subunits were found to be associated with intracellular dense core vesicles, which upon stimulation with thyrotropin-releasing hormone fuse with the plasma membrane and thus enhance Kir3-like currents (Morishige et al., 1999). These observations are in agreement with the data from immunolabeled hippocampal neurons or EGFP-tagged Kir3.1/3.2 subunits in CHO cells showing diffuse intracellular staining that could not be attributed solely to a particular compartment, such as the endoplasmic reticulum or the Golgi apparatus. In CHO cells, a fraction of the Kir3.1/3.2- and Kir3.1/3.4-EGFP signals overlapped with the intracellular marker for the endoplasmic reticulum, indicating a partial presence of the Kir3 channels in the endoplasmic reticulum while the overlap with the Golgi marker adaptin was rather weak.

However, the presence in the endoplasmic reticulum might stem from the over-expression of the proteins by the strong CMV promoter rather than a specific ER retention of the channel, since the distribution is not altered by the presence of any of the NCAM isoforms. Furthermore, the Kir3.1/3.2 channel did not gain any EndoH sensitivity by the presence of NCAM140, supporting the observations that the channels are not retained in the ER by NCAM. Therefore, this study extends the reports on the controlled transport of Kir3 channels to the membrane (Ma et al., 2001; Morishige et al., 1999) by the idea that the number of Kir3 channels in the membrane can also be controlled by the expression and/or raft-localization of NCAM140. Since raft localization of proteins has been reported to be a regulated process (see VI 3), a long-term mechanism might be operant in neurons controlling the number of G protein accessible  $K^+$  channels in the plasma membrane and thus the maximal degree of membrane hyperpolarization by neurotransmitters.

There is growing evidence that controlled transport of receptors is a regulatory principle to modulate neuronal excitability. For instance, AMPA-receptors have recently been shown to translocate from intracellular compartments to the plasma membrane of synapses upon LTP induction (for review see Lüscher et al., 2000), a mechanism thought to convert silent synapses into functional ones. Although the exact mechanism by which NCAM controls the intracellular retention of Kir3 channels is not known yet, it was possible to demonstrate that NCAM140 has to be raft-associated within intracellular organelles to inhibit channel surface localization. Furthermore, the  $NH_2$ -terminus of the Kir3.2 subunit, which had been implicated before in channel surface delivery (Stevens et al., 1997), was identified to be the main structural determinant for NCAM140 sensitivity. The  $NH_2$ -terminus of the Kir3.2 subunit does not contain any known recognition amino acid sequences, which might have given insights into the underlying mechanisms of NCAM-mediated inhibition. However, endoplasmic reticulum export signals, which are responsible for a plasma membrane targeting in other channels (Ma et al., 2001) were not found in the primary sequence of Kir3 subunits.

## **2 Two submembranous compartments contain NCAM-isoforms**

Additionally, it was shown in this study that the three major isoforms of NCAM are present in two submembranous compartments (see also Fig. 28). One compartment comprises the Triton X-100 soluble fraction containing the majority of membrane-associated

glycoproteins. The other compartment is the low-density Triton X-100 insoluble fraction of proteins, also named lipid rafts or detergent resistant microdomains, which are characterized by their accumulation of cholesterol and sphingolipids. Typically, this fraction is enriched in GPI-linked glycoproteins, among them molecules of the immunoglobulin superfamily such as F3/F11/contactin, TAG-1/axonin-1 and Thy-1. Of the three major NCAM isoforms, the GPI-linked NCAM120 was highly enriched in lipid rafts of neuroblastoma cells. This localization of NCAM120 to rafts has also been reported previously for a permanent oligodendrocyte cell line (Kramer et al., 1999). The other two NCAM isoforms, NCAM140 and NCAM180 were shown to be located both in the Triton X-100 soluble and insoluble compartments.

### **3 Palmitoylation of NCAM140 is necessary for its localization in lipid rafts**

The data raise the question about the regulatory mechanisms determining the localization of NCAM140 in the two different compartments. Mutation of the four cysteine residues representing the palmitoylation sites in the membrane proximal domain of NCAM140 reduced the capacity of NCAM140 to associate with lipid rafts (see Fig. 27). Mutation of cysteines to serines has been proven to be a useful tool to inhibit raft localization of proteins (Kabouridis et al., 1997; Zhang et al., 1998). This localization is necessary for raft-dependent signal transduction. Abrogation of palmitoylation sites not only destroys raft localization of NCAM140, but also reduces the ability of NCAM140 to activate the fyn-FAK kinase pathway, which was monitored by phosphorylation of FAK, a direct downstream effector of fyn (Schlaepfer et al., 1994). The view that raft association of NCAM140 is necessary for activation of the fyn-FAK pathway is supported by the observation that destruction of lipid rafts by removal of cholesterol with methyl- $\beta$ -cyclodextrin also attenuates NCAM140 triggered activation of the fyn-FAK kinase pathway. This study underscores the importance of NCAM140 recruitment to lipid rafts and discloses the possibility that NCAM140 signaling can be regulated by localization of NCAM140 in lipid rafts. The mechanisms controlling enzymatic acylation of the cysteine residues in NCAM are presently unknown but will be necessary for further studies to gain insights into the functional consequences of NCAM140 accumulation in rafts. Vice versa, the mechanisms removing palmitoic acid from cysteine residues to shift NCAM140 localization from lipid rafts to the non-lipid raft compartment will need to be characterized. The results are in agreement with the observations on a switch in the palmitoylation of proteins early in the critical period,

which includes a decrease in the palmitoylation of GAP-43 and other major substrates characteristic of growth cones (Patterson and Skene, 1999). Previous studies have also shown that a similar reduction in palmitoylation of growth cone proteins is sufficient to stop neurite extension, suggesting that a developmental regulation of protein palmitoylation serves to down regulate the molecular machinery for neurite outgrowth (Hess et al., 1993; Patterson and Skene, 1994).

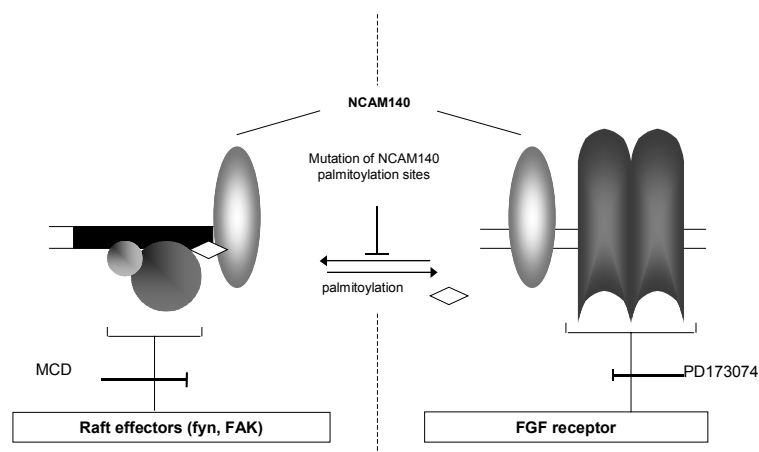


**Figure 27: Hypothetical diagram of NCAM140-distribution in the two submembranous compartments**

Within the plasma membrane, NCAM140 is partly present in lipid rafts while the majority is located outside of rafts, thus defining two submembranous compartments in which NCAM140 is present. The presence of NCAM140 in lipid rafts is regulated by palmitoylation of intracellular cysteines by yet unknown mechanisms. Upon homophilic activation, NCAM triggers distinct signal transduction pathways in the two compartments: NCAM140 phosphorylates FAK most likely via raft-associated fyn kinase in lipid rafts, while NCAM140 in the non-raft compartment facilitates FGF receptor activated downstream signaling (for detail, see Niethammer et al., submitted).

#### 4 NCAM140 regulates the transport of Kir3 channels to the cell membrane

The question whether NCAM affects Kir3.1/3.2 removal from or the transport to the membrane was illuminated by several approaches. First, a Kir3.1/3.2 construct was used, in which a flag epitope was inserted into the first extracellular loop of the Kir3.1 subunit for surface biotinylation experiments and thus quantification of membrane-bound K<sup>+</sup> channels. The insertion of the flag-epitope was necessary since the extracellular region of Kir3 channels is too small and contains no reactive amino acid side chains for biotinylation experiments. Biotinylation experiments demonstrated that in CHO cells NCAM-mediated current reduction of Kir3.1/3.2 channels is also due to a reduced surface localization like in oocytes. Furthermore, internalization assays demonstrated that the Kir3.1/3.2 channel is not

internalized faster in the presence of NCAM140, as one would expect if reduced surface localization would be due to an increased uptake of the channel. However, the Kir3.1/3.2 channels were endocytosed with the same relative kinetics independent of the co-transfected NCAM isoform. Since the Kir3.1/3.2 channels were endocytosed with slow kinetics compared to NCAM isoforms, long internalization periods of up to one hour had to be chosen, since after shorter time points hardly any internalized K<sup>+</sup> channel could be detected.

In another approach, it was tested whether Kir3.1/3.2 and Kir3.1/3.4 are internalized by different endocytosis mechanisms, which might explain their different sensitivity towards NCAM. The receptor-mediated endocytosis and the fluid-phase endocytosis were investigated by incubating Kir3.1/3.2- and Kir3.1/3.4-EGFP transfected CHO cells with fluorescent-labeled transferrin and dextran. Transferrin is the classical example of receptor-mediated endocytosis, while the latter is referred to as a fluid-phase marker. The idea was to observe any accumulation of the EGFP-labeled Kir3 channels intracellularly together with the endocytosis markers, thus giving insights into the endocytosis mechanisms of the two K<sup>+</sup> channels. However, none of the two channels accumulated with any of the endocytosis markers intracellularly, further supporting the idea that the Kir3 channels are internalized slowly in CHO cells. It is thus conceivable that NCAM interferes with the transport of the Kir3.1/3.2 channel to the plasma membrane.

## **5 Lipid rafts are involved in the transport of Kir3.1/3.2 channels to the membrane**

It was shown by this study that NCAM has to be lipid raft-associated to inhibit Kir3 transport to the cell membrane, since NCAM140 $\Delta$  did not impair surface delivery of Kir3 channels anymore. In order to dissect the potential role of lipid rafts in the NCAM-mediated surface localization of Kir3.1/3.2 channels, lipid rafts were disrupted in CHO cells by depletion of cholesterol using either methyl- $\beta$ -cyclodextrin (MCD), an agent which extracts cholesterol from the plasma membrane and thus disperses lipid rafts in the plasma membrane (Neufeld et al., 1996), or lovastatin, a blocker of the 3-HMG CoA reductase and thus of cholesterol biosynthesis. The latter treatment not only disperses lipid rafts in the plasma membrane, but also affects intracellular organelles such as the trans-Golgi network. Thus, while MCD mainly impairs signaling of raft-associated cell surface receptors such as c-ret or LAT (Tansey et al.,

2000; Harder and Kuhn, 2000) and impairs activation of the FAK kinase by NCAM140, treatment with lovastatin also destroys trans-Golgi network-associated rafts.

By this approach it was demonstrated that NCAM-mediated surface delivery of Kir3 channels is obviously not regulated by a lipid raft dependent classical “outside-in” signaling of NCAM140 from the plasma membrane into the cell, since disruption of lipid rafts in the plasma membrane by MCD did not affect the Kir3 inhibition, although it inhibited the NCAM140-mediated activation of the focal adhesion kinase, a process identified to be essential for NCAM-dependent neurite outgrowth (Beggs et al., 1997). These observations are further underlined by the results that kinase inhibitors to known NCAM-dependent signaling pathways did also not alter the surface delivery of the Kir3 channels. For instance, the inhibitors to the FGF-receptor and the MAP kinase kinase (MEK) were without effect on channel delivery. However, NCAM140-mediated inhibition of Kir3 delivery to the plasma membrane seems to depend on the association with intracellular rafts, since treatment with lovastatin/mevalonate rescued the inhibitory effect of NCAM140 on Kir3 delivery. Hence, this pharmacological approach not only gave further evidences besides the NCAM140 $\Delta$  construct for an involvement of lipid rafts, but also demonstrated that an novel lipid raft-dependent “inside-out” signaling is used by NCAM to mediate the Kir3 delivery to the membrane. This idea is also in accordance with the observations that NCAM apparently interferes with the transport of the K<sup>+</sup> channel to the membrane and not with its endocytosis.

Intracellular lipid rafts have been reported as sorting platforms both in polarized and non-polarized cells (Fig. 1) (for review, see Simons and Ikonen, 1997). For instance, lipid raft association of GPI-anchored proteins and membrane proteins was identified as an apical transport signal in polarized cells. In the TGN of polarized cells, vesicles are formed for the transport either to the basolateral side or to the apical side. While basolateral sorting is thought to be regulated predominantly via intracellular recognition motifs, the apical route transports preferentially lipid rafts carrying GPI-anchored proteins and apical transmembrane proteins. In addition to GPI-anchors and specific membrane-spanning regions, N-glycans may also be used as apical sorting signals by binding to raft-associated lectins. Basolateral signals are believed to govern localization of the protein, when both basolateral and apical sorting signals are present in the molecule (Simons and Ikonen, 1997). Although CHO cells are non-polarized cells, there is evidence that fibroblasts have apical and basolateral routes from the TGN to the plasma membrane (Simons and Ikonen, 1997; Yoshimori et al., 1996). Therefore, the above-mentioned mechanisms could also hold true for the CHO cell line used in this study.

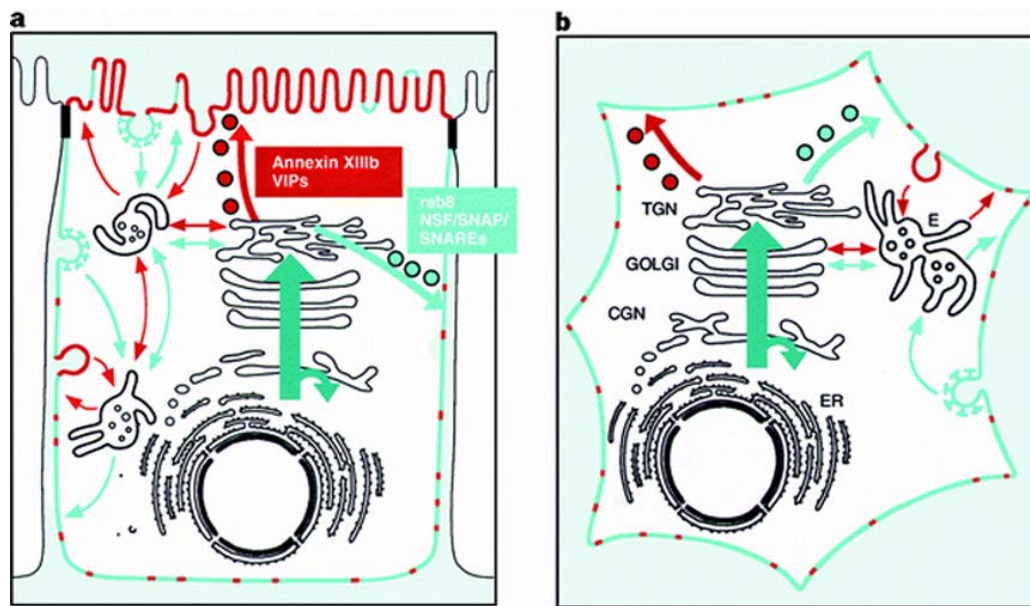


**Figure 28: A model proposed by Simons and Ikonen (1997) for two post-Golgi circuits in polarized MDCK cells (a) and unpolarized fibroblasts (b).**

After proteins have entered the TGN, they can be sorted by at least to pathways: Sorting in the raft circuit (in red) is based on sphingolipid–cholesterol microdomains functioning as sorting platforms to which vesicular integral membrane proteins (VIPs) associate as stabilizers. The other circuit (in green) employs sorting signals in the cytoplasmic tails as well as adaptor and coat proteins binding to them. The red regions of the plasma membrane are sphingolipid–cholesterol rafts and the green areas are phosphatidylcholine-enriched regions. The exact arrangement of the post-Golgi traffic map, including the return routes to the TGN, is still under investigation.

One may speculate that the fundamental principle of Kir3 sorting in the TGN is functional in the cell types investigated and that NCAM140 controls either partitioning of Kir3 to a particular transport route or insertion into the membrane. Since Kir3.1 subunits are present in the Triton X-100 insoluble low-density or lipid-raft fraction of brain lysates, Kir3.1/3.2 surface localization may be controlled by a yet unknown NCAM-dependent raft-associated protein. This idea is supported by the observation that NCAM120, albeit present in lipid rafts (Niethammer et al., submitted), does not modulate Kir3 delivery, probably due to the absence of an intracellular domain. However, the intracellular domain of NCAM140 is also not sufficient for inhibition of Kir3 transport to the plasma membrane, suggesting that the transmembrane region of NCAM140 is important for the raft-association of NCAM140.

It has been suggested that hippocampal neurons have a transport route equivalent to the apical pathway for delivery of proteins and lipids from the Golgi complex to the axons, whereas the dendrites are supplied by the basolateral routes (Dotti and Simons, 1990). Whether the NCAM-mediated reduction of Kir3 currents in oocytes, fibroblasts and hippocampal neurons is finally the product of an NCAM-dependent missorting of the Kir3 channel in the cell or a regulated intracellular retention has not been investigated yet.

Surprisingly, only little is known about the transport mechanisms of Kir3 channels in neurons: Although Kir3 channels are localized in the somata and dendrites of neurons suggesting basolateral delivery, they were also found in the axons indicating apical transport routes (Ponce et al., 1996). The immunohistochemical data of hippocampal neurons are supported by these reports. Raft-association of K<sup>+</sup> channels has so far only been reported for the Kv1.5 and the Shaker K<sup>+</sup> channel (Martens et al., 2000a; Martens et al., 2000b), but not for any of the Kir channels.

## **6 Physiological relevance of adhesion molecules regulating the number of inhibitory potassium channels**

The combined observations of this study allow speculating on the involvement of NCAM in the 5-HT<sub>1A</sub> receptor-mediated regulation of Kir3 channels. It was shown previously that the number of NCAM180-positive synapses is doubled in the hippocampus after induction of LTP (Schuster et al., 1998), which is thought to enhance synapse strength. As suggested by the present study another result of NCAM180 up-regulation would be a down-regulation of inhibitory Kir3 potassium channels and thus a reduction in the amplitudes of slow inhibitory postsynaptic potentials caused by a variety of neurotransmitters. As already discussed, palmitoylation of NCAM might also function as a regulatory mechanism for Kir3 channels. As discussed above, regulation of protein palmitoylation serves to down regulate the molecular machinery for neurite outgrowth (Hess et al., 1993; Patterson and Skene, 1994). Following this hypothesis, changes in the palmitoylation status would not only affect neuritogenesis, but would also fine-tune the excitability of the cell. As a consequence of reduced Kir3 channel activity during periods of NCAM protein up-regulation, postsynaptic cell impedance increases and neurons become more sensitive to synaptic inputs, which may be particularly important during neuritogenesis and synapse formation. In NCAM<sup>-/-</sup> mice, the increased activity of 5-HT<sub>1A</sub> receptor stimulated Kir3 channels may be causal for a lower excitability of target neurons for serotonergic fibers in the limbic system, and thus altered levels of aggression and anxiety. Although the behavioral consequences of NCAM-dependent Kir3 channel regulation remain to be elucidated on a cellular basis, this study provides first insights into some of the molecular determinants regulating neuronal long-term excitability by controlling the number of active potassium channels in the membrane.

## VII Summary

In the present study, the putative functional interplay of the neural cell adhesion molecule NCAM and the G protein-coupled inwardly rectifying potassium channels, also termed Kir3 channels, was investigated. This study was instigated by the previous study on 5-HT<sub>1A</sub> receptor signaling in NCAM-deficient (NCAM<sup>-/-</sup>) mice, where the HT<sub>1A</sub> receptor had been identified to be hyper-sensitized to its agonists 8-OH DPAT and buspirone. The 5-HT<sub>1A</sub> receptor itself, however, was unlikely to be altered in NCAM<sup>-/-</sup> mice, since receptor distribution and affinity in the different brain regions of NCAM<sup>-/-</sup> and wild type mice proved to be independent of the genotype. The option was therefore pursued that NCAM might influence Kir3 channels as the main downstream effector of 5-HT<sub>1A</sub> receptors.

In hippocampal neurons of NCAM<sup>-/-</sup> mice, Kir3-like currents were increased by ~240% compared to wild type neurons, or in other words, in the presence of NCAM Kir3-like currents were reduced by ~40% compared to hippocampal neurons in which NCAM was absent. Reconstitution of the Kir3-signaling system in the heterologous expression systems of CHO cells and oocytes showed that the inhibitory effect of NCAM on Kir3 channels is also operant in these cells: cotransfection of NCAM140 and NCAM180, those NCAM isoforms that contain an intracellular domain, together with the neuronal Kir3.1/3.2 and Kir3.1/3.3 channels reduced Kir3-mediated currents by ~70%, while cotransfection with NCAM120, a GPI-linked NCAM isoform, was without effect. The specificity of inhibition was underscored by the observations that currents of the cardiac Kir3.1/3.4 channel and members of the Kir2 family were not affected by NCAM140 or NCM180. Using cell surface biotinylation assays and green fluorescent protein-tagged Kir3 channels, it was demonstrated in oocytes and CHO cells that reduction of NCAM140 and NCAM180-mediated currents are due to a reduced surface localization of the channels. Internalization and protein expression of Kir3 channels were not affected by NCAM140, suggesting that NCAM140 regulates the transport of the Kir3 channels to the membrane. On a molecular basis, the NH<sub>2</sub>-terminus of the Kir3.2 subunit was identified as the major structural determinant for the influence of NCAM on K<sup>+</sup> channel targeting to the cell surface, but further breakdown of the Kir3.2 NH<sub>2</sub>-terminus did not identify any recognition motifs responsible for the reduced delivery to the cell surface. In search for the signaling mechanisms by which NCAM controls the Kir3 channel delivery, neither acute stimulation of NCAM nor kinase inhibitors known to mediate NCAM signaling affected Kir3 inhibition rates. Furthermore, NCAM140 and the Kir3 channels did not physically associate with each other in the cell membrane. However, it was shown for the first

time that both NCAM140 and Kir3.1/3.2 channels are localized in detergent-resistant microdomains, also called lipid rafts. Interestingly, disruption of NCAM140 raft association either by mutating NCAM140 palmitoylation sites or by dispersing intracellular but not plasma membrane rafts rescued Kir3 surface transport in the presence of NCAM140. These results point towards a novel “inside-out” signaling mechanism by which intracellular palmitoylated NCAM molecules regulate cell surface delivery and thus the amount of G protein-accessible Kir3 channels in the plasma membrane.

As a physiological consequence of this regulatory mechanism, it is conceivable that a reduced Kir3 channel activity during periods of NCAM protein up-regulation, such as development and increase of synaptic strength induced by learning and memory, increases the impedance of postsynaptic membranes and thus neurons become more sensitive to synaptic activation. Hence, this study demonstrates for the first time on a molecular basis how cell adhesion molecules can modulate synaptic strength of neurons, which is an important ingredient of nervous system function.

## VII Zusammenfassung

Im Rahmen dieser Arbeit wurde die Wechselwirkung zwischen dem neuronalen Zellerkennungsmolekül NCAM und G-Protein-aktivierten Kaliumkanälen (Kir3 Kanäle) untersucht. Diese Arbeit baute auf Untersuchungen auf, in denen gezeigt werden konnte, dass der 5-HT<sub>1A</sub>-Rezeptor bei NCAM-defizienten Mäusen (NCAM<sup>-/-</sup>) bezüglich seiner Agonisten Buspiron und 8-OH DPAT im Vergleich zu Wildtyp-Mäusen hypersensitiviert ist. Weder die Affinität, noch die Expression des 5-HT<sub>1A</sub>-Rezeptors weisen in den Gehirnen von NCAM<sup>-/-</sup>- gegenüber Wildtyp-Mäusen signifikante Unterschiede auf. Da auch der Serotonin-Metabolismus offensichtlich nicht gestört war, wurde die Möglichkeit in Betracht gezogen, dass NCAM das Effektorsystem des 5-HT<sub>1A</sub>-Rezeptors, also die Kir3-Kanäle, beeinflusst. Die ersten Experimente zeigten, dass Kir3-vermittelte Ströme in Kulturen hippocampaler Neuronen von NCAM<sup>-/-</sup>- versus Wildtyp-Mäusen signifikante Unterschiede aufwiesen. So waren die Kir3-abhängigen, einwärts-gerichteten Ströme in Neuronen von NCAM<sup>-/-</sup>-Mäusen um etwa 240% im Vergleich zu Wildtyp-Mäusen erhöht, was mit anderen Worten einer Reduktion der Kir3-Ströme in Anwesenheit von NCAM um etwa 40% entspricht. Auch in heterologen Expressionssystemen inhibierte NCAM die Kir3-Kanäle. So führte die Koexpression von NCAM140 und NCAM180, jenen Isoformen mit einer intrazellulären Domäne, zu einer 80%igen Reduktion der neuronalen Kir3.1/3.2- und Kir3.1/3.3-vermittelten Ströme, welches in etwa der Größenordnung entspricht, wie sie in hippocampalen Neuronen beobachtet wurde. Interessanterweise reagierten nicht alle NCAM-Isoformen bzw. alle Kir3-Kanäle gleich: So zeigte die Koexpression der GPI-verankerten NCAM120-Isoform keinen Effekt auf die neuronalen Kir3-Ströme. Desweiteren wurde weder der herzspezifische Kir3.1/3.4-Kanal noch der aus der Kir2-Familie stammende Kir2.1-Kanal durch die Anwesenheit von NCAM140 oder NCAM180 beeinflusst. Durch Oberflächenbiotinylierung und Fluoreszenzmarkierung der Kir3-Kanäle konnte gezeigt werden, dass NCAM140 und NCAM180 die Oberflächenlokalisation des Kir3.1/3.2-Kanals, nicht aber des Kir3.1/3.4-Kanals, um ca. 50% reduzierten. Darüber hinaus wurden Einzelleitfähigkeit und Offenwahrscheinlichkeit des Kir3-Kanals nicht durch NCAM beeinflusst, so dass die NCAM-abhängige Inhibition der Kir3-Ströme vermutlich auf eine reduzierte Membranlokalisation der K<sup>+</sup>-Kanäle zurückzuführen ist. Da weder die Proteinexpression noch die Internalisierung des Kir3.1/3.2-Kanals durch NCAM140 beeinflusst wurden, ist es naheliegend, dass NCAM den Transport des Kanals zur Membran verminderte. Als strukturelle Determinante für die NCAM-Sensitivität konnte der intrazelluläre NH<sub>2</sub>-Terminus der Kir3.2-Untereinheit

identifiziert werden. Die Inhibition durch NCAM140 konnte allerdings nicht auf ein bestimmtes Aminosäuremotiv innerhalb des NH<sub>2</sub>-Terminus eingegrenzt werden.

Ferner hatten weder die akute Stimulation von NCAM durch polyklonale NCAM-Antikörper noch der Einsatz von Kinase-Inhibitoren gegen die NCAM-vermittelten Signaltransduktionswege einen Effekt auf den Kir3-Transport zur Membran, wodurch ein klassisches „Outside-in Signaling“ von NCAM als möglicher Mechanismus unwahrscheinlich wurde. Auch waren die Kir3-Kanäle nicht direkt mit NCAM140 in der Membran assoziiert, womit ein weiterer Mechanismus für die NCAM-vermittelte Inhibition entfiel. Allerdings waren sowohl die NCAM-Isoformen als auch die Kir3-Kanäle mit detergenten-resistenten Mikrodomänen, auch lipid rafts genannt, assoziiert. Die Anwesenheit von NCAM140 in diesen Zellmembran „lipid-rafts“ scheint essentiell für seine Funktion als Oberflächen-Rezeptor zu sein. Diese Assoziation von NCAM140 mit „lipid-rafts“ wird über palmitoylierte intrazelluläre Cysteinreste vermittelt. Interessanterweise konnte die Inhibition der Kir3-Oberflächenlokalisation durch die Mutation der NCAM140-Palmitoylierungsstellen oder durch die Zerstörung von intrazellulären, nicht aber Oberflächen „lipid rafts“, aufgehoben werden. Diese Ergebnisse deuten auf einen völlig neuen „inside-out Signaling“-Mechanismus hin, mit der die maximale Zahl von aktivierbaren K<sup>+</sup>-Kanälen entweder über die Expression oder aber über die Palmitoylierung von NCAM140 bzw. NCAM180 reguliert werden kann. Eine mögliche physiologische Konsequenz dieses Regulationsmechanismus wäre, dass parallel zu einer Hochregulation der NCAM-Expression, zum Beispiel während der Ontogenese und der Festigung von synaptischen Kontakten, der elektrische Widerstand der Postsynapse aufgrund der reduzierten Anzahl von K<sup>+</sup>-Kanälen steigt und damit die Neurone bezüglich ihrer Transmission leichter erregbar werden. Die Ergebnisse zeigen damit zum ersten Mal auf molekularer Ebene auf, wie ein Zellerkennungsmolekül in die synaptischen Übertragungsprozesse eingreifen und damit so entscheidende Prozesse wie die synaptische Plastizität beeinflussen kann.

## VIII References

- Aarts, L. H., Verkade, P., van Dalen, J. J., van Rozen, A. J., Gispen, W. H., Schrama, L. H., and Schotman, P. (1999). B-50/GAP-43 potentiates cytoskeletal reorganization in raft domains. *Mol. Cell Neurosci.* *14*, 85-97.
- Aguilar-Bryan, L., Clement, J. P., Gonzalez, G., Kunjilwar, K., Babenko, A., and Bryan, J. (1998). Toward understanding the assembly and structure of KATP channels. *Physiol Rev.* *78*, 227-245.
- Ashcroft, F. M., Harrison, D. E., and Ashcroft, S. J. (1984). Glucose induces closure of single potassium channels in isolated rat pancreatic beta-cells. *Nature* *312*, 446-448.
- Ashcroft, F. M. and Rorsman, P. (1989). Electrophysiology of the pancreatic beta-cell. *Prog. Biophys. Mol. Biol.* *54*, 87-143.
- Ausrubel, F. M. (1996). *Current Protocols in Molecular Biology*. (Brooklyn, New York: Greene Publishing Associates, Inc.).
- Babenko, A. P., Aguilar-Bryan, L., and Bryan, J. (1998). A view of sur/KIR6.X, KATP channels. *Annu. Rev. Physiol* *60*, 667-687.
- Becker, C. G., Artola, A., Gerardy-Schahn, R., Becker, T., Welzl, H., and Schachner, M. (1996). The polysialic acid modification of the neural cell adhesion molecule is involved in spatial learning and hippocampal long-term potentiation. *J. Neurosci. Res.* *45*, 143-152.
- Beggs, H. E., Baragona, S. C., Hemperly, J. J., and Maness, P. F. (1997). NCAM140 interacts with the focal adhesion kinase p125(fak) and the SRC- related tyrosine kinase p59(fyn). *J. Biol. Chem.* *272*, 8310-8319.
- Brackenbury, R., Thiery, J. P., Rutishauser, U., and Edelman, G. M. (1977). Adhesion among neural cells of the chick embryo. I. An immunological assay for molecules involved in cell-cell binding. *J. Biol. Chem.* *252*, 6835-6840.
- Brown, D. A. and London, E. (1998). Functions of lipid rafts in biological membranes. *Annu. Rev. Cell Dev. Biol.* *14*, 111-136.
- Bruckner, K., Pablo, L. J., Scheiffele, P., Herb, A., Seeburg, P. H., and Klein, R. (1999). EphrinB ligands recruit GRIP family PDZ adaptor proteins into raft membrane microdomains. *Neuron* *22*, 511-524.
- Brümmendorf, T. and Rathjen, F. G. (1994). Cell adhesion molecules. 1: immunoglobulin superfamily. *Protein Profile.* *1*, 951-1058.
- Chan, K. W., Langan, M. N., Sui, J. L., Kozak, J. A., Pabon, A., Ladias, J. A., and Logothetis, D. E. (1996a). A recombinant inwardly rectifying potassium channel coupled to GTP- binding proteins. *J. Gen. Physiol* *107*, 381-397.
- Chan, K. W., Sui, J. L., Vivaudou, M., and Logothetis, D. E. (1996b). Control of channel activity through a unique amino acid residue of a G protein-gated inwardly rectifying K<sup>+</sup> channel subunit. *Proc. Natl. Acad. Sci. U. S. A* *93*, 14193-14198.

- Chen, H. C., Chan, P. C., Tang, M. J., Cheng, C. H., and Chang, T. J. (1998). Tyrosine phosphorylation of focal adhesion kinase stimulated by hepatocyte growth factor leads to mitogen-activated protein kinase activation. *J. Biol. Chem.* *273*, 25777-25782.
- Cinek, T. and Horejsi, V. (1992). The nature of large noncovalent complexes containing glycosyl- phosphatidylinositol-anchored membrane glycoproteins and protein tyrosine kinases. *J. Immunol.* *149*, 2262-2270.
- Cohen, N. A., Brenman, J. E., Snyder, S. H., and Brecht, D. S. (1996). Binding of the inward rectifier K<sup>+</sup> channel Kir 2.3 to PSD-95 is regulated by protein kinase A phosphorylation. *Neuron* *17*, 759-767.
- Cole, G. J. and Glaser, L. (1986). A heparin-binding domain from N-CAM is involved in neural cell- substratum adhesion. *J. Cell Biol.* *102*, 403-412.
- Cole, G. J., Loewy, A., Cross, N. V., Akeson, R., and Glaser, L. (1986). Topographic localization of the heparin-binding domain of the neural cell adhesion molecule N-CAM. *J. Cell Biol.* *103*, 1739-1744.
- Cremer, H., Chazal, G., Goridis, C., and Represa, A. (1997). NCAM is essential for axonal growth and fasciculation in the hippocampus. *Mol. Cell Neurosci.* *8*, 323-335.
- Cremer, H., Lange, R., Christoph, A., Plomann, M., Vopper, G., Roes, J., Brown, R., Baldwin, S., Kraemer, P., Scheff, S., and . (1994). Inactivation of the N-CAM gene in mice results in size reduction of the olfactory bulb and deficits in spatial learning. *Nature* *367*, 455-459.
- Crossin, K. L. and Krushel, L. A. (2000). Cellular signaling by neural cell adhesion molecules of the immunoglobulin superfamily. *Dev. Dyn.* *218*, 260-279.
- Cunningham, B. A., Hemperly, J. J., Murray, B. A., Prediger, E. A., Brackenbury, R., and Edelman, G. M. (1987). Neural cell adhesion molecule: structure, immunoglobulin-like domains, cell surface modulation, and alternative RNA splicing. *Science* *236*, 799-806.
- DiMagno, L., Dascal, N., Davidson, N., Lester, H. A., and Schreibmayer, W. (1996). Serotonin and protein kinase C modulation of a rat brain inwardly rectifying K<sup>+</sup> channel expressed in xenopus oocytes. *Pflugers Arch.* *431*, 335-340.
- Doherty, P., Barton, C. H., Dickson, G., Seaton, P., Rowett, L. H., Moore, S. E., Gower, H. J., and Walsh, F. S. (1989). Neuronal process outgrowth of human sensory neurons on monolayers of cells transfected with cDNAs for five human N-CAM isoforms. *J. Cell Biol.* *109*, 789-798.
- Doherty, P., Fazeli, M. S., and Walsh, F. S. (1995). The neural cell adhesion molecule and synaptic plasticity. *J. Neurobiol.* *26*, 437-446.
- Doherty, P., Fruns, M., Seaton, P., Dickson, G., Barton, C. H., Sears, T. A., and Walsh, F. S. (1990). A threshold effect of the major isoforms of NCAM on neurite outgrowth. *Nature* *343*, 464-466.

- Doherty, P., Skaper, S. D., Moore, S. E., Leon, A., and Walsh, F. S. (1992). A developmentally regulated switch in neuronal responsiveness to NCAM and N-cadherin in the rat hippocampus. *Development* *115*, 885-892.
- Doherty, P. and Walsh, F. S. (1992). Cell adhesion molecules, second messengers and axonal growth. *Curr. Opin. Neurobiol.* *2*, 595-601.
- Dotti, C. G. and Simons, K. (1990). Polarized sorting of viral glycoproteins to the axon and dendrites of hippocampal neurons in culture. *Cell* *62*, 63-72.
- Doyle, E., Nolan, P. M., Bell, R., and Regan, C. M. (1992). Hippocampal NCAM180 transiently increases sialylation during the acquisition and consolidation of a passive avoidance response in the adult rat. *J. Neurosci. Res.* *31*, 513-523.
- Dörries, U., Taylor, J., Xiao, Z., Lochter, A., Montag, D., and Schachner, M. (1996). Distinct effects of recombinant tenascin-C domains on neuronal cell adhesion, growth cone guidance, and neuronal polarity. *J. Neurosci. Res.* *43*, 420-438.
- Drake, C. T., Bausch, S. B., Milner, T. A., and Chavkin, C. (1997). GIRK1 immunoreactivity is present predominantly in dendrites, dendritic spines, and somata in the CA1 region of the hippocampus. *Proc. Natl. Acad. Sci. U. S. A* *94*, 1007-1012.
- Eckhardt, M., Bukalo, O., Chazal, G., Wang, L., Goridis, C., Schachner, M., Gerardy-Schahn, R., Cremer, H., and Dityatev, A. (2000). Mice deficient in the polysialyltransferase ST8SiaIV/PST-1 allow discrimination of the roles of neural cell adhesion molecule protein and polysialic acid in neural development and synaptic plasticity. *J. Neurosci.* *20*, 5234-5244.
- Edelman, G. M., Cunningham, B. A., Gall, W. E., Gottlieb, P. D., Rutishauser, U., and Waxdal, M. J. (1969). The covalent structure of an entire gammaG immunoglobulin molecule. *Proc. Natl. Acad. Sci. U. S. A* *63*, 78-85.
- Engel, J. (1991). Domains in proteins and proteoglycans of the extracellular matrix with functions in assembly and cellular activities. *Int. J. Biol. Macromol.* *13*, 147-151.
- Fakler, B., Brandle, U., Glowatzki, E., Weidemann, S., Zenner, H. P., and Ruppersberg, J. P. (1995). Strong voltage-dependent inward rectification of inward rectifier K<sup>+</sup> channels is caused by intracellular spermine. *Cell* *80*, 149-154.
- Fakler, B., Brandle, U., Glowatzki, E., Zenner, H. P., and Ruppersberg, J. P. (1994). Kir2.1 inward rectifier K<sup>+</sup> channels are regulated independently by protein kinases and ATP hydrolysis. *Neuron* *13*, 1413-1420.
- Fenton, R. G., Kung, H. F., Longo, D. L., and Smith, M. R. (1992). Regulation of intracellular actin polymerization by prenylated cellular proteins. *J. Cell Biol.* *117*, 347-356.
- Fields, R. D. and Itoh, K. (1996). Neural cell adhesion molecules in activity-dependent development and synaptic plasticity. *Trends Neurosci.* *19*, 473-480.
- Frangioni, J. V. and Neel, B. G. (1993). Solubilization and purification of enzymatically active glutathione S-transferase (pGEX) fusion proteins. *Anal. Biochem.* *210*, 179-187.

- Friedrich, M., Benndorf, K., Schwalb, M., and Hirche, H. (1990). Effects of anoxia on K and Ca currents in isolated guinea pig cardiocytes. *Pflugers Arch.* *416*, 207-209.
- Graeff, F. G., Guimaraes, F. S., De Andrade, T. G., and Deakin, J. F. (1996). Role of 5-HT in stress, anxiety, and depression. *Pharmacol. Biochem. Behav.* *54*, 129-141.
- Gribble, F. M., Tucker, S. J., and Ashcroft, F. M. (1997). The essential role of the Walker A motifs of SUR1 in K-ATP channel activation by Mg-ADP and diazoxide. *EMBO J.* *16*, 1145-1152.
- Harder, T. and Kuhn, M. (2000). Selective accumulation of raft-associated membrane protein LAT in T cell receptor signaling assemblies. *J. Cell Biol.* *151*, 199-208.
- Harkins, A. B., Dlouhy, S., Ghetti, B., Cahill, A. L., Won, L., Heller, B., Heller, A., and Fox, A. P. (2000). Evidence of elevated intracellular calcium levels in weaver homozygote mice. *J. Physiol* *524 Pt 2*, 447-455.
- Henry, P., Pearson, W. L., and Nichols, C. G. (1996). Protein kinase C inhibition of cloned inward rectifier (HRK1/KIR2.3) K<sup>+</sup> channels expressed in *Xenopus* oocytes. *J. Physiol* *495 (Pt 3)*, 681-688.
- Hess, D. T., Patterson, S. I., Smith, D. S., and Skene, J. H. (1993). Neuronal growth cone collapse and inhibition of protein fatty acylation by nitric oxide. *Nature* *366*, 562-565.
- Hess, E. J. (1996). Identification of the weaver mouse mutation: the end of the beginning. *Neuron* *16*, 1073-1076.
- Hibino, H., Horio, Y., Inanobe, A., Doi, K., Ito, M., Yamada, M., Gotow, T., Uchiyama, Y., Kawamura, M., Kubo, T., and Kurachi, Y. (1997). An ATP-dependent inwardly rectifying potassium channel, KAB-2 (Kir4. 1), in cochlear stria vascularis of inner ear: its specific subcellular localization and correlation with the formation of endocochlear potential. *J. Neurosci.* *17*, 4711-4721.
- Hille, B. (1992). G protein-coupled mechanisms and nervous signaling. *Neuron* *9*, 187-195.
- Ho, K., Nichols, C. G., Lederer, W. J., Lytton, J., Vassilev, P. M., Kanazirska, M. V., and Hebert, S. C. (1993). Cloning and expression of an inwardly rectifying ATP-regulated potassium channel. *Nature* *362*, 31-38.
- Hoffman, S. and Edelman, G. M. (1983). Kinetics of homophilic binding by embryonic and adult forms of the neural cell adhesion molecule. *Proc. Natl. Acad. Sci. U. S. A* *80*, 5762-5766.
- Hooper, N. M. (1997). Glycosyl-phosphatidylinositol anchored membrane enzymes. *Clin. Chim. Acta* *266*, 3-12.
- Huang, C. L., Jan, Y. N., and Jan, L. Y. (1997). Binding of the G protein betagamma subunit to multiple regions of G protein-gated inward-rectifying K<sup>+</sup> channels. *FEBS Lett.* *405*, 291-298.

- Huang, C. L., Slesinger, P. A., Casey, P. J., Jan, Y. N., and Jan, L. Y. (1995). Evidence that direct binding of G beta gamma to the GIRK1 G protein-gated inwardly rectifying K<sup>+</sup> channel is important for channel activation. *Neuron* *15*, 1133-1143.
- Inanobe, A., Yoshimoto, Y., Horio, Y., Morishige, K. I., Hibino, H., Matsumoto, S., Tokunaga, Y., Maeda, T., Hata, Y., Takai, Y., and Kurachi, Y. (1999). Characterization of G-protein-gated K<sup>+</sup> channels composed of Kir3.2 subunits in dopaminergic neurons of the substantia nigra. *J. Neurosci.* *19*, 1006-1017.
- Inoue, H., Nojima, H., and Okayama, H. (1990). High efficiency transformation of *Escherichia coli* with plasmids. *Gene* *96*, 23-28.
- Isomoto, S., Kondo, C., and Kurachi, Y. (1997). Inwardly rectifying potassium channels: their molecular heterogeneity and function. *Jpn. J. Physiol* *47*, 11-39.
- Jelacic, T. M., Kennedy, M. E., Wickman, K., and Clapham, D. E. (2000). Functional and biochemical evidence for G-protein-gated inwardly rectifying K<sup>+</sup> (GIRK) channels composed of GIRK2 and GIRK3. *J. Biol. Chem.* *275*, 36211-36216.
- Jorgensen, O. S. (1995). Neural cell adhesion molecule (NCAM) as a quantitative marker in synaptic remodeling. *Neurochem. Res.* *20*, 533-547.
- Kabouridis, P. S., Magee, A. I., and Ley, S. C. (1997). S-acylation of LCK protein tyrosine kinase is essential for its signalling function in T lymphocytes. *EMBO J.* *16*, 4983-4998.
- Kadmon, G., Kowitz, A., Altevogt, P., and Schachner, M. (1990). Functional cooperation between the neural adhesion molecules L1 and N-CAM is carbohydrate dependent. *J. Cell Biol.* *110*, 209-218.
- Karschin, C. and Karschin, A. (1997). Ontogeny of Gene Expression of Kir Channel Subunits in the Rat. *Mol. Cell Neurosci.* *10*, 131-148.
- Keilhauer, G., Faissner, A., and Schachner, M. (1985). Differential inhibition of neurone-neurone, neurone-astrocyte and astrocyte-astrocyte adhesion by L1, L2 and N-CAM antibodies. *Nature* *316*, 728-730.
- Keller, P. and Simons, K. (1998). Cholesterol is required for surface transport of influenza virus hemagglutinin. *J. Cell Biol.* *140*, 1357-1367.
- Kennedy, M. E., Nemecek, J., Corey, S., Wickman, K., and Clapham, D. E. (1999). GIRK4 confers appropriate processing and cell surface localization to G-protein-gated potassium channels. *J. Biol. Chem.* *274*, 2571-2582.
- Kofuji, P., Davidson, N., and Lester, H. A. (1995). Evidence that neuronal G-protein-gated inwardly rectifying K<sup>+</sup> channels are activated by G beta gamma subunits and function as heteromultimers. *Proc. Natl. Acad. Sci. U. S. A* *92*, 6542-6546.
- Kofuji, P., Hofer, M., Millen, K. J., Millonig, J. H., Davidson, N., Lester, H. A., and Hatten, M. E. (1996). Functional analysis of the weaver mutant GIRK2 K<sup>+</sup> channel and rescue of weaver granule cells. *Neuron* *16*, 941-952.

- Kolkova, K., Novitskaya, V., Pedersen, N., Berezin, V., and Bock, E. (2000a). Neural cell adhesion molecule-stimulated neurite outgrowth depends on activation of protein kinase C and the Ras-mitogen-activated protein kinase pathway. *J. Neurosci.* *20*, 2238-2246.
- Kolkova, K., Pedersen, N., Berezin, V., and Bock, E. (2000b). Identification of an amino acid sequence motif in the cytoplasmic domain of the NCAM-140 kDa isoform essential for its neurotogenic activity. *J. Neurochem.* *75*, 1274-1282.
- Kornblihtt, A. R., Umezawa, K., Vibe-Pedersen, K., and Baralle, F. E. (1985). Primary structure of human fibronectin: differential splicing may generate at least 10 polypeptides from a single gene. *EMBO J.* *4*, 1755-1759.
- Kozak, M. (1986). Point mutations define a sequence flanking the AUG initiator codon that modulates translation by eukaryotic ribosomes. *Cell* *44*, 283-292.
- Kramer, E. M., Klein, C., Koch, T., Boytinck, M., and Trotter, J. (1999). Compartmentation of Fyn kinase with glycosylphosphatidylinositol- anchored molecules in oligodendrocytes facilitates kinase activation during myelination. *J. Biol. Chem.* *274*, 29042-29049.
- Krapivinsky, G., Gordon, E. A., Wickman, K., Velimirovic, B., Krapivinsky, L., and Clapham, D. E. (1995). The G-protein-gated atrial K<sup>+</sup> channel IKACH is a heteromultimer of two inwardly rectifying K<sup>(+)</sup>-channel proteins. *Nature* *374*, 135-141.
- Krapivinsky, G., Kennedy, M. E., Nemeč, J., Medina, I., Krapivinsky, L., and Clapham, D. E. (1998). Gbeta binding to GIRK4 subunit is critical for G protein-gated K<sup>+</sup> channel activation. *J. Biol. Chem.* *273*, 16946-16952.
- Kronenberg, M., Siu, G., Hood, L. E., and Shastri, N. (1986). The molecular genetics of the T-cell antigen receptor and T-cell antigen recognition. *Annu. Rev. Immunol.* *4*, 529-591.
- Krushel, L. A., Cunningham, B. A., Edelman, G. M., and Crossin, K. L. (1999). NF-kappaB activity is induced by neural cell adhesion molecule binding to neurons and astrocytes. *J. Biol. Chem.* *274*, 2432-2439.
- Kubo, Y., Baldwin, T. J., Jan, Y. N., and Jan, L. Y. (1993). Primary structure and functional expression of a mouse inward rectifier potassium channel. *Nature* *362*, 127-133.
- Laemmli, U. K. (1970). Cleavage of structural proteins during the assembly of the head of bacteriophage T4. *Nature* *227*, 680-685.
- Lesage, F., Guillemare, E., Fink, M., Duprat, F., Heurteaux, C., Fosset, M., Romey, G., Barhanin, J., and Lazdunski, M. (1995). Molecular properties of neuronal G-protein-activated inwardly rectifying K<sup>+</sup> channels. *J. Biol. Chem.* *270*, 28660-28667.
- Liao, Y. J., Jan, Y. N., and Jan, L. Y. (1996). Heteromultimerization of G-protein-gated inwardly rectifying K<sup>+</sup> channel proteins GIRK1 and GIRK2 and their altered expression in weaver brain. *J. Neurosci.* *16*, 7137-7150.
- Little, E. B., Crossin, K. L., Krushel, L. A., Edelman, G. M., and Cunningham, B. A. (2001). A short segment within the cytoplasmic domain of the neural cell adhesion molecule (N-CAM) is essential for N-CAM-induced NF-kappa B activity in astrocytes. *Proc. Natl. Acad. Sci. U. S. A* *98*, 2238-2243.

- Little, E. B., Edelman, G. M., and Cunningham, B. A. (1998). Palmitoylation of the cytoplasmic domain of the neural cell adhesion molecule N-CAM serves as an anchor to cellular membranes. *Cell Adhes. Commun.* *6*, 415-430.
- Lüscher, C., Jan, L. Y., Stoffel, M., Malenka, R. C., and Nicoll, R. A. (1997). G protein-coupled inwardly rectifying K<sup>+</sup> channels (GIRKs) mediate postsynaptic but not presynaptic transmitter actions in hippocampal neurons. *Neuron* *19*, 687-695.
- Lüscher, C., Nicoll, R. A., Malenka, R. C., and Muller, D. (2000). Synaptic plasticity and dynamic modulation of the postsynaptic membrane. *Nat. Neurosci.* *3*, 545-550.
- Ma, D., Zerangue, N., Lin, Y. F., Collins, A., Yu, M., Jan, Y. N., and Jan, L. Y. (2001). Role of ER Export Signals in Controlling Surface Potassium Channel Numbers. *Science* *291*, 316-319.
- Mackie, K., Sorkin, B. C., Nairn, A. C., Greengard, P., Edelman, G. M., and Cunningham, B. A. (1989). Identification of two protein kinases that phosphorylate the neural cell-adhesion molecule, N-CAM. *J. Neurosci.* *9*, 1883-1896.
- Mark, M. D. and Herlitze, S. (2000). G-protein mediated gating of inward-rectifier K<sup>+</sup> channels. *Eur. J. Biochem.* *267*, 5830-5836.
- Martens, J. R., Navarro-Polanco, R., Coppock, E. A., Nishiyama, A., Parshley, L., Grobaski, T. D., and Tamkun, M. M. (2000a). Differential targeting of Shaker-like potassium channels to lipid rafts. *J. Biol. Chem.* *275*, 7443-7446.
- Martens, J. R., Sakamoto, N., Sullivan, S. A., Grobaski, T. D., and Tamkun, M. M. (2000b). Isoform-specific localization of voltage-gated K<sup>+</sup> channels to distinct lipid raft populations: Targeting of Kv1.5 to caveolae. *J. Biol. Chem.* *276*, 8409-8414.
- McNicholas, C. M., Wang, W., Ho, K., Hebert, S. C., and Giebisch, G. (1994). Regulation of ROMK1 K<sup>+</sup> channel activity involves phosphorylation processes. *Proc. Natl. Acad. Sci. U. S. A* *91*, 8077-8081.
- Melkonian, K. A., Ostermeyer, A. G., Chen, J. Z., Roth, M. G., and Brown, D. A. (1999). Role of lipid modifications in targeting proteins to detergent-resistant membrane rafts. Many raft proteins are acylated, while few are prenylated. *J. Biol. Chem.* *274*, 3910-3917.
- Mohammadi, M., Froum, S., Hamby, J. M., Schroeder, M. C., Panek, R. L., Lu, G. H., Eliseenkova, A. V., Green, D., Schlessinger, J., and Hubbard, S. R. (1998). Crystal structure of an angiogenesis inhibitor bound to the FGF receptor tyrosine kinase domain. *EMBO J.* *17*, 5896-5904.
- Montixi, C., Langlet, C., Bernard, A. M., Thimonier, J., Dubois, C., Wurbel, M. A., Chauvin, J. P., Pierres, M., and He, H. T. (1998). Engagement of T cell receptor triggers its recruitment to low-density detergent-insoluble membrane domains. *EMBO J.* *17*, 5334-5348.
- Morishige, K., Inanobe, A., Yoshimoto, Y., Kurachi, H., Murata, Y., Tokunaga, Y., Maeda, T., Maruyama, Y., and Kurachi, Y. (1999). Secretagogue-induced exocytosis recruits G protein-gated K<sup>+</sup> channels to plasma membrane in endocrine cells. *J. Biol. Chem.* *274*, 7969-7974.

- Muller, D., Wang, C., Skibo, G., Toni, N., Cremer, H., Calaora, V., Rougon, G., and Kiss, J. Z. (1996). PSA-NCAM is required for activity-induced synaptic plasticity. *Neuron* *17*, 413-422.
- Murase, S. and Schuman, E. M. (1999). The role of cell adhesion molecules in synaptic plasticity and memory. *Curr. Opin. Cell Biol.* *11*, 549-553.
- Neufeld, E. B., Cooney, A. M., Pitha, J., Dawidowicz, E. A., Dwyer, N. K., Pentchev, P. G., and Blanchette-Mackie, E. J. (1996). Intracellular trafficking of cholesterol monitored with a cyclodextrin. *J. Biol. Chem.* *271*, 21604-21613.
- Nichols, C. G. and Lopatin, A. N. (1997). Inward rectifier potassium channels. *Annu. Rev. Physiol* *59*, 171-191.
- Ochsenbauer, C., Dubay, S. R., and Hunter, E. (2000). The Rous sarcoma virus Env glycoprotein contains a highly conserved motif homologous to tyrosine-based endocytosis signals and displays an unusual internalization phenotype. *Mol. Cell Biol.* *20*, 249-260.
- Ono, K., Tomasiewicz, H., Magnuson, T., and Rutishauser, U. (1994). N-CAM mutation inhibits tangential neuronal migration and is phenocopied by enzymatic removal of polysialic acid. *Neuron* *13*, 595-609.
- Orr, H. T., Lancet, D., Robb, R. J., Lopez de Castro, J. A., and Strominger, J. L. (1979). The heavy chain of human histocompatibility antigen HLA-B7 contains an immunoglobulin-like region. *Nature* *282*, 266-270.
- Patterson, S. I. and Skene, J. H. (1994). Novel inhibitory action of tunicamycin homologues suggests a role for dynamic protein fatty acylation in growth cone-mediated neurite extension. *J. Cell Biol.* *124*, 521-536.
- Patterson, S. I. and Skene, J. H. (1999). A shift in protein S-palmitoylation, with persistence of growth-associated substrates, marks a critical period for synaptic plasticity in developing brain. *J. Neurobiol.* *39*, 423-437.
- Peiro, S., Comella, J. X., Enrich, C., Martin-Zanca, D., and Rocamora, N. (2000). PC12 cells have caveolae that contain TrkA. *J. Biol. Chem.* *275*, 37846-37852.
- Persohn, E., Pollerberg, G. E., and Schachner, M. (1989). Immunoelectron-microscopic localization of the 180 kD component of the neural cell adhesion molecule N-CAM in postsynaptic membranes. *J. Comp Neurol.* *288*, 92-100.
- Pollerberg, E. G., Sadoul, R., Goridis, C., and Schachner, M. (1985). Selective expression of the 180-kD component of the neural cell adhesion molecule N-CAM during development. *J. Cell Biol.* *101*, 1921-1929.
- Ponce, A., Bueno, E., Kentros, C., Vega-Saenz, d. M., Chow, A., Hillman, D., Chen, S., Zhu, L., Wu, M. B., Wu, X., Rudy, B., and Thornhill, W. B. (1996). G-protein-gated inward rectifier K<sup>+</sup> channel proteins (GIRK1) are present in the soma and dendrites as well as in nerve terminals of specific neurons in the brain. *J. Neurosci.* *16*, 1990-2001.

- Prekeris, R., Klumperman, J., Chen, Y. A., and Scheller, R. H. (1998). Syntaxin 13 mediates cycling of plasma membrane proteins via tubulovesicular recycling endosomes. *J. Cell Biol.* *143*, 957-971.
- Probstmeier, R., Kuhn, K., and Schachner, M. (1989). Binding properties of the neural cell adhesion molecule to different components of the extracellular matrix. *J. Neurochem.* *53*, 1794-1801.
- Regan, C. M. and Fox, G. B. (1995). Polysialylation as a regulator of neural plasticity in rodent learning and aging. *Neurochem. Res.* *20*, 593-598.
- Retzer, M. D., Kabani, A., Button, L. L., Yu, R. H., and Schryvers, A. B. (1996). Production and characterization of chimeric transferrins for the determination of the binding domains for bacterial transferrin receptors. *J. Biol. Chem.* *271*, 1166-1173.
- Rogalski, S. L., Appleyard, S. M., Pattillo, A., Terman, G. W., and Chavkin, C. (2000). TrkB activation by brain-derived neurotrophic factor inhibits the G protein-gated inward rectifier Kir3 by tyrosine phosphorylation of the channel. *J. Biol. Chem.* *275*, 25082-25088.
- Ronn, L. C., Hartz, B. P., and Bock, E. (1998). The neural cell adhesion molecule (NCAM) in development and plasticity of the nervous system. *Exp. Gerontol.* *33*, 853-864.
- Rosen, C. L., Lisanti, M. P., and Salzer, J. L. (1992). Expression of unique sets of GPI-linked proteins by different primary neurons in vitro. *J. Cell Biol.* *117*, 617-627.
- Ruoslahti, E. and Pierschbacher, M. D. (1987). New perspectives in cell adhesion: RGD and integrins. *Science* *238*, 491-497.
- Ruppersberg, J. P. (2000). Intracellular regulation of inward rectifier K<sup>+</sup> channels. *Pflugers Arch.* *441*, 1-11.
- Ruppersberg, J. P. and Fakler, B. (1996). Complexity of the regulation of Kir2.1 K<sup>+</sup> channels. *Neuropharmacology* *35*, 887-893.
- Rutishauser, U. (1990). Neural cell adhesion molecule as a regulator of cell-cell interactions. *Adv. Exp. Med. Biol.* *265*, 179-183.
- Rutishauser, U. and Jessell, T. M. (1988). Cell adhesion molecules in vertebrate neural development. *Physiol Rev.* *68*, 819-857.
- Saffell, J. L., Williams, E. J., Mason, I. J., Walsh, F. S., and Doherty, P. (1997). Expression of a dominant negative FGF receptor inhibits axonal growth and FGF receptor phosphorylation stimulated by CAMs [published erratum appears in *Neuron* 1998 Mar;20(3):619]. *Neuron* *18*, 231-242.
- Saiki, R. K., Gelfand, D. H., Stoffel, S., Scharf, S. J., Higuchi, R., Horn, G. T., Mullis, K. B., and Erlich, H. A. (1988). Primer-directed enzymatic amplification of DNA with a thermostable DNA polymerase. *Science* *239*, 487-491.
- Sambrook, J., Fritsch, E. F., and Maniatis, T. (1989). *Molecular cloning: A Laboratory Manual*. (Cold Spring Harbor: Cold Spring Harbor Laboratory).

- Santoni, M. J., Barthels, D., Vopper, G., Boned, A., Goridis, C., and Wille, W. (1989). Differential exon usage involving an unusual splicing mechanism generates at least eight types of NCAM cDNA in mouse brain. *EMBO J.* 8, 385-392.
- Schachner, M. (1991). Cell surface recognition and neuron-glia interactions. *Ann. N. Y. Acad. Sci.* 633, 105-112.
- Schachner, M. (1997). Neural recognition molecules and synaptic plasticity. *Curr. Opin. Cell Biol.* 9, 627-634.
- Schachner, M. and Martini, R. (1995). Glycans and the modulation of neural-recognition molecule function. *Trends Neurosci.* 18, 183-191.
- Schlaepfer, D. D., Hanks, S. K., Hunter, T., and van der Geer P. (1994). Integrin-mediated signal transduction linked to Ras pathway by GRB2 binding to focal adhesion kinase. *Nature* 372, 786-791.
- Schmidt, A., Hannah, M. J., and Huttner, W. B. (1997). Synaptic-like microvesicles of neuroendocrine cells originate from a novel compartment that is continuous with the plasma membrane and devoid of transferrin receptor. *J. Cell Biol.* 137, 445-458.
- Schuch, U., Lohse, M. J., and Schachner, M. (1989). Neural cell adhesion molecules influence second messenger systems. *Neuron* 3, 13-20.
- Schuster, T., Krug, M., Hassan, H., and Schachner, M. (1998). Increase in proportion of hippocampal spine synapses expressing neural cell adhesion molecule NCAM180 following long-term potentiation. *J. Neurobiol.* 37, 359-372.
- Signorini, S., Liao, Y. J., Duncan, S. A., Jan, L. Y., and Stoffel, M. (1997). Normal cerebellar development but susceptibility to seizures in mice lacking G protein-coupled, inwardly rectifying K<sup>+</sup> channel GIRK2. *Proc. Natl. Acad. Sci. U. S. A* 94, 923-927.
- Simons, K. and Ikonen, E. (1997). Functional rafts in cell membranes. *Nature* 387, 569-572.
- Slesinger, P. A., Reuveny, E., Jan, Y. N., and Jan, L. Y. (1995). Identification of structural elements involved in G protein gating of the GIRK1 potassium channel. *Neuron* 15, 1145-1156.
- Sontheimer, H., Kettenmann, H., Schachner, M., and Trotter, J. The Neural Cell Adhesion Molecule (N-CAM) Modulates K<sup>+</sup> Channels in Cultured Glial Precursor Cells. *Eur. J. Neurosci.* 3, 230-236. 1990.
- Sporns, O., Edelman, G. M., and Crossin, K. L. (1995). The neural cell adhesion molecule (N-CAM) inhibits proliferation in primary cultures of rat astrocytes. *Proc. Natl. Acad. Sci. U. S. A* 92, 542-546.
- Springer, T. A. (1990). Adhesion receptors of the immune system. *Nature* 346, 425-434.
- Stefanova, I., Horejsi, V., Ansotegui, I. J., Knapp, W., and Stockinger, H. (1991). GPI-anchored cell-surface molecules complexed to protein tyrosine kinases. *Science* 254, 1016-1019.

- Stevens, E. B., Woodward, R., Ho, I. H., and Murrell-Lagnado, R. (1997). Identification of regions that regulate the expression and activity of G protein-gated inward rectifier K<sup>+</sup> channels in *Xenopus* oocytes. *J. Physiol* *503* ( Pt 3), 547-562.
- Stork, O., Welzl, H., Cremer, H., and Schachner, M. (1997). Increased intermale aggression and neuroendocrine response in mice deficient for the neural cell adhesion molecule (NCAM). *Eur. J. Neurosci.* *9*, 1117-1125.
- Stork, O., Welzl, H., Wotjak, C. T., Hoyer, D., Delling, M., Cremer, H., and Schachner, M. (1999). Anxiety and increased 5-HT<sub>1A</sub> receptor response in NCAM null mutant mice. *J. Neurobiol.* *40*, 343-355.
- Tansey, M. G., Baloh, R. H., Milbrandt, J., and Johnson, E. M., Jr. (2000). GFR $\alpha$ -mediated localization of RET to lipid rafts is required for effective downstream signaling, differentiation, and neuronal survival. *Neuron* *25*, 611-623.
- Thiery, J. P., Brackenbury, R., Rutishauser, U., and Edelman, G. M. (1977). Adhesion among neural cells of the chick embryo. II. Purification and characterization of a cell adhesion molecule from neural retina. *J. Biol. Chem.* *252*, 6841-6845.
- Thomas, U., Kim, E., Kuhlendahl, S., Koh, Y. H., Gundelfinger, E. D., Sheng, M., Garner, C. C., and Budnik, V. (1997). Synaptic clustering of the cell adhesion molecule fasciclin II by discs-large and its role in the regulation of presynaptic structure. *Neuron* *19*, 787-799.
- Tomasiewicz, H., Ono, K., Yee, D., Thompson, C., Goridis, C., Rutishauser, U., and Magnuson, T. (1993). Genetic deletion of a neural cell adhesion molecule variant (N-CAM-180) produces distinct defects in the central nervous system. *Neuron* *11*, 1163-1174.
- Towbin, H., Staehelin, T., and Gordon, J. (1979). Electrophoretic transfer of proteins from polyacrylamide gels to nitrocellulose sheets: procedure and some applications. *Proc. Natl. Acad. Sci. U. S. A* *76*, 4350-4354.
- van't Hof, W. and Resh, M. D. (1997). Rapid plasma membrane anchoring of newly synthesized p59fyn: selective requirement for NH<sub>2</sub>-terminal myristoylation and palmitoylation at cysteine-3. *J. Cell Biol.* *136*, 1023-1035.
- Wang, W., Hebert, S. C., and Giebisch, G. (1997). Renal K<sup>+</sup> channels: structure and function. *Annu. Rev. Physiol* *59*, 413-436.
- Wickman, K. and Clapham, D. E. (1995). Ion channel regulation by G proteins. *Physiol Rev.* *75*, 865-885.
- Williams, E. J., Mittal, B., Walsh, F. S., and Doherty, P. (1995). FGF inhibits neurite outgrowth over monolayers of astrocytes and fibroblasts expressing transfected cell adhesion molecules. *J. Cell Sci.* *108* ( Pt 11), 3523-3530.
- Wischmeyer, E., Doring, F., and Karschin, A. (1998). Acute suppression of inwardly rectifying Kir2.1 channels by direct tyrosine kinase phosphorylation. *J. Biol. Chem.* *273*, 34063-34068.

- Wischmeyer, E., Doring, F., Wischmeyer, E., Spauschus, A., Thomzig, A., Veh, R., and Karschin, A. (1997). Subunit interactions in the assembly of neuronal Kir3.0 inwardly rectifying K<sup>+</sup> channels. *Mol. Cell Neurosci.* *9*, 194-206.
- Wischmeyer, E. and Karschin, A. (1996). Receptor stimulation causes slow inhibition of IRK1 inwardly rectifying K<sup>+</sup> channels by direct protein kinase A-mediated phosphorylation. *Proc. Natl. Acad. Sci. U. S. A* *93*, 5819-5823.
- Xavier, R., Brennan, T., Li, Q., McCormack, C., and Seed, B. (1998). Membrane compartmentation is required for efficient T cell activation. *Immunity.* *8*, 723-732.
- Xiao, Z. C., Taylor, J., Montag, D., Rougon, G., and Schachner, M. (1996). Distinct effects of recombinant tenascin-R domains in neuronal cell functions and identification of the domain interacting with the neuronal recognition molecule F3/11. *Eur. J. Neurosci.* *8*, 766-782.
- Yoshimori, T., Keller, P., Roth, M. G., and Simons, K. (1996). Different biosynthetic transport routes to the plasma membrane in BHK and CHO cells. *J. Cell Biol.* *133*, 247-256.
- Zerangue, N., Schwappach, B., Jan, Y. N., and Jan, L. Y. (1999). A new ER trafficking signal regulates the subunit stoichiometry of plasma membrane K(ATP) channels. *Neuron* *22*, 537-548.
- Zhang, W., Tribble, R. P., and Samelson, L. E. (1998). LAT palmitoylation: its essential role in membrane microdomain targeting and tyrosine phosphorylation during T cell activation. *Immunity.* *9*, 239-246.

## IX APPENDIX

### 1 ABBREVIATIONS

∅	“without”, diameter
× g	g-force
aa	amino acid
A	adenine
Acc	accession number
Amp	ampicillin
APS	ammoniumperoxodisulfate
ATCC	<i>American Type Culture Collection</i>
ATP	adenosine triphosphate
bp	base pairs
BSA	bovine serum albumine
C	Cytosine
cDNA	complementary deoxyribonucleic acid
CHO	Chinese Hamster Ovary
CMV	cytomegalie virus
CTP	cytosine triphosphate
dATP	2'-desoxyadenosinetriphosphate
dCTP	2'-desoxycytidinetriphosphate
DEPC	diethylpyrocarbonate
DIC	differential interference image
DMEM	Dulbeccos modified eagle medium
dGTP	2'-desoxyguanosinetriphosphate
DMSO	dimethylsulfoxide
DNA	deoxyribonucleic acid
DNase	deoxyribonuclease
dNTP	2'-desoxyribonucleotide-5'-triphosphate
DRM	detergent-resistant microdomains
DTT	dithiothreitol
<i>E. coli</i>	<i>escherichia coli</i>
EDTA	ethylendiamintetraacetic acid
EGFP	enhanced green fluorescent protein
f.c.	final concentration
FCS	fetal calf serum
FGF	fibroblast growth factor
G	guanosine
GCG	Genetic Computer Group
GMEM	Glasgow modified eagle medium
h	human, hour
HEPES	2-(4-(2-Hydroxyethyl)-piperzino)-ethansulfonic acid
IB	immunoblotting
IH	immunohistochemistry
IP	immunopräzipitation
IPTG	isopropyl-β-D-thiogalactoside
Kana	kanamycin

kb	kilo base pairs
Kir	K <sup>+</sup> inwardly rectifying channel
LB	Luria Bertani
MCD	methylcyclodextrin
MEM	minimal essential medium
MESNa	2-mercaptoethanesulfonic acid
MOPS	(4-(N-morpholino)-propan)-sulfonic acid
mRNA	messenger ribonucleic acid
Nt	nucleotide
OD <sub>x</sub>	optic density
ORF	open reading frame
PAGE	polyacrylamide gel electrophoresis
PBS	phosphate-buffered saline
PCR	polymerase chain reaction
PDI	protein-disulfide isomerase
PEG	polyethyleneglycol
PMSF	phenylmethylsulfonylfluoride
RIPA buffer	radioimmunoprecipitation buffer
rpm	rounds per minute
psi	pounds per square inch
RNA	ribonucleic acid
RNase	ribonuclease
RT	room temperature
SDS	sodium dodecyl sulfate
SOE	splicing by overlap extension
T	thymine
TABS	(N-tris(Hydroxymethyl)methyl-3-aminopropane-sulfonic acid
Tab.	table
TBS	Tris-buffered saline
TE	tris-EDTA
TEMED	N,N,N',N'-tetraethylenamine
Tet	tetracycline
TGN	Trans-Golgi network
T <sub>m</sub>	melting temperature
TM	transmembrane segment
Tris	tris(-hydroxymethyl)-aminomethane
U	unit (enzymatic)
V	volt
v/v	volume per volume
Vol.	volume
w/v	weight per volume
ZMNH	Zentrum für Molekulare Neurobiologie Hamburg

Amino acids were abbreviated using the one letter code.

## 2 Oligonucleotides

Nr.	PRIMER	Sequence (5' - 3')	remarks
1	EGFP/EcoEhe-up	AAC GAA TTC <u>GGC GCC</u> ATG GTG AGC AAG GGC GAG GAG CTG	EheI site
2	EGFP/XhoIEhe-dn	AAA CTC GAG <u>GGC GCC</u> CTT GTA CAG CTC GTC CAT GCC GAG	EheI site
3	EGFPint368-up	TGG TGA ACC GCA TCG AGC	For sequencing
4	EGFPint368-dn	GCT CGA TGC GGT TCA CCA	For sequencing
5	pDsred/EcoEhe-up	AAC GAA TTC <u>GGC GCC</u> ATG GTG CGC TCC TCC AAG AAC GTC	EheI site
6	pDsred/EcoEhe-dn	AAA CTC GAG <u>GGC GCC</u> CAG GAA CAG GTG GTG GCG GCC CTC	EheI site
7	pDsredintern-up	AAG ACT CCT CCC TGC AGG ACG	For sequencing
8	pDsredintern-dn	CGT CCT GCA GGG AGG AGT CTT	For sequencing
9	EGFPEcoRISall-up	AAC GAA TTC GTC GAC ATG GTG AGC AAG GGC GAG GAG	
10	EGFPXhoI-dn	AAA CTC GAG TTA CTT GTA CAG CTC GTC CAT	
11	NCAMintEcoRI pos1474	ACA GGA GTC CTT <u>GGA ATT CAT</u>	EcoRI site
12	NCAMICStart/BamHI-up	CTA GGA TCC <u>GCC ACC</u> ATG GAC ATC ACC TGC TAC	Kozak sequence <b>Initiation</b>
13	NCAMXhoI-Stop-dn	GGC GAA TTC <u>TCG AGG TCA</u> TGC TTT GCT CTC	XhoI site <b>Stop codon</b>
14	NCAMquik-3cys-up	TTC CTG AAC AAG AGT GGC CTG CTC ATG AGC ATC GCT GTT AAC CTG AGC GGC AAA GCG G	
15	NCAMquik-3cys-dn	CCG CTT TGC CGC TCA GGT TAA CAG CGA TGC TCA TGA GCA GGC CAC TCT TGT TCA GGA A	
16	NCAMquik-1cys(1pos)-up	GTG GTC ATG GAC ATC AAC AGC TAC TTC CTG	
17	NCAMquik-1cys(1pos)-dn	CAG GAA GTA GCT GGT GAT GTC CAT GAC CAC	
18	Kir3.2(95)-up	TGA TTT TTA CCA TGG TTT ACA CAG TGA CCT GGC	
19	Kir3.2(95)-dn	GCC AGG TCA CTG TGT AAA CCA TGG TAA AAA TCA	
20	Kir3.2(75)-up	CGC TAC CTG AGC GAT ATC TTC	
21	Kir3.2(75)-dn	GAA GAT ATC GCT CAG GTA GCG	
22	Kir3.2(54, 57, 68)-up	AGG TAC ATG AGG AAA AGC GGA AAG TGC AAT GTT CAT CAC GGC AAC GTG CAG GAG	
23	Kir3.2(54, 57, 68)-dn	CTC CTG CAC GTT GCC GTG ATG AAC ATT GCA CTT TCC GCT TTT CCT CAT GTA CCT	
24	Kir3.4Y(12)D/I(14)R/LLAA-up	CGC GAT GAC GTC CCC AGA GCC ACA GAC CGT ACG CGC GCG GCG GCC GAG	

25	Kir3.4Y(12)D/I(14)R/LLAA-dn	CTC GGC CGC CGC GCG CGT ACG GTC TGT GGC TCT GGG GAC GTC ATC GCG	
26	Kir3.2/3.4 exchangepos.23	CCT GGC CTG CTT AGG CAA CTT GGG GT CCA GGG AGT GAC TCC	Primer for SOE
27	Kir3.2/3.4 exchangepos.50	GTC TTT CCT CAC GTA CCT CTG GCG TGG CTT CTT GC CTC GGC	Primer for SOE
28	Kir3.2/Nt/Sal-up	ACT GGT CGA CCT GAA GTG GAG ATT CAA CCT A	
29	Kir3.2/Nt/XhoI-dn	CAG CTC GAG TAA TGT GGT GAA GAT ATC GGT	
30	Kir3.4/Nt/Sal-up	CTG GTC GAC CTC AAG TGG CGC TTC AAC TTG	
31	Kir3.4/Nt/XhoI-dn	CAG CTC GAG CAG GGT GGT GAA GAG GTC ACT	
32	Kir3.4/ctk/XhoI-dn	GGT CTC GAG TCT CTT CTT GGG CTG GCT GAT	
33	Kir3.2/ctk/Sal-up	AGG GTC GAC ACC CTG GTC TTT TCC ACC CAT	
34	Kir3.2/ct/XhoI-dn	CCC CTC GAG AAT GTG GGA ATT CCT AAG	
35	Kir3.2/ct/Sal-up	CCC GTC GAC GCT TCC ATC AGA GCC AAG	
36	Kir3.4/ct/XhoI-dn	CCC CTC GAG GAT GTG GGA GTT GCG GAG	
37	Kir3.4/ct/Sal-up	CCC GTC GAC GCC TCC ATC CGG GCC AGG	
38	Kir3.1HindIII-up	GCC ACC GAA GCT TCA AAA GA	HindIII site
39	Kir3.4- stop/XhoI-dn	CCC CTC GAG TCA CAT TGA GCC CCT TGT	
40	Kir3.2- stop/XhoI-dn	CCC CTC GAG CTA AAC TTT GGA TTC ATT	
41	Kir3.4-tag/XhoI-dn	CCC CTC GAG CAT TGA GCC CCT TGT	
42	Kir3.2-tag/XhoI-dn	CCC CTC GAG AAC TTT GGA TTC ATT	

### 3 Accession numbers

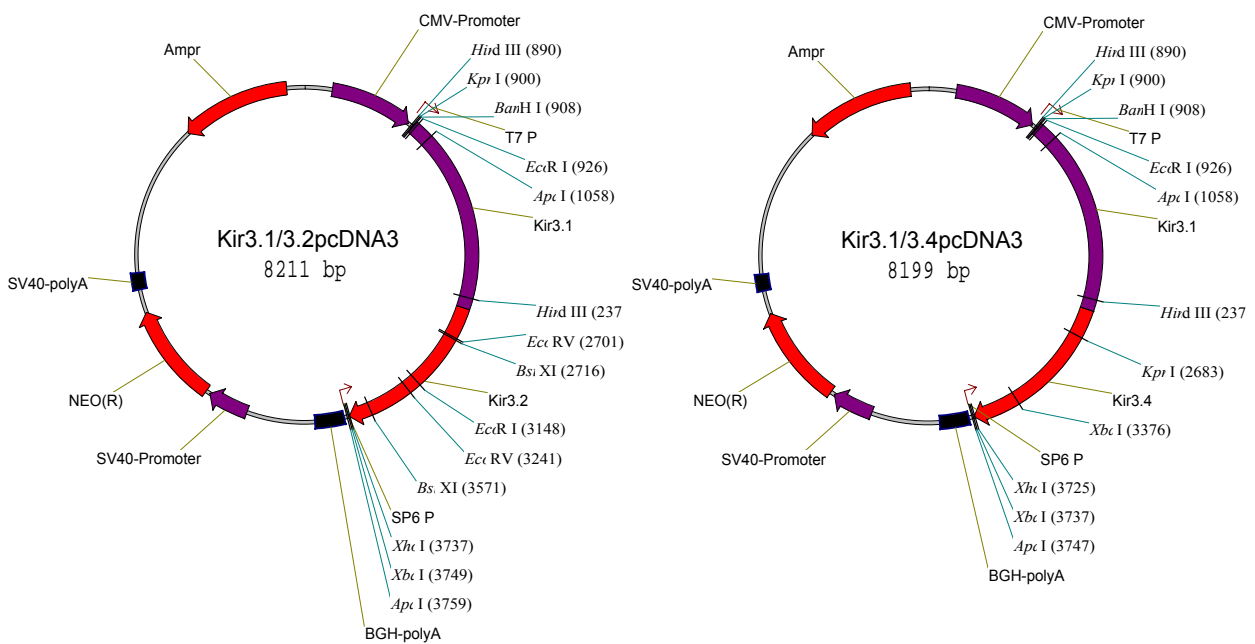
Protein	Organism	accession number
NCAM120	<i>mouse</i>	Y00051
NCAM140	<i>rat</i>	X06564
NCAM180	<i>rat</i>	Not available
Kir3.1	<i>rat</i>	Y12259
Kir3.2	<i>human</i>	C78480
Kir3.3	<i>rat</i>	C77929
Kir3.4	<i>human</i>	C47208

## 4 Plasmids

Primers are cited referring to their number in the oligonucleotide table (see IV 2)

### 4.1 Kir3 plasmids

The concatemeric Kir3.1/3.2pcDNA3 (or psGEM) and Kir3.1/3.4pcDNA3 (or psGEM) plasmids were obtained from the lab of Dr. A. Karschin (Wischmeyer et al., 1997).



#### 4.1.1 Construction of Kir3.1/3.2 and Kir3.1/3.4-hybrids

##### 4.1.1.1 COOH and NH<sub>2</sub> exchange

For construction of the COOH-terminal and NH<sub>2</sub>-terminal chimeras of Kir3.2 and 3.4, standard PCR technique was used. The COOH-termini of Kir3.2 or 3.4 were exchanged by amplifying sequences with PCR II (see Fig. 29) using primers C and D. The corresponding Kir3.2 and 3.4 core channels with the 3' end of Kir3.1 were amplified with PCR I using primers A and B. The NH<sub>2</sub>-termini were exchanged by amplifying the 3' end of Kir3.1 and base pairs 1-249 of Kir3.2 and Kir3.4 with PCR I using primers A and B and the corresponding core channels were amplified by PCR II with the primers C and D. In parallel, silent restriction sites were introduced for SalI and XhoI into the PCR products, as depicted in the diagram. PCR products of PCR I and PCR II were subcloned into pBluescript II KS via HindIII/XhoI and Sal/XhoI, respectively. Chimeras were produced by fusing the PCR I product of Kir3.2 or Kir3.4 with their XhoI site in-frame on the SalI site of the corresponding PCR product II. The sequence of all PCR-amplified products was verified by DNA sequence analysis. The mutated cDNA was introduced into the psGEM plasmid by substituting the Kir3.1/3.2 wild type HindIII/XhoI Fragment by the mutated HindIII/XhoI fragments.

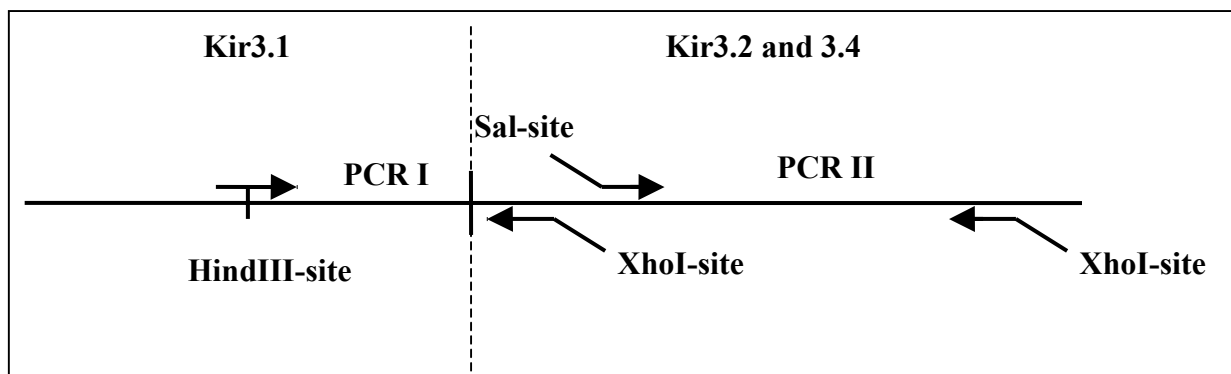


**Figure 29: Schematic diagram of Kir3.2 and Kir3.4 chimera production.**

Primers were designed such that PCR I amplified the NH<sub>2</sub>-termini and PCR II the core channel for the NH<sub>2</sub>-terminus exchange. For COOH exchange, primers were designed such that PCR I amplified the core channel and PCR II the corresponding COOH terminus of Kir3.2 and Kir3.4.

Hybrid name	Amino acids of Kir3.2 and Kir3.4	Primers no. A and B Primers no. C and D	Cloned in plasmids
Kir3.1/3.2 C-term 3.4	1-234 of Kir3.2 231-419 of Kir3.4	38, 34 37, 39	psGEM
Kir3.1/3.4 C-term 3.2	1-231 of Kir3.4 234-423 of Kir3.2	38, 36 35, 40	psGEM
Kir3.1/3.4 C-term complete 3.2	1-198 of Kir3.4 201-423 of Kir3.2	38, 32 33, 40	psGEM
Kir3.1/3.2 N-term 3.4	1-83 of Kir3.4 86-423 of Kir3.2	38, 31 28, 40	psGEM
Kir3.1/3.4 N-term 3.2	1-86 of Kir3.2 83-419 of Kir3.4	38, 29 30, 39	psGEM

**Table 2: Exchange of the NH<sub>2</sub> and COOH termini between Kir3.2 and Kir3.4.**

Listed are the hybrid channels and amino acid positions of Kir3.2 and Kir3.4 where the NH<sub>2</sub> and COOH termini were exchanged. Primers refer to the schematic drawing of Fig. 1.

Amino acids 1-35 and 1-54 of Kir3.2 were substituted with the corresponding amino acids of Kir3.4 using the PCR technique of splicing by overlap extension (SOEing; Retzer et al., 1996). The final PCR products were digested by HindIII/XhoI and cloned into the psGEM plasmid as described above.

Hybrid name	Amino acids of Kir3.2 and Kir3.4	Primers and template for PCR1	Primers and template for PCR2
Kir3.1/3.4(1-23)-3.2	1-23 of Kir3.4 30-423 of Kir3.2	38, 26 Template: Kir3.1/3.4pcDNA <sub>3</sub>	PCR1 product, 40 Template: Kir3.1/3.2
Kir3.1/3.4(1-50)-3.2	1-50 of Kir3.4 53-423 of Kir3.2	38, 27 Template: Kir3.1/3.4pcDNA <sub>3</sub>	PCR1 product, 40 Template: Kir3.1/3.2

**Table 3: Exchange of parts of NH<sub>2</sub> termini between Kir3.2 and Kir3.4.**

Listed are the hybrid channels and amino acid positions of Kir3.2 at which parts of the NH<sub>2</sub> terminus were exchanged.

#### 4.1.1.2 Single amino acid mutations in Kir3.2 and Kir3.4

Mutation of the indicated amino acids in the NH<sub>2</sub>-terminus of Kir3.2 and Kir3.4 were performed using the Quikchange Mutagenesis kit (Stratagene). The HindIII/XhoI fragments of Kir3.1/3.2 and Kir3.1/3.4 were subcloned into the pBlueKS plasmid and all mutations were performed on these plasmids. In case of multiple amino acid exchange, mutations were performed successively. The mutated HindIII/XhoI fragments were finally ligated into the HindIII/XhoI linearized Kir3.1/3.2-psGEM plasmid.

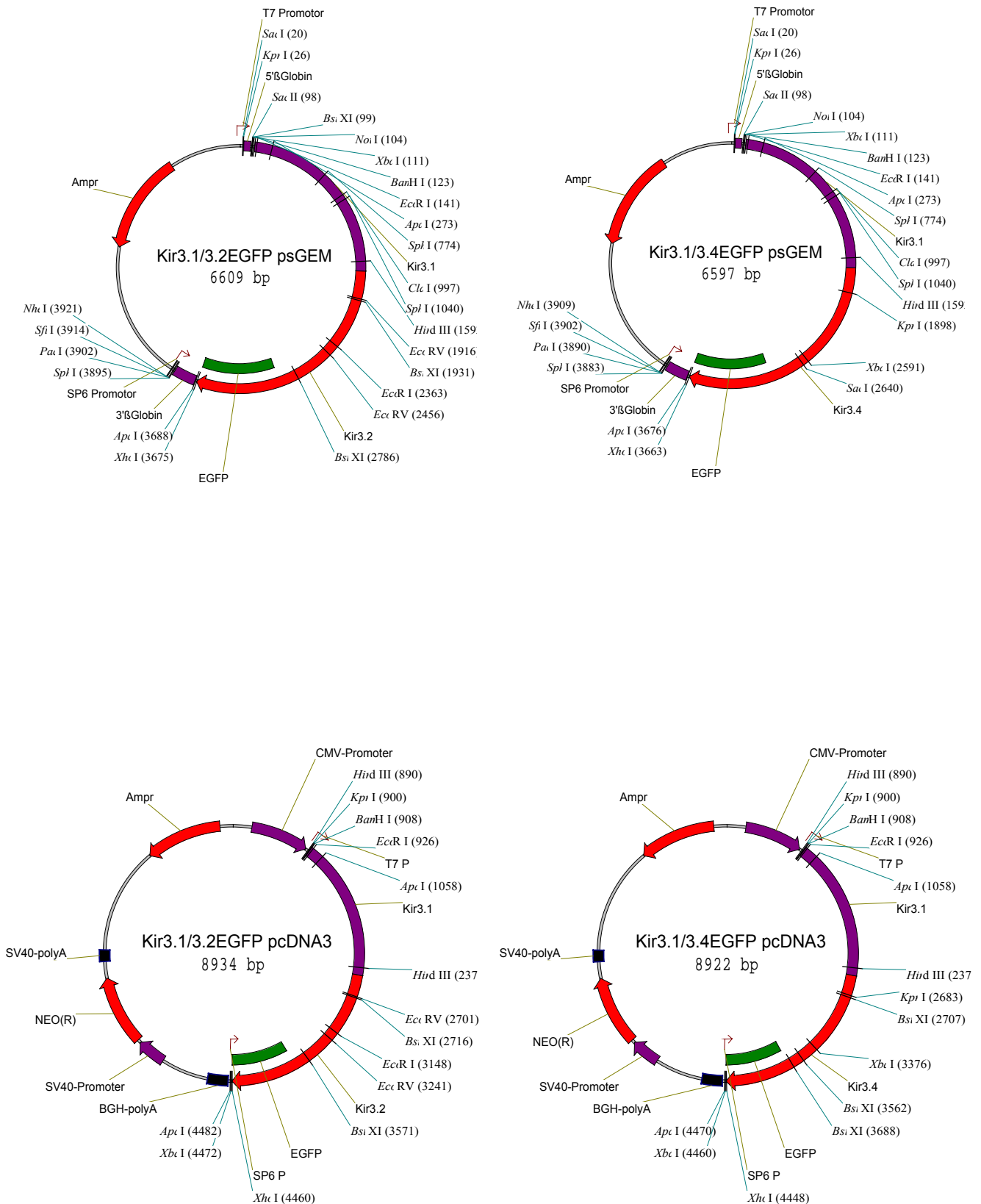
Mutant name	Position and amino acids exchange	Primers and template for Mutation	Cloned in the plasmids
Kir3.1/3.2(54, 57, 68)	54, V → M 57, D → S 68, Q → R	22, 23 Template: Kir3.1/3.2pBlue	psGEM
Kir3.1/3.2(54, 57, 68, 75, 95)	54, V → M 57, D → S 68, Q → R 75, T → S 95, V → T	a) 18, 19 b) 20, 21 Template: Kir3.1/3.2(54, 57, 68)pBlue	psGEM
Kir3.1/3.4Δendocytosis signals	32, Y → D 34, I → R 42, 43, LL → AA	24, 25 Template: Kir3.1/3.4pBlue And Kir3.1/3.4EGFPpBlue	psGEM and the Kir3.1/3.4 EGFP plasmid in pcDNA <sub>3</sub>

**Table 4: Point mutations within the amino acid sequences of Kir3.2 and Kir3.4.**

Listed are the mutant channels, the amino acid position of mutation and the corresponding amino acid that was introduced instead.

#### 4.1.2 Construction of Kir3.1/3.2 and Kir3.1/3.4-EGFP and 6xHis-tag chimeras

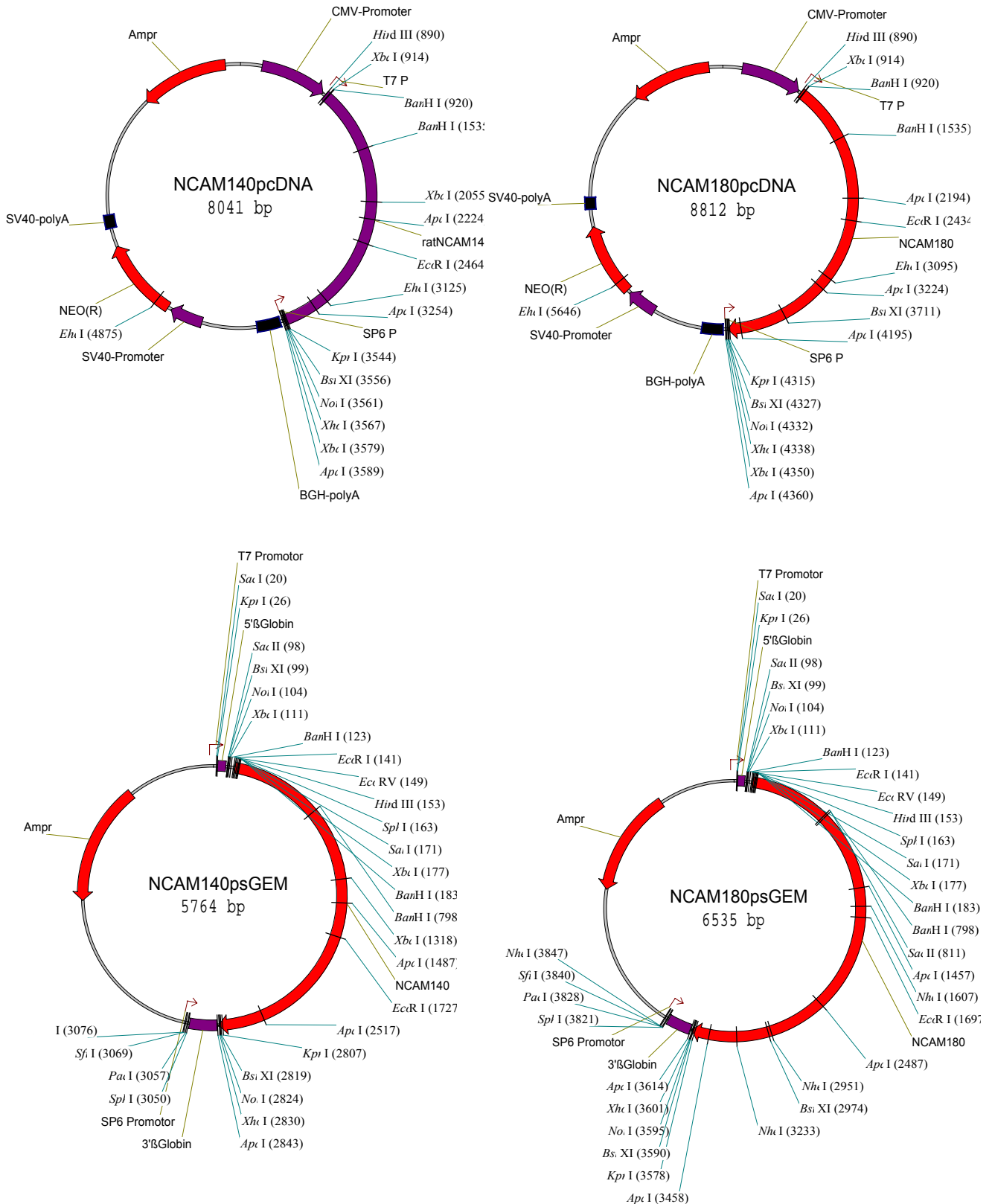
Kir-EGFP and 6xHis-tag chimeras were constructed by removing the stop codon and introducing an XhoI site at the 3' end of the coding sequences of Kir3.2 and 3.4 using standard PCR technique using the primers 42 and 41, respectively. For construction of the 6xHis-tag chimeras, the PCR product was cloned in-frame into the pcDNA3 Myc/His plasmid. For construction of the EGFP chimeras, Sall and XhoI sites were introduced by PCR to the 5' and 3' end of the EGFP cDNA (Clontech) using the primers 9 and 10. The Sall site of EGFP cDNA was fused in-frame to the 3' end XhoI site of the Kir3.2 and 3.4 subunits and the resulting chimeras were subcloned via HindIII/XhoI into pcDNA3 and psGEM.





#### 4.2.2 NCAM140 and NCAM180 in pcDNA3 and psGEM

NCAM140 and NCAM180 (both in pcDNA3) were obtained from Dr. P. Maness, University of South Carolina, USA. The cDNA for NCAM140 and NCAM180 was cut out of pcDNA3 by HindIII/XhoI and ligated into the HindIII/XhoI linearized psGEM.

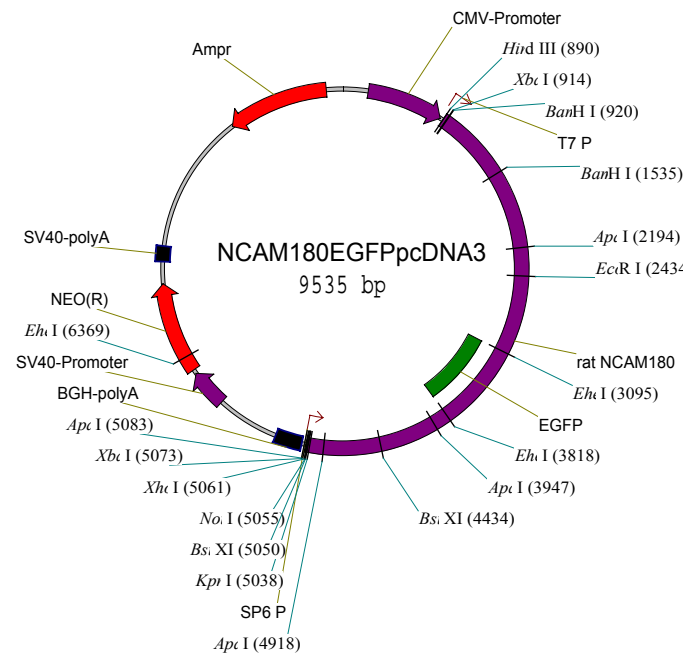
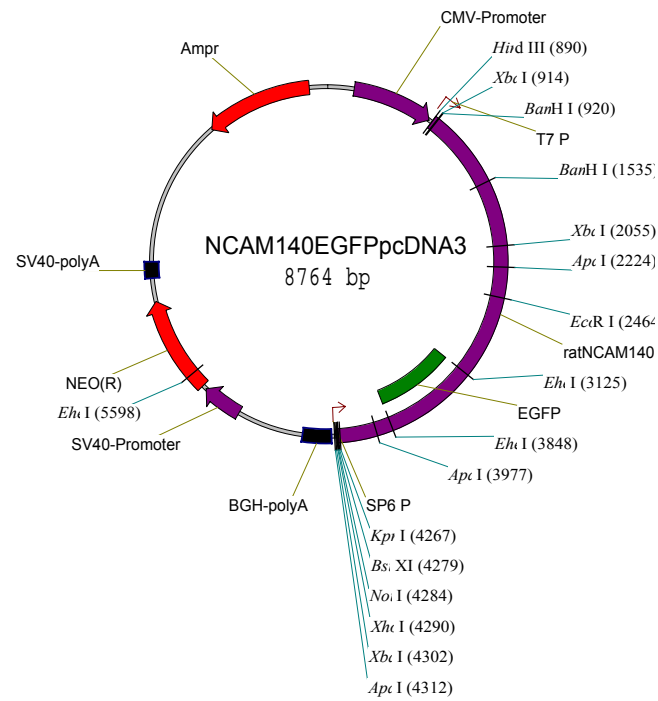


### **4.2.3 NCAM 140 $\Delta$ in pcDNA3 and psGEM**

An NCAM140 fragment (pos 1474-2583) was amplified by PCR using primers 11 and 13 and subcloned after EcoRI/XhoI digestion into pBlueKS. All mutations were performed on this NCAM140 fragment in pBlueKS. The 4 intracellular cysteines were mutated into serines using the Quikchange Mutagenesis kit (Stratagene) by successive mutations using primers 14, 15 and 16, 17. The mutated EcoRI/XhoI fragment was re-introduced into the EcoRI/XhoI linearized NCAM140pcDNA3 plasmid. (Restriction map is identical to NCAM140pcDNA3).

### **4.2.4 NCAM140-, NCAM180- and NCAM140 $\Delta$ -EGFP in pcDNA3**

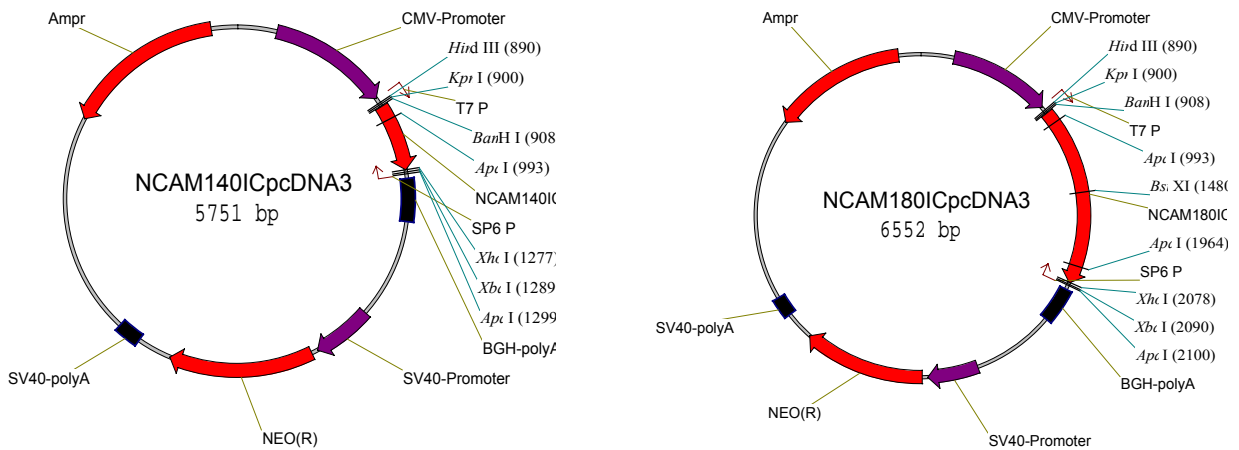
An NCAM180 fragment (pos 1474-2883) was amplified by PCR using primers 11 and 13 and was subcloned after EcoRI/XhoI digestion into pBlueKS. A single EheI restriction site (pos. 1873) within the extracellular domain of all trans-membranous NCAM isoforms was used to introduce the cDNA of the EGFP protein. EheI restriction sites were introduced by PCR to the 5' and 3' end of the EGFP cDNA (Clontech) using primers 1 and 2. The PCR product was subcloned via EcoRI and XhoI into pBlueKS and excised via EheI. All three NCAM (140, 140 $\Delta$  and 180) EcoRI/XhoI pBlueKS fragments were linearized by EheI digestion, dephosphorylated and the EGFP cDNA was ligated into the plasmids. Finally, all modified EcoRI/XhoI fragments were re-introduced into the EcoRI/XhoI linearized NCAM140pcDNA<sub>3</sub> plasmid. (Restriction map of NCAM140 $\Delta$ -EGFP is identical to NCAM140-EGFPpcDNA<sub>3</sub>).



All four constructs were also tagged with the red fluorescent protein using the pDsred plasmid as a template by the same method as the EGFP-tagged constructs.

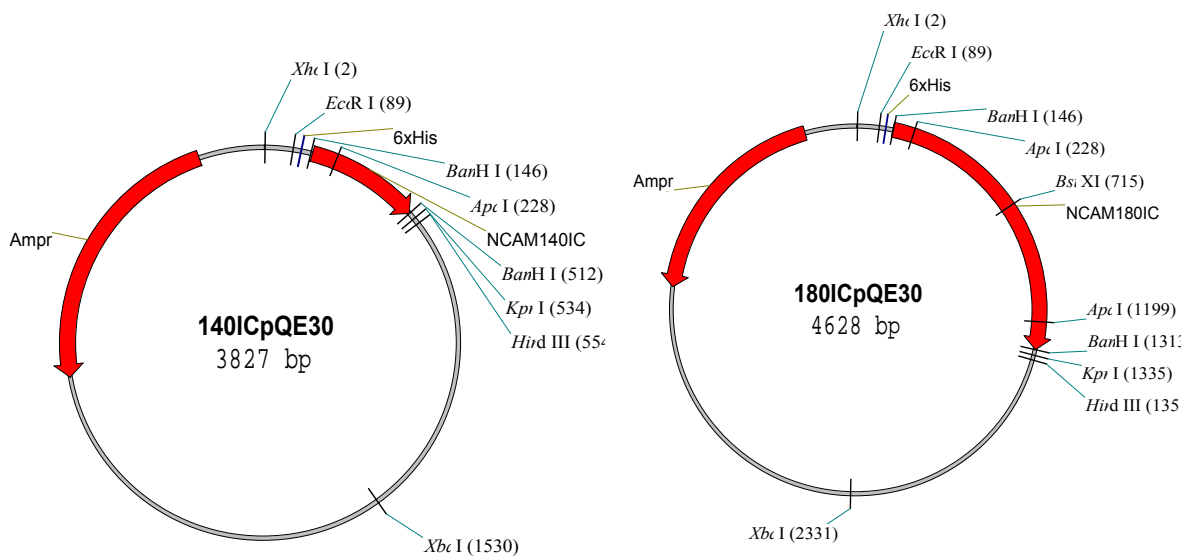
#### 4.2.5 NCAM140IC and NCAM180ICpcDNA3 and psGEM

The intracellular domains of NCAM140 and NCAM180 were amplified by PCR using the primers 12 and 13. The primers were designed such that a BamHI restriction site and a Kozak sequence (Kozak, 1986) were introduced to the 5' end and an XhoI site to the 3' end of the intracellular domain. The PCR product was BamHI/XhoI digested and ligated into the BamHI/XhoI linearized pcDNA3 and psGEM plasmids.



#### 4.2.6 NCAM140IC and NCAM180ICpQE30

The intracellular domains of NCAM140 (bp. 2135-2550) and NCAM180 (bp. 2135-2850) were amplified by PCR introducing BamHI restriction sites at the 5' and 3' end. The PCR product was cloned into the pQE30 plasmid after BamHI digestion.



## **5 Publications and poster presentations**

### **5.1 Poster presentations:**

Delling, M., Wischmeyer, E., Dityatev, A., Gercken, G., Karschin, A. and Schachner, M. Modulation of G protein-activated inwardly rectifying potassium channels by the neural cell adhesion molecule NCAM. Meeting of the federation of european neuroscience societies (FENS), Brighton, 24th-28th June 2000

Delling, M., Wischmeyer, E., Dityatev, A., Gercken, G., Veh, R., Karschin, A. and Schachner, M. Modulation of G protein-activated inwardly rectifying potassium channels by the neural cell adhesion molecule NCAM. Meeting of the German-Scandinavian Society of Physiology, Berlin, 10th-13th March 2001

### **5.2 Publications:**

Stork, O., Welzl, H., Wotjak, C.T., Hoyer, D., Delling, M., Cremer, H. and Schachner, M. Anxiety and increased 5-HT<sub>1A</sub> response in NCAM null mutant mice, *J. Neurobiol.* 1999; 40, 343-55.

Delling, M., Wischmeyer, E., Dityatev, A., Veh, R., Gercken, G., Karschin, A. and Schachner, M.

The neural cell adhesion molecule NCAM regulates cell surface delivery of G protein-activated inwardly rectifying potassium channels via lipid rafts, submitted.

Niethammer, P., Delling, M., Sytnyk, V., Dityatev, A. and Schachner, M. Co-signaling of NCAM via lipid rafts and the FGF receptor is required for neuritogenesis, submitted.

## 6 Curriculum vitae

### Persönliche Daten

Name: Markus Delling  
Geburtstag: 31. 01. 1972  
Geburtsort: Hamburg

### Schulbildung

1978 Einschulung in Hamburg  
1982 Übergang zum Gymnasium Oberalster  
1991 Abitur in Hamburg

### Akademischer Werdegang

Oktober 91 Beginn des Chemiestudiums in Hamburg  
Dezember 93 Vordiplom im Studiengang Chemie an der Universität Hamburg (Note „Sehr gut“)  
Oktober 94 Studienaufenthalt in England an der Universität  
bis März 95 Southampton. Bearbeitung jeweils eines „Third Year Project“ in physikalischer und anorganischer Chemie  
November 96 Diplomprüfung im Studiengang Chemie an der Universität Hamburg (Gesamtnote „sehr gut“)  
Januar 97 Diplomarbeit in der Abteilung für Biochemie und  
bis Oktober 97 Molekularbiologie des Fachbereiches Chemie der Universität Hamburg mit dem Thema „Tyrosinphosphorylierung in Alveolarmakrophagen nach Stimulation mit Quarzstäuben und metalloxid-beschichteten Silicapartikeln“ (Note „sehr gut“)  
Dezember 97 Promotion am Zentrum für molekulare Neurobiologie Hamburg  
bis März 01 bei Frau Professor Dr. Melitta Schachner

### Beruflicher Werdegang

1.10.94-1.3.95 Erasmus-Stipendium  
1.1.98-31.3.99 Wissenschaftlicher Mitarbeiter an der Universität Hamburg  
1.4.99-31.3. 01 Promotionsstipendium der Studienstiftung des Deutschen Volkes

## Danksagung

Sehr herzlich bedanken möchte ich mich bei Frau Professor Melitta Schachner, die mich während meiner Zeit in Ihrem Institut fachlich wie auch persönlich sehr unterstützt und gefördert hat. Außerdem möchte ich Ihr für die Freiheit bei der Ausgestaltung dieser Arbeit und Ihren zügig vorgenommenen Korrekturen danken.

Besonderer Dank gilt auch Herrn Professor Gercken für die Betreuung dieser externen Promotion und die interessanten wie auch unterhaltsamen Seminare.

Besonders möchte ich mich auch bei PD Dr. Erhard Wischmeyer und Professor Andreas Karschin bedanken, die mich von Beginn an sehr unterstützt haben und mir mit den Oozytendaten wie auch durch ihre intensiven Diskussionen sehr weitergeholfen haben.

Im gleichem Atemzug muss auch Dr. Alexander Dityatev genannt werden, der mir nicht nur die Elektrophysiologie näher gebracht hat, sondern auch durch seine Hilfe und zahlreichen Diskussionen und Anregungen sehr zum erfolgreichen Abschluss dieser Arbeit beigetragen hat.

Bei Philipp Niethammer bedanke ich mich für die ausgesprochen kreative Zusammenarbeit während seiner Diplomarbeit. Ohne seine Hilfe wäre das NCAM140 $\Delta$  Konstrukt sicher nicht so gut charakterisiert worden.

Bei meinem Laborkollegen Ulrich Bormann möchte ich mich für die freundschaftliche und „lustige“ Zusammenarbeit im Labor bedanken, ohne die manches sicherlich wesentlich schwerer zu ertragen gewesen wäre.

Bei Volodja Sytnyk bedanke ich mich für die Hilfe am konfokalen Laserscanning-Mikroskop.

Dr. Ralf Kleene danke ich für seine Diskussionen und Anregungen bezüglich der „lipid rafts“ und Endozytosemechanismen.

Allen Mitarbeitern des Institutes danke ich für die nette Zusammenarbeit, die stete Diskussionsbereitschaft und die Freundschaft, die uns verbunden hat.

Meiner Freundin Corinna danke ich für ihre Unterstützung und Hilfe bei den Korrekturen.

Nicht zuletzt danke ich besonders der Studienstiftung des Deutschen Volkes für ein zweijähriges Doktorandenstipendium.

## **Erklärung**

Hiermit versichere ich, dass ich die vorliegende Arbeit selbständig angefertigt habe. Fremde Hilfe ist, soweit sie in Anspruch genommen wurde, vermerkt.

Diese Arbeit ist zuvor keiner Prüfungsbehörde in gleicher oder ähnlicher Form vorgelegt worden.

Hamburg, den 11.06.2001

(Markus Delling)